RESEARCH DEPARTMENT

An introduction to the theory of aerials

Report No. E-085

(1963/27)

THE BRITISH BROADCASTING CORPORATION
ENGINEERING DIVISION

RESEARCH DEPARTMENT

AN INTRODUCTION TO THE THEORY OF AERIALS

Report No. E-085

(1963/27)

W Proctor Wilson

H. Page, M.Sc., M.I.E.E.

(W. Proctor Wilson)

This Report is the property of the British Broadcasting Corporation and may not be reproduced in any form without the written permission of the Corporation.

Report No. E-085

AN INTRODUCTION TO THE THEORY OF AERIALS

Section Title Page

LIST OF PRINCIPAL SYMBOLS

1 INTRODUCTION 1
  1.1. Reciprocal Properties of an Aerial Used for Transmission or Reception 1
  1.2. Field Radiated by a Doublet 3
  1.3. The Image of a Current Element over a Perfectly-Conducting Plane 6

2 LOW- AND MEDIUM-FREQUENCY AERIALS 7
  2.1. The Radiation Characteristics of the Idealised Vertical Aerial 7
    2.1.1. The Vertical Radiation Pattern 7
    2.1.2. Calculation of the Radiated Power 13
    2.1.3. The Radiation Resistance 17
    2.1.4. Ground-Wave Field Strength 20
  2.2. The Radiation Characteristics of the Practical Vertical Aerial 21
    2.2.1. The Effect of Imperfectly-Conducting Ground on the Vertical Radiation Pattern 21
    2.2.2. The Aerial Current Distribution 24
    2.2.3. The Radiation Characteristics 26
    2.2.4. The Base Impedance 28
    2.2.5. The Characteristic Impedance of a Vertical Cylindrical Aerial 30
  2.3. Radiation Coupling Between Spaced Aerials 32
    2.3.1. Definition of Mutual Impedance Between Aerials 32
    2.3.2. Calculation of Mutual Impedance 33
    2.3.3. The Mutual Impedance Between Similar Parallel Aerials 34
    2.3.4. Examples of Calculations on Coupled Aerials 37
    2.3.5. Receiving Aerials 39

3 HIGH-FREQUENCY AERIALS 43
  3.1. General Considerations 43
  3.2. The Curtain Array 46
  3.3. The End-Fire Array 54
  3.4. The Rhombic Aerial 58

Section Title Page

4. VERY-HIGH AND ULTRA-HIGH FREQUENCY AERIALS 64
- 4.1. General Considerations 64
- 4.2. The Folded Dipole 67
- 4.3. The Concept of Equivalent Generators 70
- 4.4. Balanced-to-Unbalanced Impedance Transformations 70
- 4.5. The Radiation Pattern of an Aerial Mounted on a Cylindrical Mast 74
- 4.6. Aerials Having a Uniform Horizontal Radiation Pattern . . . 77
- 4.7. Slot in Infinite Perfectly-Conducting Flat Sheet 80
- 4.8. Slot in Finite Perfectly-Conducting Flat Sheet 86
- 4.9. Longitudinal Slot in Infinitely-Long Cylinder 86

5. ACKNOWLEDGEMENTS 91

6. REFERENCES 91

7. APPENDICES 92
- 7.1. The z-Component of the Electric Force near a Vertical Aerial Carrying a Sinusoidal Current Distribution 92
- 7.2. The Mutual Impedance Between Similar Vertical Aerials . . . 95
- 7.3. The Field in the Direction of a Doublet Mounted Near an Infinitely-Long Cylinder Immersed in a Plane-Wave Field . . 97
  - 7.3.1. Generalised Expression for the Field 97
  - 7.3.2. Values of the Coefficients for a Horizontally-Polarised Transmitting Doublet 100
  - 7.3.3. Values of the Coefficients for a Vertically-Polarised Transmitting Doublet 101
  - 7.3.4. Field in Direction of Tangential Receiving Doublet Spaced a Distance b from the Axis of the Cylinder . 102
  - 7.3.5. Field in Direction of Vertical Receiving Doublet Spaced a Distance b from the Axis of the Cylinder . 102
  - 7.3.6. Field in Direction of Radial Receiving Doublet Spaced a Distance b from the Axis of the Cylinder . 103
  - 7.3.7. Value of H_z at the Surface of the Cylinder due to Horizontally-Polarised Transmitting Doublet 103

LIST OF SYMBOLS

a = radius of cylindrical aerial or supporting mast

b = distance of aerial from axis of cylindrical supporting mast

c = velocity of light

h = height of aerial

r = distance from aerial to point under consideration

E = electric force

E_g = ground-wave field strength (electric force)

H = magnetic force

I_L = r.m.s. value of the current at the maximum of a sinusoidal distribution (loop current)

P = power radiated by aerial

R_L = radiation resistance referred to loop current

Z_{11}, Z_{22} = self impedance of aerials 1 and 2 respectively

Z_{12} = mutual impedance between aerials 1 and 2

$\beta = \frac{2\pi}{\lambda}$

ϵ_0 = permittivity of free space

ϵ_r = permittivity of ground relative to free space

ϵ_n = Neumann's number ($\epsilon_n = 1$ for $n = 0$, $\epsilon_n = 2$ for $n \neq 0$)

η_0 = characteristic impedance of free space

θ_0 = angle of zero radiation in the vertical radiation pattern

λ = wavelength

μ_0 = permeability of free space

ρ_v, ρ_h = reflection coefficient of the ground for vertically-polarised and horizontally-polarised plane waves respectively

σ = conductivity of the ground

ω = angular frequency

Co-ordinate systems: Cartesian: (x, y, z)
Spherical: (r, θ, ϕ)
Cylindrical: (ρ, z, ϕ)

© BBC 2004. All rights reserved. Except as provided below, no part of this document may be reproduced in any material form (including photocopying or storing it in any medium by electronic means) without the prior written permission of BBC Research & Development except in accordance with the provisions of the (UK) Copyright, Designs and Patents Act 1988.

The BBC grants permission to individuals and organisations to make copies of the entire document (including this copyright notice) for their own internal use. No copies of this document may be published, distributed or made available to third parties whether by paper, electronic or other means without the BBC's prior written permission. Where necessary, third parties should be directed to the relevant page on BBC's website at http://www.bbc.co.uk/rd/pubs/ for a copy of this document.

Report No. E-085

(1963/27)

August 1963

AN INTRODUCTION TO THE THEORY OF AERIALS

1. INTRODUCTION

The function of the aerial, when transmitting, is to propagate the electromagnetic waves flowing from the source into space. It may be regarded as a leaky waveguide, the degree of guidance in launching the waves being controlled by the configuration of the aerial.

The two important characteristics are:

i. *the radiation pattern* i.e. the intensity of the radiation as a function of direction, at a large constant distance from the aerial. It is obviously desirable to concentrate the available energy in the required directions, rather than to allow it to be radiated in directions where it will be either harmful or wasted. The greater the control required over the shape of the radiation pattern the more complex the aerial, so that in practice a compromise must be sought between complexity and performance.

ii. *the impedance*, which determines the design of the network coupling the aerial to the source, and also the working currents and voltages. In the case of aerials which are required to cover a band of frequencies it is necessary to know how both the radiation pattern and the impedance change over the band.

The methods used in calculating these performance characteristics are introduced in sections classified according to the frequency band. These theoretical methods are of quite general application, and those developed in the earlier sections of the report form the foundation for the later work. The classification is used merely to draw attention to the associated practical problems, the importance of which usually depends on the frequency band under consideration. The initial number of both the figures and the equations give the sections in which they are to be found. Rationalised M.K.S. units are used throughout.

1.1. Reciprocal Properties of an Aerial Used for Transmission or Reception

Since the aerial and the associated propagation medium constitute a linear passive system, the radiation pattern of the aerial is the same whether it be used for transmission or reception. This can be proved by supposing the field due to the transmitting aerial, T, in Fig. 1.1, to be measured by means of a distant receiving aerial, R, which rotates round the transmitting aerial at a constant distance from it; the radius vector joining T and R is at an angle θ to the axis of T. If a zero-impedance generator of voltage V in series with the transmitting aerial induces a current I to flow in the receiving aerial, we can write $I \propto V.f(\theta)$; $f(\theta)$ is the function of θ which describes the radiation pattern of T when transmitting. Applying

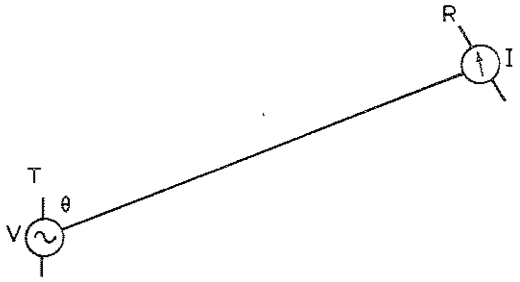

Fig. 1.1 - Reciprocal properties of an aerial used for transmission or reception

the reciprocity theorem, it follows that a zero-impedance generator of voltage V in series with R induces a current I to flow in T; since $I \propto V.f(\theta)$, $f(\theta)$ also describes the radiation pattern of T as a receiving aerial. The same argument holds if an arbitrary impedance is connected in series with T.

The radiation pattern is defined as that obtained when the receiving aerial, R, is oriented to correspond with the polarisation of the radiated wave, i.e. to maximum pick-up. In some problems it may be convenient to calculate the radiation pattern corresponding to one particular component of the radiated wave; the reciprocity principle applies to this case also.

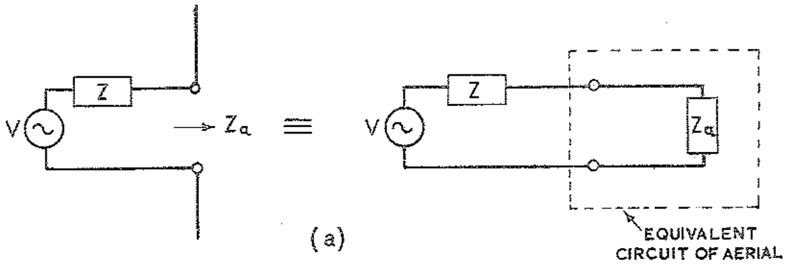

(a) Transmitting aerial energised from generator of voltage V and internal impedance Z

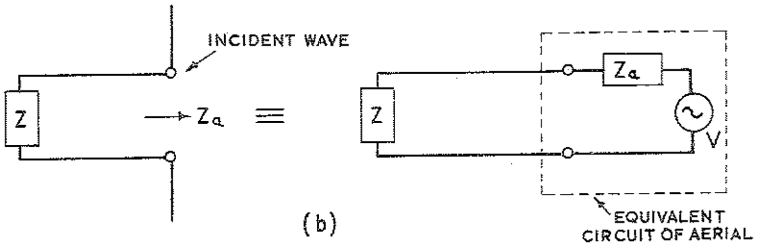

(b) Receiving aerial terminated in receiver of impedance Z; V = open-circuit voltage induced by incident wave

Fig. 1.2 - Equivalent circuit of an aerial used for transmission or reception

The equivalent circuit of a transmitting aerial is shown in Fig. 1.2(a). V is the open-circuit voltage of the applied generator of internal impedance Z, and Z_a is the impedance of the aerial measured when transmitting. For reception, we regard the aerial as a network in which the voltage, V, induced at the open-circuited output terminals by the incident wave is either measured or calculated. The equivalent circuit is then as shown in Fig. 1.2(b); Z_a is the impedance of the aerial measured when transmitting and Z is the input impedance of the receiver.

In calculating the radiation pattern or impedance of an aerial it is therefore immaterial whether we consider it to be transmitting or receiving, and we shall consider whichever case is the easier to analyse. This means that usually we shall take the aerial to be transmitting, although in a few cases it is more convenient to consider it as receiving.

1.2. Field Radiated by a Doublet

In carrying out calculations on a radiating system it is often convenient to imagine it as being composed of a large number of infinitesimal elements; by summing the contributions from the separate elements the effect of the complete system can be calculated.

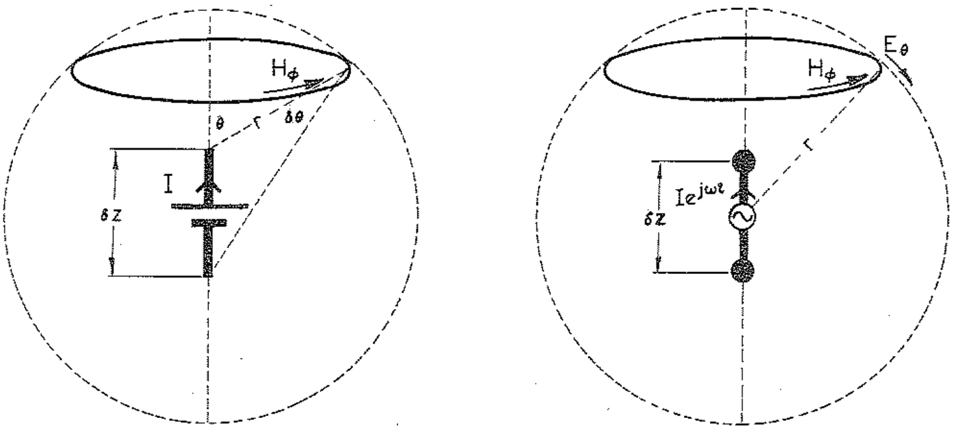

(a) Current element (b) Doublet

Fig. 1.3

This concept is useful even in the case of a circuit carrying a direct current. We suppose the element, shown in Fig. 1.3(a), to be immersed in a conducting medium, but insulated from it except at the ends. A current I is maintained by means of a battery, and spreads out into the conducting medium. The current distribution within the medium is equivalent to the sum of two uniform radial distributions, one associated with each pole of the element. The current density of each distribution at a radius r is $I/4\pi r^2$ and the associated current through the spherical cap of semi-angle θ is $\frac{1}{2}I(1-\cos\theta)$. The current flowing through the spherical cap due to the element is thus

$$\frac{I}{2}\{(1-\cos\theta)-(1-\cos\overline{\theta-\delta\theta})\} = \frac{I}{2}\sin\theta\;\delta\theta = \frac{I\sin^2\theta\;\delta z}{2r}$$

where δz is the length of the element and $r \gg \delta z$.

From considerations of symmetry the lines of magnetic force lie in circles perpendicular to and with their centres on the axis of the element. The only component of magnetic force is therefore H_ϕ, ϕ being the angle from the datum in the horizontal plane. Since the current through the spherical cap is equal to the line integral of the magnetic force round the periphery, we have

$$H_\phi = \frac{I \sin\theta \ \delta z}{4\pi r^2} \tag{1.1}$$

The corresponding element in the alternating-current case is the doublet energised by a series generator, as shown in Fig. 1.3(b), i.e. an infinitesimally short filament whose radius is small compared with its length, terminated in large capacitances carrying oscillating charges. The generator voltage, and hence the current, is assumed to vary sinusoidally with time; the current will be written $Ie^{j\omega t}$ where ω is the angular frequency. The steady magnetic field in Fig. 1.3(a) becomes an alternating magnetic field in Fig. 1.3(b); as a limiting case we may consider radiation into free space. The voltage of the battery in Fig. 1.3(a) would of course then tend to infinity, but provided the current is maintained by some means the foregoing reasoning is not affected.

We will endeavour to find a solution for the field which reduces to Equation (1.1) when $\omega \to 0$, with I replaced by $Ie^{j\omega t}$, and which also satisfies Maxwell's equations in free space. Spherical co-ordinates are the most convenient for this problem;* since the medium is non-conducting, and since also all the derivatives with respect to ϕ vanish (from considerations of symmetry) and $\partial/\partial t$ may be replaced by $j\omega$, we have

$$j\omega\epsilon_0 E_r = \frac{1}{r}\ \frac{\partial H_\phi}{\partial\theta} + \frac{\cos\theta}{r\sin\theta} H_\phi \tag{1.2}$$

$$j\omega\epsilon_0 E_\theta = -\frac{H_\phi}{r} - \frac{\partial H_\phi}{\partial r} \tag{1.3}$$

$$j\omega\epsilon_0 E_\phi = \frac{H_\theta}{r} + \frac{\partial H_\theta}{\partial r} - \frac{1}{r}\frac{\partial H_r}{\partial\theta} \tag{1.4}$$

$$-j\omega\mu_0 H_r = \frac{1}{r}\frac{\partial E_\phi}{\partial\theta} + \frac{\cos\theta}{r\sin\theta} E_\phi \tag{1.5}$$

$$-j\omega\mu_0 H_\theta = -\frac{E_\phi}{r} - \frac{\partial E_\phi}{\partial r} \tag{1.6}$$

$$-j\omega\mu_0 H_\phi = \frac{E_\theta}{r} + \frac{\partial E_\theta}{\partial r} - \frac{1}{r}\frac{\partial E_r}{\partial\theta} \tag{1.7}$$

where ϵ_0 is the permittivity of free space = $10^{-9}/36\pi$ farads/m, and μ_0 is the permeability of free space = $4\pi . 10^{-7}$ henrys/m.

For the time being we will assume that, as in the case of the element carrying a direct current, $H_\theta = H_r = 0$, and $H_\phi \propto \sin\theta$; we therefore write

$$H_\phi = \sin\theta \, . \, \Psi \tag{1.8}$$

where Ψ is expected to be a function of t and r only

---

*E.C. Jordan, "Electromagnetic Waves and Radiating Systems", Prentice-Hall, pp. 17 and 113.

From Equation (1.2) $$E_r = \frac{-j2\cos\theta}{\omega\epsilon_0 r}\,\Psi \qquad (1.9)$$

From Equation (1.3) $$E_\theta = \frac{j\sin\theta}{\omega\epsilon_0}\left\{\frac{\Psi}{r} + \frac{\partial\Psi}{\partial r}\right\} \qquad (1.10)$$

From Equation (1.4) $$E_\phi = 0 \qquad (1.11)$$

From Equations (1.7)-(1.10), since $\epsilon_0\mu_0 = (1/c^2)$ (where c is the velocity of light) we have

$$\frac{\partial^2\Psi}{\partial r^2} + \frac{2}{r}\frac{\partial\Psi}{\partial r} - \left(\frac{2}{r^2} - \beta^2\right)\Psi = 0 \qquad (1.12)$$

where $\beta = (\omega/c) = (2\pi/\lambda)$ and λ is the wavelength. As θ does not appear in Equation (1.12) our assumption that $H_\phi \propto \sin\theta$ is justified.

When r is very large the only component of the field is that corresponding to radiation into free space, the velocity of propagation being that of light; it must therefore include a factor $e^{-j\beta r}$. The power flow per unit solid angle is independent of r (no power is absorbed by the medium) so that $H_\phi \propto (1/r)$. Since we must also satisfy Equation (1.1) when $\omega = 0$, let us try a solution of the form

$$\Psi = M\left(\frac{N}{r} + \frac{1}{r^2}\right)e^{j(\omega t - \beta r)} \qquad (1.13)$$

where M, N are expected to be constants. Substituting for Ψ we find that Equation (1.12) is satisfied providing $N = j\beta$. There is one other independent solution of the second-order differential Equation (1.12); it is found by changing the sign of β in Equation (1.13), but is inadmissible in our case as it does not represent an outward-travelling wave. Since $N = 0$ when $\omega = 0$, we can satisfy Equation (1.1) by putting $M = (I\delta z/4\pi)$. Our suggested solution for Ψ is therefore justified. Substituting for Ψ in Equations (1.8)-(1.10)

$$H_\phi = \frac{I\delta z\sin\theta}{4\pi}\left(\frac{j\beta}{r} + \frac{1}{r^2}\right)e^{j(\omega t - \beta r)} \qquad (1.14)$$

$$E_r = 60I\delta z\cos\theta\left(\frac{1}{r^2} - \frac{j}{\beta r^3}\right)e^{j(\omega t - \beta r)} \qquad (1.15)$$

$$E_\theta = 30I\delta z\sin\theta\left(\frac{j\beta}{r} + \frac{1}{r^2} - \frac{j}{\beta r^3}\right)e^{j(\omega t - \beta r)} \qquad (1.16)$$

Equations (1.14)-(1.16) give the components of magnetic and electric force at a distance r from a doublet of length δz carrying a current $Ie^{j\omega t}$. The components proportional to $1/r$, $1/r^2$ and $1/r^3$ are sometimes called the radiation, induction and electrostatic fields respectively. The induction and electrostatic fields fall off rapidly with distance from the doublet, and are small compared with the radiation field for $r > \lambda$.

When $r >> \lambda$ Equations (1.14)-(1.16) reduce to

$$H_\phi = \frac{jI\delta z\beta \sin\theta}{4\pi r} e^{j(\omega t - \beta r)} \tag{1.17}$$

$$\frac{E_r}{E_\theta} \rightarrow 0 \text{ as } r \rightarrow \infty \tag{1.18}$$

$$E_\theta = \frac{j30I\delta z\beta \sin\theta}{r} e^{j(\omega t - \beta r)} \tag{1.19}$$

In other words, when $r >> \lambda$ the only field components are H_ϕ and E_θ; they are perpendicular in space and in phase in time, and their directions are shown in Fig. 1.3(b). The ratio $\eta = (E_\theta/H_\phi)$ is defined as the wave impedance of the medium; for free space, from Equations (1.17) and (1.19) we have

$$\eta_0 = 120\pi \approx 377 \text{ ohms} \tag{1.20}$$

The current in the doublet and the associated fields are both manifestations of the radiation of electromagnetic waves. The current satisfies the boundary condition required by the existence of the field, and it is immaterial which we regard as the "cause", and which as the "effect". It is often convenient to regard the current as the "cause" and then to calculate the field from the current. This is because we either know (or assume) the current distribution in a transmitting aerial; we can then regard it as equivalent to a large number of doublets placed end to end, each carrying the appropriate current. By summing the contributions from individual doublets the field due to the complete aerial can be calculated.

So far we have taken r to be large compared with δz, which in turn is large compared with the radius of the doublet. But since the radius is assumed to be vanishingly small we can make r as small as we please in calculating the field associated with a complete aerial.

1.3. The Image of a Current Element over a Perfectly-Conducting Plane

In some aerial problems it is permissible to regard the ground as virtually perfectly conducting, and in these cases the concept of "images" is helpful.

In electrostatics it is convenient to consider the effect of a perfectly-conducting infinite plane in the presence of a charge $+q$, Fig. 1.4(a), as being equivalent to a charge $-q$ placed at the image point. There is a corresponding equivalence for current elements; for instance, the image of a *vertical* current element is an equal *positive* current element, Fig. 1.4(b), while the image of a *horizontal* current element is an equal *negative* current element, Fig. 1.4(c). For these arrangements, from considerations of symmetry we see that there is no component of tangential electric force at the surface of the plane, and its presence does not therefore affect the field. However, the space above the plane is screened from the image; insofar as the field above the plane is concerned, it therefore follows that the plane is equivalent in its effect to an image source.

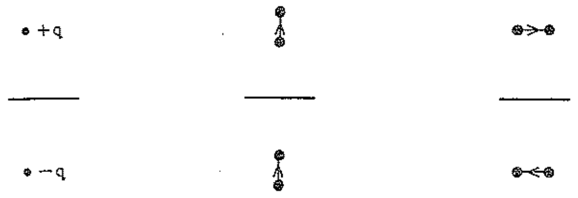

Fig. 1.4 - Images of charges and current elements over a perfectly-conducting plane

(a) Image of fixed charge

(b) Image of vertical current element

(c) Image of horizontal current element

2. LOW- AND MEDIUM-FREQUENCY AERIALS

The low- and medium-frequency bands cover 30–300 kc/s and 300 kc/s–3 Mc/s respectively. They are used mainly for local broadcasting services, radio-navigation, and communication systems which entail transmission along (or nearly along) the ground. Since the ground is virtually perfectly-conducting at these relatively low frequencies, vertical aerials are used in order to achieve the maximum field for a given power in the required directions. If uniform radiation in all horizontal directions is required, a single vertical wire or mast is employed; two or more such radiators are used for a directional system, the spacing between them and the relative amplitude and phase of the currents supplied to the individual aerials being arranged to give the required radiation pattern.

2.1. The Radiation Characteristics of the Idealised Vertical Aerial

There is as yet no rigorous solution to what at first sight appears a simple problem - the radiation from a vertical cylindrical aerial energised at the base. Unfortunately the current distribution along the aerial cannot be calculated exactly; some approximate solutions have been obtained and three of these are discussed in Section 2.2.2. In practical cases the radiation characteristics are often calculated making the assumption that the current distribution is the sinusoidal standing-wave pattern we should get on an open-circuited coaxial transmission line of the same length as the aerial, along which a wave is propagated with the velocity of light; for brevity this will be called a "sinusoidal" current distribution. Although the aerial radiates, whereas the transmission line does not, the two current distributions do not differ appreciably; in fact the aerial current tends to a sinusoidal distribution for the limiting case of an infinitesimally thin filament (see footnote on p. 24).

Another assumption which is often made in calculating the performance of aerials in the low- and medium-frequency bands is that the ground behaves as a perfectly-conducting plane surface. These two assumptions considerably simplify the mathematical analysis, and enable us to learn a great deal about the radiation characteristics of vertical aerials. We will therefore treat this idealised case first; but later we will consider the effect of both assumptions on the radiation characteristics, and obtain a closer approximation to the practical case.

2.1.1. The Vertical Radiation Pattern

Fig. 2.1 shows the vertical aerial of height h, energised at the base. The peak value of the current at the maximum of the sinusoidal distribution will be designated I. The effect of the perfectly-conducting ground plane is equivalent to the image current shown dotted. At a point height z above ground level, the current may be written

$$I_z = I\sin(\beta\overline{h-z})e^{j\omega t}$$

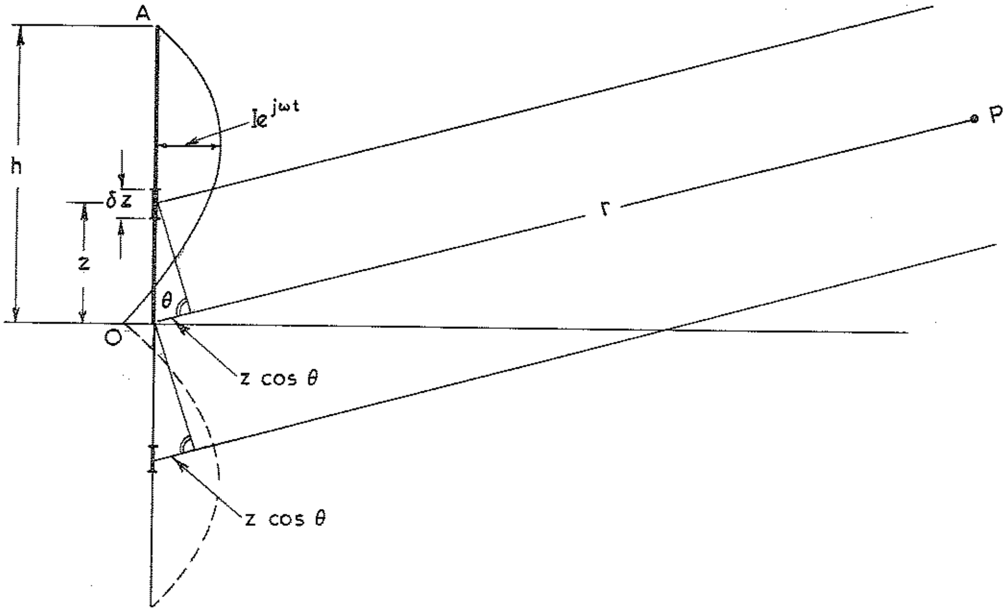

Fig. 2.1 - Vertical aerial radiating over perfectly-conducting ground

We will calculate the electric force at a point P distance r from O, OP being at an angle θ to the vertical; r is assumed to be so large compared with h and λ that lines joining any point on the aerial to P may be considered parallel. From Section 1.2 it follows that the only component of electric force at P is E_θ, in a direction perpendicular to OP. The contributions to the electric force at P due to the element δz and its image are substantially equal in magnitude; but they differ in phase because of the difference in the path lengths to the point P. Relative to an element at O, the contribution from the element δz leads and that from the image lags by an angle $\beta z\cos\theta$. It follows from Equation (1.19) that the combined contribution from these two elements is

$$\frac{j30I\sin(\beta\overline{h-z})\beta\sin\theta}{r}\left\{e^{j(\omega t-\beta\overline{r-z\cos\theta})}+e^{j(\omega t-\beta\overline{r+z\cos\theta})}\right\}\delta z$$

$$=\frac{j60I\beta\sin\theta\; e^{j(\omega t-\beta r)}}{r}\sin(\beta\overline{h-z})\cos(\beta z\cos\theta)\delta z$$

Since the phase of the current is the same at all points on the aerial the total electric force at P is

$$\frac{j60I\beta\sin\theta\ e^{j(\omega t-\beta r)}}{r}\int_0^h \sin(\beta\overline{h-z})\cos(\beta z\cos\theta)dz$$

$$= \frac{j60I}{r\sin\theta}\{\cos(\beta h\cos\theta)-\cos(\beta h)\}e^{j(\omega t-\beta r)}$$

The phase of the electric force is therefore the same as for a doublet at the base of the aerial carrying a current in phase with the aerial current. If we call the r.m.s. value of the current at the maximum of the sinusoidal distribution (often called the loop current) I_L, the r.m.s. value of the electric force is given by

$$E_\theta = \frac{60I_L}{r\sin\theta}\{\cos(\beta h\cos\theta)-\cos(\beta h)\} \qquad (2.1)$$

In this and other cases where the exponential time term is omitted r.m.s. values are implied.

Equation (2.1) applies strictly to a cylindrical aerial whose radius is vanishingly small; but it clearly applies also to the case of an aerial whose radius is small compared with the wavelength. The electric force, E_θ, is the field component measured in most practical cases, and is usually referred to as the field strength.

(a) $h = 0.25\lambda$
(b) $h = 0.50\lambda$
(c) $h = 0.55\lambda$
(d) $h = 0.60\lambda$

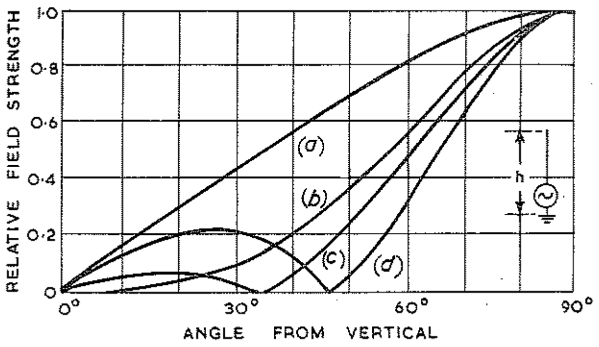

Fig. 2.2 - Vertical radiation patterns of vertical aerials, assuming perfectly-conducting ground and a sinusoidal standing-wave current distribution

The vertical radiation patterns for aerials of different heights are shown in Fig. 2.2, the curves being normalised to have the same value at $\theta = 90°$. For heights short compared with the wavelength the field strength is proportional to $\sin\theta$. The shape of the pattern remains substantially the same for heights up to $0{\cdot}25\lambda$, but as h increases further the radiation at small angles to the vertical decreases rapidly.

For heights greater than $0{\cdot}5\lambda$ a zero appears in the pattern at an angle to the vertical which increases with aerial height. The aerial may be thought of as approximately equivalent to a doublet at the same height as that of the loop current; as the height increases the distance between this doublet and its image increases, and when the spacing exceeds half a wavelength cancellation of the two contributions can occur. To cause the vertical radiation pattern of any aerial to differ significantly from that of a doublet it is necessary to "spread-out" the system over a distance of at least half a wavelength. In theory there are exceptions to this rule (see Section 3.1) but they are of no practical significance. The "spreading" may occur along a line, as in the case considered, over a surface, or throughout a volume.

The method we have used for calculating the radiation pattern can be applied to any aerial system comprising radiating wires, providing the current distribution is known. The field is calculated by summing the contributions associated with the component doublets, the integration being carried out either mathematically or graphically.

The shape of the vertical radiation pattern is an important factor in the design of transmitting aerials for broadcasting on low and medium frequencies; here the aim is to minimise the effect of the fading which occurs when two or more signals are received, one propagated along the ground (the ground wave) and the others reflected from the ionosphere (the reflected waves). Both the amplitude and phase of a reflected wave may change due to variations in the ionosphere, so that the resultant signal at the receiver waxes and wanes. The fading is often accompanied by distortion of the transmitted programme, and is particularly severe if the carrier amplitude falls to a low level leaving effectively enhanced sidebands.

In Fig. 2.3 the received field strength is plotted as a function of distance from the transmitter, for the ground wave and for a single-hop reflected wave; perfect reflection at an ionospheric layer taken to be 110 km high is assumed. The ground-wave field strength takes into account the attenuation introduced by the imperfectly-conducting ground, which cannot be neglected even at low frequencies if the distances involved are long. The strength of the reflected wave, on the other hand, can be calculated on the basis of the curves shown in Fig. 2.2 since it is not attenuated by the atmosphere.

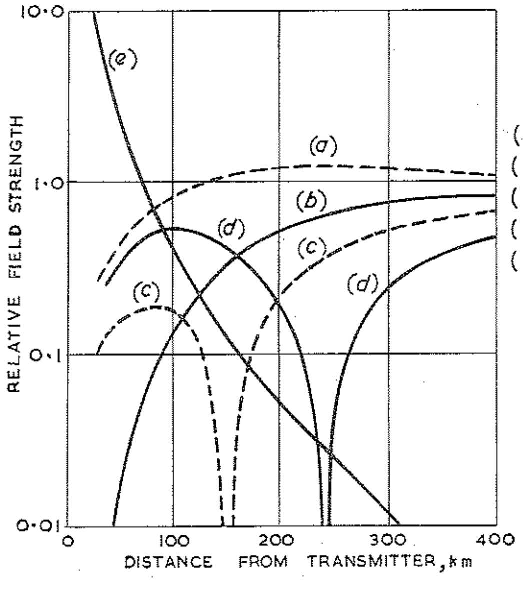

(a) h = 0.25λ
(b) h = 0.50λ
(c) h = 0.55λ
(d) h = 0.60λ
Reflected-wave field strength assuming perfectly-conducting ground, perfectly-reflecting ionosphere and a sinusoidal aerial-current distribution.
(e) Ground-wave field strength for a conductivity of 10^{-2} mho/m and a frequency of 1 Mc/s

Fig. 2.3 - Ground-wave and reflected-wave field strength curves corresponding to the vertical radiation patterns shown in Fig. 2.2

For any given aerial height there is a distance for which the ground and reflected waves are comparable, so that severe fading is then possible. Since the ground wave is decreasing rapidly with distance from the transmitter and the reflected wave is increasing, reception conditions deteriorate very rapidly beyond this point.

We do not however change over from a predominantly ground-wave service to a predominantly reflected-wave service, since the amplitude and phase of the reflected wave are very dependent on ionospheric conditions. Rather we change from a region of slight fading to one of intense fading. Subjective tests show that perceptible distortion of the programme occurs when the reflected wave exceeds one quarter of the ground wave; the measured median reflection coefficient of the ionosphere is also about one quarter. It follows that we can regard the range at which the ground wave is equal to the reflected wave (calculated assuming a perfectly-reflecting ionosphere, as in Fig. 2.3) as determining the limit of the useful service area.

It will be seen from Fig. 2.3 that there is an aerial height giving the maximum service area, this optimum height depending on the attenuation of the ground wave; such an aerial is often described as having "antifading" characteristics. If the attenuation is high (due, for example, to low ground conductivity or the use of a high frequency or both) the ground wave falls off rapidly with distance from the transmitting aerial. This entails using a reduced aerial height and accepting a smaller service area. On the other hand, if the attenuation is low a greater aerial height is permissible and a larger service area is achieved.

Table 1 shows typical values of optimum aerial heights, the corresponding value of θ_0 (the angle from the vertical of the zero in the vertical radiation pattern) and the radius of the service area. The two values of ground conductivity, σ, correspond to the extremes likely to be encountered in practice. It is necessary to emphasise here that in calculating the vertical radiation pattern we have considerably simplified the picture, by assuming a sinusoidal aerial-current distribution and perfectly-conducting ground. We have taken the imperfect conductivity of the ground into account only in calculating the ground wave. As we shall see in Section 2.2.3 it is possible to approach these idealised conditions in practice; Table 1 may therefore be taken as realistic.

TABLE 1

Optimum Aerial-Height and Service-Area Radius

f	λ	$\sigma = 10^{-2}$ mho/m			$\sigma = 10^{-3}$ mho/m		
		Optimum aerial-height	θ_0	Service-area radius	Optimum aerial-height	θ_0	Service-area radius
200 kc/s	1500 m	$0{\cdot}60\lambda$	48°	350 km	$0{\cdot}53\lambda$	27°	180 km
500 kc/s	600 m	$0{\cdot}58\lambda$	44°	250 km	$0{\cdot}50\lambda$	0°	80 km
1000 kc/s	300 m	$0{\cdot}54\lambda$	32°	160 km	$0{\cdot}50\lambda$	0°	50 km
1500 kc/s	200 m	$0{\cdot}51\lambda$	16°	100 km	$0{\cdot}50\lambda$	0°	40 km

In the low-frequency band masts of the optimum height (approximately 3000 ft) introduce prohibitive engineering difficulties and are never used. Even in the medium-frequency band masts of the height required are expensive, and it is desirable to use the minimum height giving the required antifading characteristics.

In one arrangement, shown in Fig. 2.4(a), a "top" is added to the aerial, and constitutes a capacitance into which current can flow. The current distribution is a portion of a sinusoid, as shown in Fig. 2.4(b). In the case of a mast radiator the "top" usually takes the form of a metallic disc, in order to achieve the required capacitance with a structure of relatively small dimensions. This is a convenient mechanical arrangement, and at the same time means that the radiation from the "top" is negligible. On the other hand, for a wire aerial it is convenient to make the aerial in the form of a T or inverted L, and if the "top" is extensive the radiation from it may not be negligible.

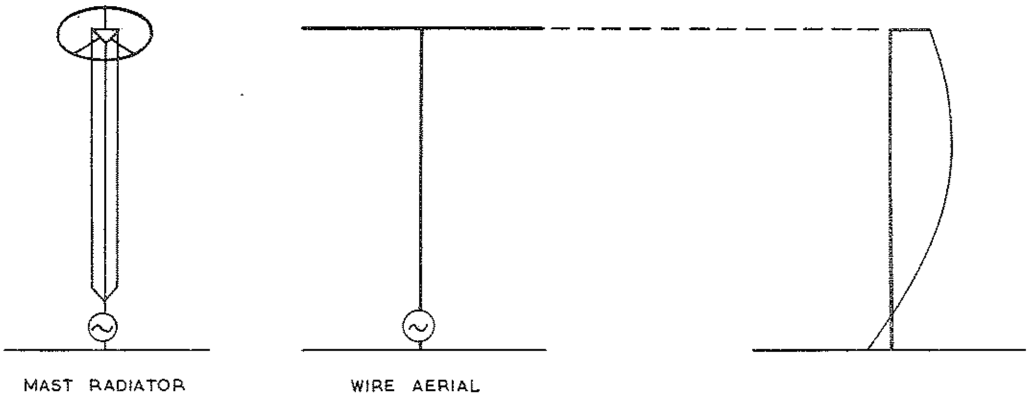

(a) Mechanical arrangement (b) Aerial current distribution

Fig. 2.4 - Aerial with capacitance top

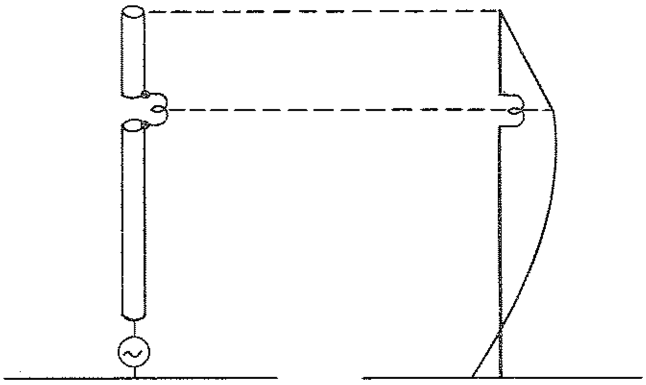

(a) Mechanical arrangement (b) Aerial current distribution

Fig. 2.5 - Series-loaded aerial

Another arrangement used for mast radiators is shown in Fig. 2.5(a). One section of the mast is insulated from the other, a reactance being connected across the gap; this is sometimes described as series loading. The current distribution, shown in Fig. 2.5(b), takes the form of portions of two sinusoidal distributions. A combination of a capacitance "top" and series loading can also be used. The radiation patterns for any of these arrangements can be calculated, making the assumption that the aerial current distribution is the same as for the corresponding dissipationless transmission line. Since both methods raise the height of the current maximum, the effective height of the mast is increased; in practice increases of 10%-20% can be achieve by these means.

The arrangement we have discussed here, a single vertical aerial between 0·5λ and 0·6λ high energised at the base, is only one method of obtaining antifading characteristics. However, it is the only method in common use, because it is both convenient and not unduly expensive. It is possible to use instead a number of aerials in ring formation, or a number of aerials on the same vertical axis. Both arrangements give uniform radiation in all horizontal directions and can be designed to have antifading characteristics.

2.1.2. Calculation of the Radiated Power

Two methods have been developed for calculating the radiated power, the "Poynting-vector method" and the "Induced-EMF method"; as both are instructive we will apply them in turn to the case of the idealised vertical aerial radiating into free space.

(i) The Poynting-vector method

The aerial is assumed to be at the centre of a sphere having a radius large compared with the wavelength; the power radiated is then found by integrating the power flow per unit area over the spherical surface. For an aerial over perfectly-conducting ground (Fig. 2.6), as no power flows through the ground plane we need to integrate only over the hemispherical surface.

We have seen in Section 1.2 that, at a distance from the aerial large compared with the wavelength, the only field components, E_θ and H_ϕ, are in phase; from Equation (1.20) we have $(E_\theta/H_\phi) = 120\pi$. It follows that the corresponding power flow per unit area is in the direction of the radius vector r, and equal to $|E_\theta^2|/120\pi$, where E_θ is the r.m.s. value of the electric force. Consider a narrow strip on the hemisphere bounded by radii at angles of θ and $(\theta + \delta\theta)$ to the vertical;

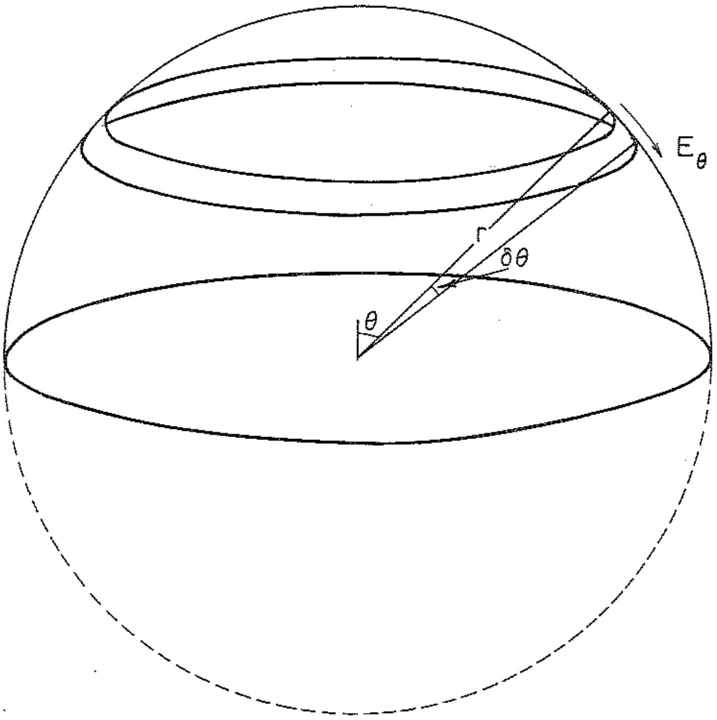

Fig. 2.6 - Calculation of radiated power by the Poynting-vector method

since the area of the strip is $2\pi r^2 \sin\theta\,\delta\theta$ the power flowing through it is $(|E_\theta|^2/60)r^2 \sin\theta\,\delta\theta$. Substituting for E_θ from Equation (2.1) the radiated power, P, is given by

$$P = 60 I_L^2 \int_0^{\pi/2} \frac{\{\cos(\beta h \cos\theta) - \cos(\beta h)\}^2}{\sin\theta}\, d\theta$$

We can write
$$\int_0^{\pi/2} \frac{\{\cos(\beta h \cos\theta) - \cos(\beta h)\}^2}{\sin\theta}\, d\theta$$

$$= \int_0^{1} \frac{\{\cos(\beta h v) - \cos(\beta h)\}^2}{(1-v^2)}\, dv$$

where $v = \cos\theta$

$$= \frac{1}{2}\int_0^{1} \{\cos(\beta h v) - \cos(\beta h)\}^2 \left\{\frac{1}{(1+v)} + \frac{1}{(1-v)}\right\} dv$$

Changing the sign of the variable in the last term of the integral, and remembering that $\cos(\beta h v) = \cos(-\beta h v)$, we have

$$P = \frac{1}{2}\int_{-1}^{1} \frac{\{\cos(\beta h v) - \cos(\beta h)\}^2}{(1+v)}\, dv$$

Writing $u = (1+v)$, after simplification we obtain

$$P = 15 I_L^2\{\sin(2\beta h)Si(4\beta h) - 2\sin(2\beta h)Si(2\beta h) - \\ - \cos(2\beta h)Ki(4\beta h) + 4\cos^2(\beta h)Ki(2\beta h)\} \tag{2.2}$$

where
$$Si(x) = \int_0^x \frac{\sin u}{u}\, du \tag{2.3}$$

usually called the "sine integral", and

$$Ki(x) = \int_0^x \frac{(1-\cos u)}{u}\, du = \gamma + \log(x) - Ci(x) \tag{2.4}$$

γ is Euler's constant, 0·5772, and

$$Ci(x) = \int_\infty^x \frac{\cos u}{u}\, du \tag{2.5}$$

usually called the "cosine integral".

(ii) The Induced-EMF method

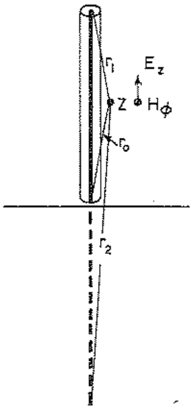

Fig. 2.7 - Calculation of radiated power by the Induced-EMF method

Suppose next the aerial is surrounded by a closely-fitting cylinder, as shown in Fig. 2.7. The power flow per unit area normal to the surface of the cylinder is $-\text{Re}(E_z H_\phi^*)$, where E_z is the z-component of the electric force and H_ϕ^* is the conjugate of the ϕ component of the magnetic force at the point Z; the minus sign arises from the conventions we have used for defining the directions of E_z and H_ϕ. The *outward* power flow per unit length of the cylinder is therefore $-\text{Re}(E_z I_z^*)$, since I_z, the current flowing at the point Z, is the line integral of the magnetic force round the cylinder at the point Z. The total outward power flow through the cylindrical surface is therefore

$$-\text{Re} \, . \int_0^h E_z I_z dz$$

The conjugate sign can be omitted since we will take I_z as the phase reference. Using Equations (1.15) and (1.16) we can resolve the E_r and E_θ field components for a doublet to find the E_z component, and then integrate to take account of the complete aerial and its image. The result is shown in Section 7.1 to be

$$E_z = j30I_L \left\{ 2\cos(\beta h) \frac{e^{-j\beta r_0}}{r_0} - \frac{e^{-j\beta r_1}}{r_1} - \frac{e^{-j\beta r_2}}{r_2} \right\} \qquad (2.6)$$

where r_0, r_1 and r_2 are respectively the distances to the base and the extremities of the aerial and its image, as shown in Fig. 2.7. We see that $-\text{Re}(E_z I_z)$ is finite at the top and bottom of the aerial, so that there is no power flow through the infinitesimally small end caps of the cylinder.

The *total* outward power flow from the aerial, P, is therefore given by

$$P = -30I_L^2 \, \text{Im} \, . \int_0^h \left\{ 2\cos(\beta h) \frac{e^{-j\beta r_0}}{r_0} - \frac{e^{-j\beta r_1}}{r_1} - \frac{e^{-j\beta r_2}}{r_2} \right\} \sin(\beta \overline{h-z}) \, dz$$

The result is shown in Section 7.2 to be the same as that given by the Poynting-vector method.

This method, as so far described, is similar to the Poynting-vector method but with a closely-fitting cylinder replacing the hemispherical surface. There is another way of looking at this method which is instructive. Equation (2.6) gives E_z at any point, and can be used to find the value at the surface of the aerial; the result for an aerial of finite radius is given in Section 7.1. But since we assume the aerial to be perfectly-conducting there cannot be a tangential component of electric force at the surface, and the only way to satisfy the boundary condition is to postulate generators spaced at intervals along the aerial. Generators of voltage $-E_z \delta z$ spaced δz apart maintain an electric force E_z (the electric force is *minus* the potential gradient). These are the generators, therefore, which are required to maintain the assumed sinusoidal current distribution and the power supplied by them,

$$-\mathrm{Re}\,.\int_0^h E_z I_z dz$$

is equal to the radiated power.*

It follows that if, after assuming the current distribution on an aerial, we calculate the resulting tangential electric force at the surface, E_z, either:

(i) there are distributed generators of voltage $-E_z\delta z$ spaced at intervals δz along the aerial, and these generators maintain the assumed current distribution exactly, or

(ii) if it is known that the system of generators described in (i) above does not exist, the assumed current distribution is incorrect; the current will deviate from the assumed distribution to such an extent as to make E_z zero at all points along the aerial.

Fig. 2.8 shows the calculated value of E_z for an aerial carrying a sinusoidal current distribution. It applies to a mast 0·55λ high, radius 0·0025λ, but is typical of other cases. Re . E_z is the component in phase with the aerial current and Im . E_z is the component in phase quadrature with the aerial current. We see that a complicated system of generators would be required to maintain the assumed distribution.

If the aerial were energised at the base E_z would be zero along the aerial, with sudden discontinuities at the top and at the base, where the aerial terminates; if the gap across which the generator is connected were infinitesimal, E_z would be infinite at the base. E_z for the base-energised aerial is shown dotted in Fig. 2.8;

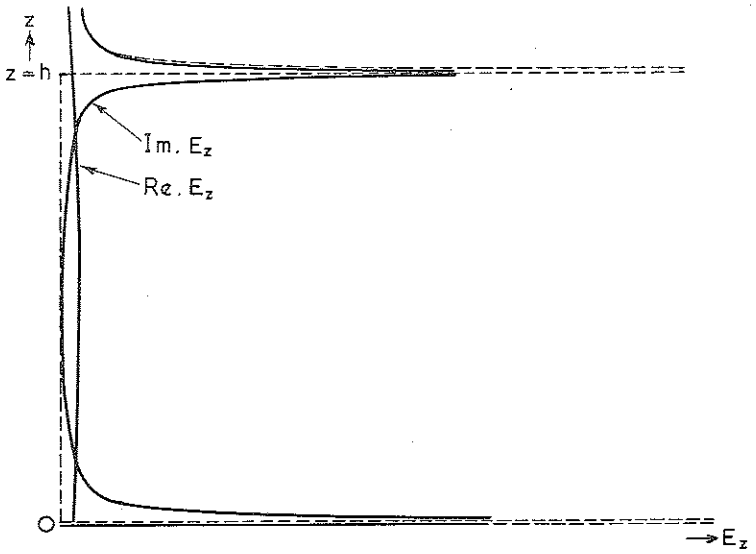

Fig. 2.8 - E_z as a function of z for a vertical aerial, height 0·55λ, radius 0·0025λ

it is very nearly the same as that for the aerial carrying a sinusoidal current. A relatively small change in the current distribution is therefore sufficient to change the full-line curves in Fig. 2.8 to the dotted curve. Since E_z at a given point is determined mainly by the current flowing *at* the point, in the case of a base-energised aerial we conclude that the deviations from a sinusoidal distribution occur mainly near the top and bottom. Moreover, it follows from Section 7.1 that the thinner the aerial the more steeply does $\mathrm{Im}\,.\,E_z$ increase at the extremities, and hence the more closely do the full-line curves approach the dotted curve; in other words, the closer does the current distribution approach a sinusoid.

---

*The originator of the title by which this method is known regarded any element of the circuit as subject to an EMF induced by the remainder of the circuit; the radiation from that element was given by the real part of the product of the induced EMF and the current.

Since E_z is zero along an aerial energised at the base, it is sometimes stated that in the induced-EMF method a "non-existent" quantity is integrated to give the radiated power; this is referred to as the "radiation paradox". But we must expect anomalies if an incorrect assumption is made, for instance that the current distribution is *exactly* sinusoidal for a base-energised aerial. In calculating the radiated power by the induced-EMF method we are not integrating a "non-existent" quantity, but quite correctly calculating the power flowing from the only sources consistent with a sinusoidal current distribution - the distributed generators. The result also applies *approximately* if the current distribution is *approximately* sinusoidal, as is the case for a relatively thin base-fed aerial.

2.1.3. The Radiation Resistance

The power radiated by the aerial can be expressed as in Equation (2.2) or in the form

$$P = I^2 R \qquad (2.7)$$

where I is the current at the input terminals. R is defined as the resistance by which the square of the input current must be multiplied to give the radiated power, and is described as the "radiation resistance referred to the input current". R is therefore the resistive component of the input impedance of the aerial.

It is often convenient to regard the input terminals as being at the current loop. It follows from Equations (2.2) and (2.7) that R_L, the radiation resistance referred to the loop current (or the loop radiation resistance) is given by

$$R_L = 15\{\sin(2\beta h)Si(4\beta h) - 2\sin(2\beta h)Si(2\beta h) - $$

$$- \cos(2\beta h)Ki(4\beta h) + 4\cos^2(\beta h)Ki(2\beta h)\} \qquad (2.8)$$

The functions $Si(x)$ and $Ki(x)$ are defined by Equations (2.3) and (2.4), and are well tabulated;[1, 2] they are plotted in Fig. 2.9. Sometimes the value of $Ci(x)$ rather than $Ki(x)$ is tabulated; Equation (2.4) gives the relationship between these two functions. Fig. 2.10 shows R_L as a function of the aerial height, h.

If the input terminals are not at the current loop the radiation resistance referred to the input current can be derived in terms of R_L; we merely equate the radiated power expressed in terms of the loop current to that expressed in terms of the input current. For a sinusoidal current distribution the radiation resistance referred to the input (or base) current is $R_L\,\mathrm{cosec}^2(\beta h)$. However, a word of warning is necessary in applying this result for the *idealised* aerial to the *practical* aerial.

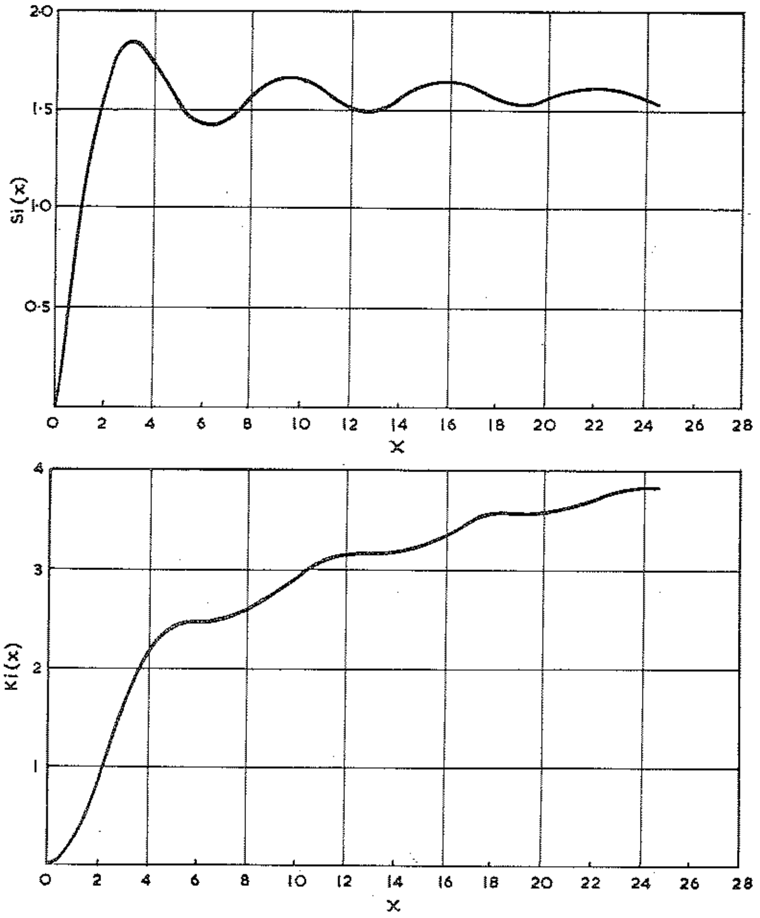

Fig. 2.9 - $Si(x)$ and $Ki(x)$ functions

If the current distribution does not conform precisely to a sinusoidal standing-wave pattern there are two difficulties. First, our calculation of the radiated power is in error; second, the assumed relationship between the input and loop currents is not correct. As we shall see later, in practice the deviations of the current distribution from the assumed sinusoid are relatively small, and important only in the vicinity of the current node. It follows that the power calculated in terms of the loop current, and hence R_L, are approximately correct. On the other hand, the value of the radiation resistance referred to the input current may be greatly in error when h is approximately $0{\cdot}5\lambda$, since in practice the ratio between the input and loop currents departs substantially from the ratio for a sinusoid. Equation (2.8) therefore gives a close approximation to R_L; it can also be used to give a reasonably good approximation to the input resistance, except for a range of values of h in the neighbourhood of $0{\cdot}5\lambda$. A method which is not subject to this restriction is given in Section 2.2.4. It is therefore preferable to work always in terms of the loop radiation resistance, using the method given in Section 2.2.4 to obtain the input impedance of the aerial.

Let us consider next some practical cases.

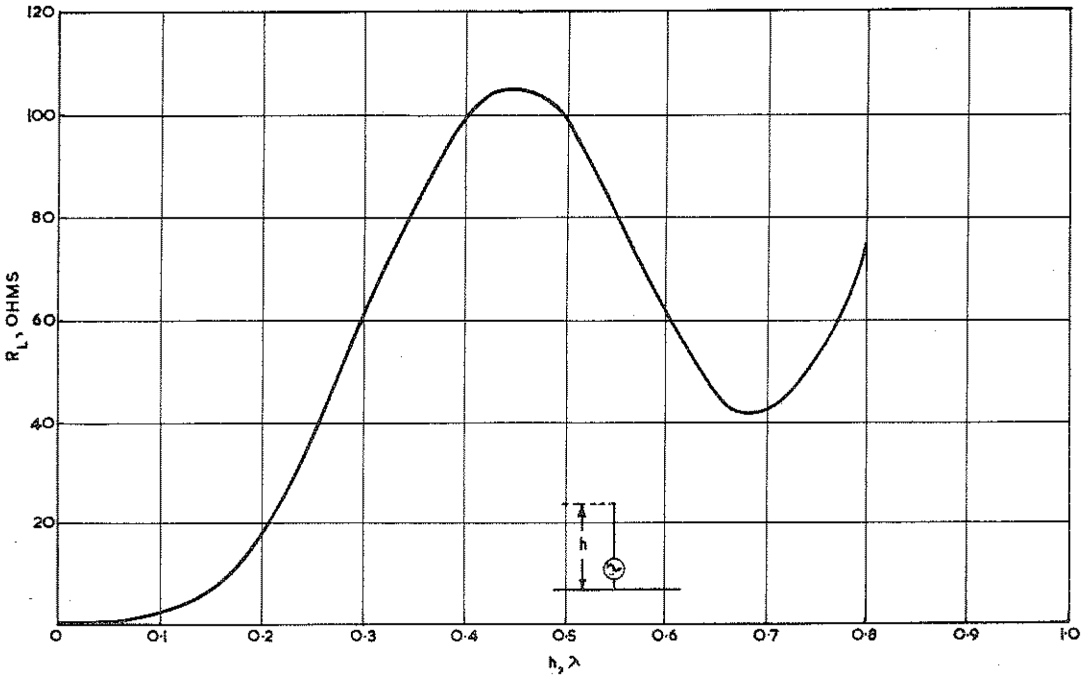

Fig. 2.10 - Radiation resistance of aerial referred to loop current

Example 1: $h = 0{\cdot}25\lambda$

$R_L = 36{\cdot}56$ ohms

I_L for a radiated power of 100 kW is 52·2 amps

It follows that, for an aerial 0·5λ long in free space, $R_L = 73{\cdot}1$ ohms.

Example 2: $h = 0{\cdot}5\lambda$

$R_L = 100$ ohms

I_L for a radiated power of 100 kW is 31·6 amps

The effect of the perfectly-conducting ground is to increase R_L from the free-space value of 73·1 ohms to 100 ohms.

Example 3: $h = 0{\cdot}125\lambda$

$R_L = 3{\cdot}4$ ohms

The base resistance is $3{\cdot}4 \operatorname{cosec}^2(\pi/4) = 6{\cdot}8$ ohms

The base current for a radiated power of 100 kW is 116 amps.

So far we have considered only simple vertical aerials. If an antifading aerial has a capacitance top or series loading the loop radiation resistance is less than that for a simple aerial having the same vertical radiation pattern; the value can be calculated using one of the methods described in Section 2.1.2. On the other hand, a capacitance top is often added to a low aerial with the object of increasing the radiation resistance. In this case a large top changes the current distribution on the vertical portion of the aerial from linear to substantially constant, thus approximately quadrupling the radiation resistance.

The value of the radiation resistance of a doublet in free space is of theoretical interest. A doublet can be regarded as the limiting case of a very short aerial together with its image; the equivalent current in the doublet is the mean of the linear distribution in each half of the short aerial. However, it is simpler to calculate the radiation resistance direct from Equation (1.19). We imagine the doublet, of length δz carrying a r.m.s. current I, to be at the centre of the sphere in Fig. 2.6. Integrating over the surface we obtain

$$P = \int_0^{\pi} \frac{1}{120\pi}\left(\frac{30I\delta z\beta\sin\theta}{r}\right)^2 2\pi r^2 \sin\theta\, d\theta = 30\beta^2 I^2 \delta z^2 \int_0^{\pi/2} \sin^3\theta\, d\theta = 20\beta^2 I^2 \delta z^2$$

The radiation resistance of the doublet, R_d, is therefore given by

$$R_d = 20\beta^2\delta z^2 \qquad (2.9)$$

2.1.4. Ground-Wave Field Strength

The ground-wave field strength, E_g, is given by putting $\theta = 90°$ in Equation (2.1); combining this with Equation (2.7) we obtain

$$\frac{E_g r}{\sqrt{P}} = \frac{60}{\sqrt{R_L}}\{1-\cos(\beta h)\} \qquad (2.10)$$

In other words, the product of E_g and r divided by the square root of the power is a constant for a given aerial; the greater the concentration of energy along the ground the larger the value of $E_g r/\sqrt{P}$. This parameter, which is shown in Fig. 2.11, can therefore be regarded as a figure of merit for comparing the ground-wave field strengths for different aerials. For a short aerial, for example, the value of $E_g r/\sqrt{P}$ is 9·5; the field strength at, say, 1 km from the aerial over flat perfectly-conducting ground is therefore 9·5 millivolts per metre (mV/m) for a radiated power of 1 watt, or 300 mV/m for a radiated power of 1 kilowatt. The value of $E_g r/\sqrt{P}$ increases from 9·5 at low values of h to a maximum of 14 at $h = 0{\cdot}63\lambda$ and thereafter decreases rapidly. This is the type of curve we would expect from consideration of the vertical radiation patterns shown in Fig. 2.2. As the aerial height increases the reduction in radiation upwards, compared with that along the ground, necessarily implies an increase in the ground-wave field strength for a given power. $E_g r/\sqrt{P}$ eventually decreases on account of the radiated power associated with the large subsidiary lobe.

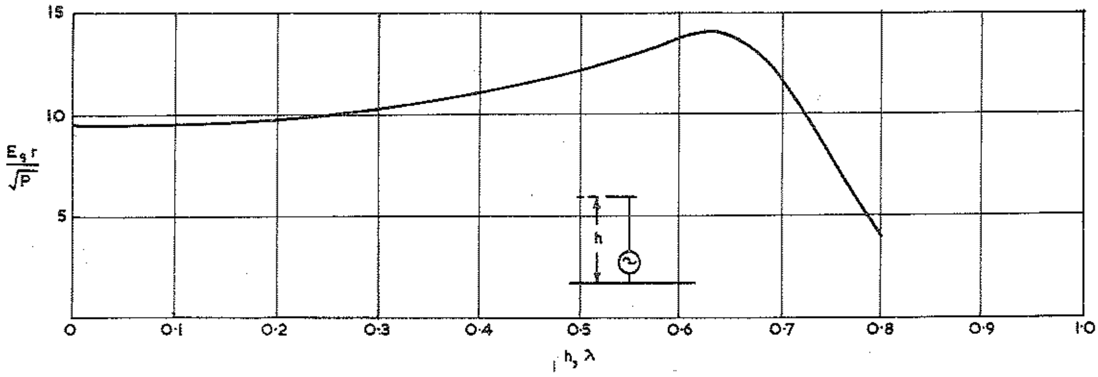

Fig. 2.11 - $E_g r/\sqrt{P}$ for a vertical aerial, height h

Looking next at that part of the diagram corresponding to small values of h we see that $E_g r/\sqrt{P}$ is substantially independent of h. We might conclude from this that, if the vertical radiation pattern meets the requirements, a very short aerial has no technical disadvantages, and has the merit of cheapness. This would be true only if our assumption of perfectly-conducting ground were correct, and if there were no disadvantages associated with the very high base current and the correspondingly high base voltage. In practice, if a very short aerial is used a substantial fraction of the power may be lost in the ground, in tuning coils and in aerial insulators; the fraction lost in this way increases as the aerial height is reduced. A compromise must therefore be sought between performance and cost.

The above considerations lead us to divide our aerial requirements in the low and medium-frequency bands into two main classes:

(i) The first class includes those cases for which a sinusoidal vertical radiation pattern is acceptable, and where the cost of a high aerial merely to achieve a higher ground-wave field strength is not warranted. The aerial height is chosen to be a compromise between overall cost and loss of power in the ground and matching circuit. For transmission the aerials are usually between $0{\cdot}1\lambda$ and $0{\cdot}25\lambda$ high, and are often provided with capacitance tops. For reception very short (and hence very inefficient) aerials are usually used.

(ii) The second class comprises those transmitting aerials for broadcasting which are required to give the maximum service area. The aerial height is between $0{\cdot}5\lambda$ and $0{\cdot}6\lambda$; the size of the capacitance top or the amount of series loading, if used, would be such as not to reduce the loop radiation resistance unduly - a value not less than about 30 ohms is aimed at in practice.

2.2. The Radiation Characteristics of the Practical Vertical Aerial

In dealing with the idealised aerial in Section 2.1 we assumed that the ground is perfectly conducting, and also that the aerial current distribution is a sinusoidal standing-wave pattern. We will next examine the effect of departures from these idealised conditions.

2.2.1. The Effect of Imperfectly-Conducting Ground on the Vertical Radiation Pattern

In analysing the radiation from an aerial over imperfectly-conducting ground it is convenient to take the expression for the field and to regard it as the sum of three components:

(i) the direct wave, i.e. the wave received in the absence of the ground,

(ii) the ground-reflected wave, i.e. the direct wave multiplied by the reflection coefficient of the ground for a plane wave of the appropriate polarisation and angle of incidence, delayed in time relative to component (i) as a result of the greater path length, and

(iii) the surface wave.

We will group the first two components together and call the sum the *space-wave*. Since the reflection coefficient for both vertically- and horizontally-polarised plane waves is -1 at grazing incidence (i.e. along the surface of the ground) the space wave is zero at the surface; the only field component here is the surface wave. The space wave predominates elsewhere, except over a small region just above the surface of the ground, where the space and surface waves are comparable.

In the case of imperfectly-conducting ground it is convenient to regard the total field as comprising the space-wave (the sum of the direct and the ground-reflected waves) and the surface wave. On the other hand, in the case of perfectly-conducting ground it is more convenient to group the ground-reflected wave and the surface wave together,* regarding the sum as a single contribution from an image of the aerial, with a ground reflection-coefficient of +1 for all angles of incidence.

The space-wave field strength is inversely proportional to distance from the aerial, since there is no attenuation in the atmosphere at the frequencies under consideration. The surface wave, on the other hand, is attenuated more rapidly than inversely as the distance, as a result of the power dissipated in the ground; it is eventually entirely absorbed in the ground. This means that the vertical radiation pattern of our aerial is no longer the produce of independent functions of the distance and direction, as it is in the case of perfectly-conducting ground. It is therefore more appropriate to plot the vertical radiation pattern of the space wave only, remembering that the surface wave corresponding to the particular distance must be added to complete the picture of reception at a given point. This is convenient inasmuch as the reflected-wave field strength depends only on the space wave (except over a small region which is of no practical interest) and the ground-wave field strength depends only on the surface wave.

The reflection coefficient for a plane vertically-polarised wave incident on flat ground is given by**

$$\rho_v = \frac{(\epsilon_r - j60\lambda\sigma)\cos\theta - \sqrt{\{(\epsilon_r - j60\lambda\sigma) - \sin^2\theta\}}}{(\epsilon_r - j60\lambda\sigma)\cos\theta + \sqrt{\{(\epsilon_r - j60\lambda\sigma) - \sin^2\theta\}}} \qquad (2.11)$$

where ϵ_r is the ratio of the permittivity of the ground to that of free space, and σ is the conductivity. Fig. 2.12 shows ρ_v for a frequency of 1 Mc/s and two values of σ, 10^{-2} and 10^{-3} mhos/m, corresponding to ground of good and poor conductivity respectively. The reflection coefficient is virtually constant over the range of angles of interest in calculating the reflected-wave field strength ($0° - 50°$) from the vertical; furthermore, over this same range, when $\sigma = 10^{-2}$ mhos/m ρ_v is virtually the same as for perfectly-conducting ground.

The vertical radiation pattern of the space wave for a vertical doublet height h above ground level is the sum of two contributions, the direct wave and the direct wave multiplied by ρ_v; the latter contribution is delayed relative to the former (as a result of the path difference) by a phase angle $2\beta h\cos\theta$. By regarding the aerial as composed of collinear doublets and summing the contributions, we can calculate the vertical radiation pattern of any aerial, provided the current distribution is known. The pattern for a 0·55 λ aerial carrying a sinusoidal current distribution is shown in Fig. 2.13; in this diagram the field strength is normalised with respect to the ground wave for an aerial (carrying the same current) over perfectly-conducting ground.

---

*In this limiting case the surface wave is finite only at grazing incidence ($\theta = 90°$).

**E.C. Jordan, Electromagnetic Waves and Radiating Systems, Prentice-Hall, p. 141. The definition of ρ_v is illustrated in Fig. 3.1.

From Fig. 2.13 we see that the effect of the finite conductivity is to increase the angle of minimum radiation, i.e. it is equivalent to an increase in the effective height of the aerial. This results from the increased phase lag on reflection at the ground, and can be compensated by a small reduction in the aerial height. More important, the zero in the vertical radiation pattern is blurred, and the subsidiary lobe is increased. For $\sigma = 10^{-2}$ mhos/m the minimum field strength is 3% of the ground-wave field strength for perfectly-conducting ground; for $\sigma = 10^{-3}$ mhos/m the corresponding figure is 11%. Poorly conducting ground not only increases the strength of the reflected wave; more important, it reduces the distant ground-wave field strength

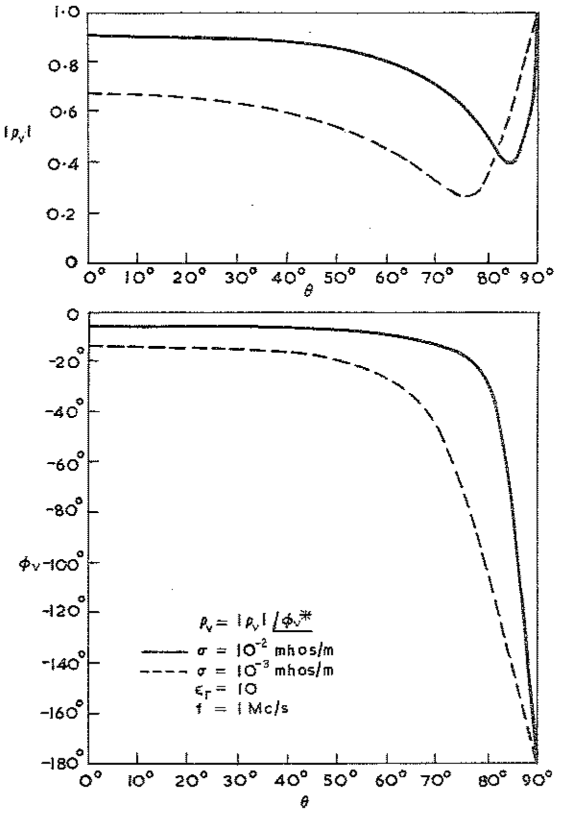

Fig. 2.12 - The modulus and phase angle of the reflection coefficient, ρ_v, for vertically-polarised plane waves

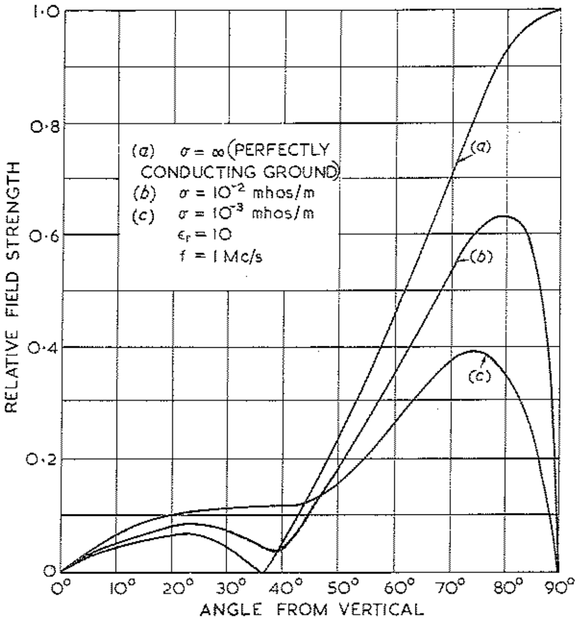

Fig. 2.13 - Vertical radiation pattern of 0·55λ aerial, assuming a sinusoidal current distribution

---

*The symbol $\angle$ is used to designate the phase angle of a complex quantity.

The foregoing discussion has been in terms of an aerial without an extensive earth system. It is usual to bury wires just below the surface of the ground in order to reduce loss in the immediate vicinity of the aerial; but typical earth systems rarely exceed 0·5 λ in radius and have a negligible effect on the vertical radiation pattern.[3]

2.2.2. The Aerial Current Distribution

In any radiation problem we must formulate Maxwell's equations in the space outside the aerial in a form suitable for satisfying the boundary conditions; in our case the tangential electric force must be zero over the surface of the perfectly-conducting cylindrical aerial. The most suitable mathematical form of the solution will depend on the precise shape of the surface; it will be different, for instance, if the corners of the cylinder are slightly rounded rather than sharp, although we can see intuitively that this cannot affect the current distribution significantly.

Rigorous solutions for the current distribution have been obtained for cases where the shape of the aerial is chosen to be convenient for mathematical analysis. On the other hand, the solutions applying to cylindrical aerials introduce approximations at some stage. But even these approximate solutions involve a lengthy mathematical analysis and it is not possible to deal with them in detail here. Three are worthy of mention, in order to illustrate both the methods of grappling with an intractable problem, and also the attendant difficulties.

It is possible to formulate an integral equation satisfied by the aerial current by equating the tangential electric force along the aerial to zero. However, it is not possible to obtain an explicit solution of this equation because the electric force at any point is a function of the current at *all* points on the aerial.* The best we can do is to check whether any suggested current distribution satisfies the integral equation. Hallén[4] overcame this difficulty by splitting the integral equation into two parts, one of which was much smaller than the other; he then calculated the smaller term approximately, thus obtaining a first approximation to the current distribution. This result was the inserted in the original integral equation to obtain a closer approximation to the current distribution, and so on. By a series of successive approximations a solution was obtained in the form of a power series in $1/\Omega$, where $\Omega = 60 \log(2h/a)$, h being the height and a the radius of the aerial. Clearly the choice of the parameter to use in the power series is important, since there is a possibility that the series may not converge. Gray,[5] for instance, obtained a power series using a slightly different parameter, and claims it gives results in better agreement with measurements than that of Hallén.

Böhm[6] used a method based on the transmission line analogy; he took as a first approximation to the aerial current a sinusoidal distribution, or the *primary* current. The system of distributed generators needed to maintain the primary

*A similar difficulty does not arise in the theory of transmission lines because it is assumed that the spacing between the go and return wires is so small that the conditions to be satisfied at any point are determined only by conditions *at* the point. The condition of zero tangential electric force at the surface of each wire then gives the well-known transmission line equations. As the radius of the aerial decreases the tangential electric force at a point becomes increasingly determined *only* by the current flowing at that point; it follows that the current distribution then reverts to that for an open-circuited transmission line, viz. a sinusoidal standing-wave pattern.

current follows from the induced-EMF method (see Section 2.1.2). The difference between the true current and the primary current, the *secondary* current, is therefore maintained by this system of distributed generators, reversed in sign, together with the base generator. The secondary current can then be calculated by regarding the aerial as approximating to a uniform transmission line, thus giving a second approximation to the aerial current.* This method is similar to that of Hallén and could be similarly continued in an iterative manner, but published results have so far been restricted to the second approximation.

Schelkunoff's method[7] is based on the solution for a biconical aerial with a generator applied between the apices; the radiation from this aerial is the same as for an inverted cone over perfectly-conducting ground. A transverse electromagnetic wave, the "principal wave", is propagated in the "aerial region" as if along a transmission line having a characteristic impedance determined by the angle of the cone. At the "boundary sphere" separating the "aerial region" and the "free-space region" a disturbance is set up which causes an infinite series of "complementary waves" to be generated. These are propagated outwards into free space and inwards towards the generator. The coefficients of the complementary waves are found by satisfying the continuity conditions at the boundary sphere; this is a laborious process involving a series of successive approximations. The aerial current follows from the value of the tangential magnetic force at the surface of the cone. A cylindrical aerial is regarded as a series of elements each approximating to a frustum of a cone, and the average characteristic impedance calculated (see Section 2.2.5). The equivalent conical aerial is taken to be one having the same characteristic impedance.

The results obtained by the three methods discussed are in reasonably good agreement, bearing in mind the difficulty of the problem. They demonstrate that the aerial behaves approximately like a transmission line of constant characteristic impedance; the larger the ratio of the height to the radius, h/a, the higher the characteristic impedance (see Section 2.2.5). The aerial current may be regarded as the sum of two components, one in-phase and one in phase-quadrature with that for the idealised aerial. The *in-phase component* is distributed approximately sinusoidally, but is "compressed" slightly, corresponding to a wave propagated along the aerial with a velocity less than that of light; the apparent velocity falls as the characteristic impedance of the aerial is reduced. The corresponding radiation pattern could be calculated from the known distribution of the in-phase component. But, for the important case of aerials approximately $0{\cdot}5\lambda$ high, a sufficiently good estimate for most purposes can be made as follows.

---

*In the methods used by Hallén and Böhm it is assumed that the current flows along a thin filament at the axis of the aerial. The field at a distance from this axis equal to the radius of the aerial is taken to be the same as that at the surface of the actual aerial; this procedure requires justification. In both methods the radius of the aerial, a, enters the result in the form log a. The actual aerial is equivalent to a series of thin filaments spaced round the periphery, the contributions of which must be summed. The term log a in the result should therefore be replaced by

$$\frac{2}{\pi}\int_{0}^{\pi/2} \log(2a\cos\phi)\,d\phi$$

The proof that this is equal to log a, thus justifying the procedure used by Hallén and Böhm, is left as an exercise for the reader.

If the velocity factor (the ratio of the effective velocity of propagation along the aerial to that of light) is v, the height of the maximum of the current distribution is approximately $h/2v$, and the vertical radiation pattern will be like that for an idealised aerial greater in height by $h\{1/v - 1\}/2$. There is therefore an "equivalent" practical aerial, shorter than the idealised aerial by an amount $h\{1/v - 1\}/2$, which has the same vertical radiation pattern.

The *phase-quadrature* component of the aerial current is in phase with the applied voltage, and the product of the two at the base therefore gives the power flowing from the generator.* The phase-quadrature component is concentrated towards the base of the aerial, so that its vertical radiation pattern is similar to that for a low aerial. As a result, the radiation pattern for the complete current distribution exhibits a blurred minimum, the degree of blurring increasing as the characteristic impedance of the aerial is reduced. The measured pattern for a typical mast radiator 0·55λ high, over perfectly-conducting ground, is shown in Fig. 2.14.[3] The measured pattern in Fig. 2.14 is like the idealised case for an aerial 0·58λ high; in this case the velocity factor v is therefore 0·90.

The complete current distribution takes the form of a sinusoid (with zeros 0·5 vλ apart) having a minimum blurred by the phase quadrature component. The ratio of the maximum to the minimum in this distribution is a measure of the difference between the idealised and practical aerials; by equating the radiated and input powers we can show that the ratio is approximately equal to R_L/Z_0. For a typical mast radiator (R_L = 70 ohms and Z_0 = 230 ohms) the maximum to minimum current ratio is about 0·3; for a typical thin wire aerial of the same height the ratio would be about 0·15.

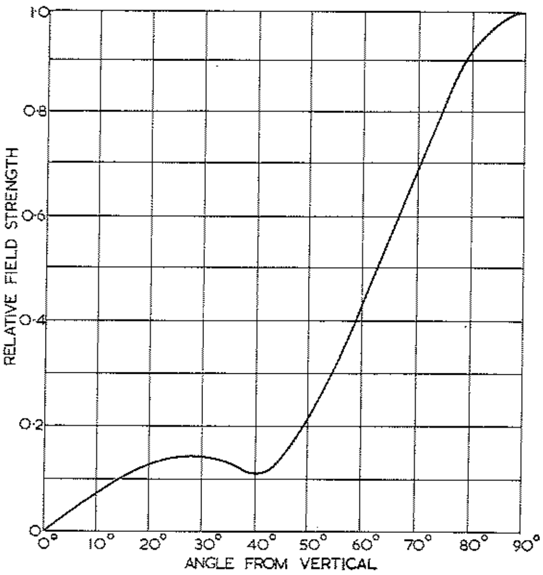

Fig. 2.14 - Measured vertical radiation pattern of 0·55λ aerial over perfectly-conducting ground; Z_0 = 245 ohms

2.2.3. The Radiation Characteristics

The differences between the radiation patterns of the idealised aerial considered in Section 2.1 and the practical aerial considered in Section 2.2 are important mainly if antifading characteristics are required. The chief difference is that the vertical radiation pattern of the base-driven aerial exhibits a blurred minimum, the effect of imperfectly-conducting ground re-inforcing that of the aerial current distribution. Other effects occasion no difficulty, involving merely a small modification to the aerial height.

---

*Here the phase reference is that of the current in the idealised aerial; in power engineering on the other hand, the phase reference is usually taken to be that of the applied voltage. In the latter case the power flow is given by the product of the voltage and the *in-phase* components of current.

The blurring of the radiation pattern associated with the aerial current results from the concentration near the base of the phase-quadrature component. This difficulty can be overcome by feeding the power in at the position of the current loop, rather than at the base; the base is then connected to ground through a reactance such as to locate the current loop at the required height, the current distribution then being similar to that shown in Fig. 2.5(b). One method is shown in Fig. 2.15(a), where the lower section of the mast is used as the outer of a transmission line through which the power is fed.

We can go further, and feed power in simultaneously at the position of the current loop and also at the base, as in Fig. 2.15(b). The driving circuits can be designed so that power is fed *in* at the loop but *abstracted* at the base, in any desired ratio. If the site were perfectly-conducting the vertical radiation pattern would therefore be the same as for a base-fed aerial with a *negative* phase-quadrature component of current. This arrangement can therefore be designed to overcome the deleterious effect of imperfectly-conducting ground, which is equivalent to a *positive* phase-quadrature component of aerial current. The vertical radiation pattern of the practical aerial energised at the loop and base simultaneously is then similar to that for the idealised aerial considered in Section 2.1.

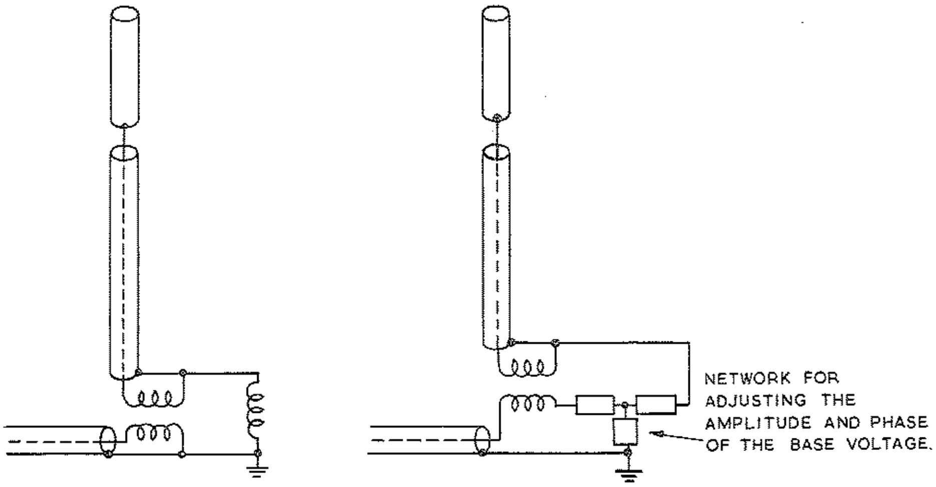

NETWORK FOR ADJUSTING THE AMPLITUDE AND PHASE OF THE BASE VOLTAGE.

(a) Energised at loop

(b) Energised at loop and base simultaneously

Fig. 2.15 - Methods of energising a vertical aerial

We have shown that, for aerials approximately 0·5λ high, the practical aerial of height

$$h\left(\frac{3}{2}-\frac{1}{2v}\right)$$

has substantially the same vertical radiation pattern as an idealised aerial of height h. For a given loop current, the ratio of the ground-wave field strengths of these equivalent aerials is

$$\frac{1-\cos\left(\beta h\,\frac{3}{2}-\frac{1}{2v}\right)}{1-\cos(\beta h)}$$

Since the radiation patterns are the same, the square of this fraction is the ratio of the radiated powers, and hence of the loop radiation resistances. The loop radiation resistance of the practical aerial can therefore be derived; the method is approximate, but adequate for most practical purposes.

For the base-fed aerial, the ground-wave field strength will be less, and the loop radiation resistance greater, than that for the equivalent aerial energised at the loop and base simultaneously, on account of the radiated power associated with the phase quadrature component of aerial current; but in practical cases the differences are small.

2.2.4. The Base Impedance

The theoretical methods described in Section 2.2.2 give the input current for a given generator voltage, and hence the base impedance of the aerial. However, the formulae involve extremely laborious computation, and are in any case subject to the same doubts as those arising in determining the aerial current distribution. There is an added difficulty; the fields associated with the end caps (or the evanescent fields within the cylinder near the top and bottom, if there are no end caps) are neglected. If, for instance, the generator is applied across an infinitesimal gap the added parallel susceptance on this account is infinite.

Apart from these limitations there are usually other considerations to take into account in a practical case: the effect of stay attachments, base insulator, lead-in, and, if a conventional mast rather than a cylindrical aerial is used, that of the non-circular cross-section and the lattice construction. These difficulties make the use of the more refined theoretical methods of doubtful value for accurate calculation of the base impedance; moreover, in a practical case an approximate estimate of the impedance is usually sufficient, because it is inexpensive to provide an aerial coupling network catering for a range of impedance.

An approximate equivalent circuit sufficient for most practical needs is shown in Fig. 2.16. The aerial, of height h and radius a, is regarded as a transmission line of constant characteristic impedance, Z_0, and of electrical length h/v; the velocity factor v depends on the characteristic impedance, a typical value for a mast radiator being 0·9. The transmission line is terminated $0{\cdot}25\lambda$ from the open-circuited end in a resistance R_L, the loop radiation resistance for an aerial having a velocity factor v, calculated as described in Section 2.2.3. The capacitance across the base insulator and the effect of the lead-in depends on the mechanical arrangement and must be assessed separately. R_g is a series resistance to take account of local ground loss; its value depends on the height of the aerial and the form of the earth system. For a high aerial with an extensive earth system R_g is small compared with the radiation resistance referred to the base; on the other hand, for a low aerial R_g is large compared with the radiation resistance. A low- or medium-frequency receiving aerial, for instance, is usually a small fraction of a wavelength high; the equivalent circuit is then a small capacitance which is proportional to the height of the aerial, in series with a resistance determined entirely by the loss in the ground. It is usual in carrying out laboratory measurements on receivers to connect in series with the generator a "dummy" aerial, i.e. a network simulating an agreed "standard" receiving-aerial impedance.

A formula for the characteristic impedance of a cylindrical aerial whose height is large compared with the radius is derived in Section 2.2.5, Equation (2.12); it is based on the result derived by Howe[8] for the electrostatic capacitance per unit length. At the quarter-wave resonance frequency the impedance is resistive and approximately equal to 36 ohms; at the half-wave resonance frequency the impedance is resistive and approximately equal to $Z_0^2/100$ ohms. The higher the value of Z_0 the more rapidly does the impedance change with frequency. One advantage of increasing the lateral dimensions of the aerial (and so reducing Z_0) is to increase the bandwidth, i.e. the frequency range corresponding to a specified impedance ratio. Another advantage is that the base voltage in the vicinity of half-wave resonance is reduced. For one or other of these

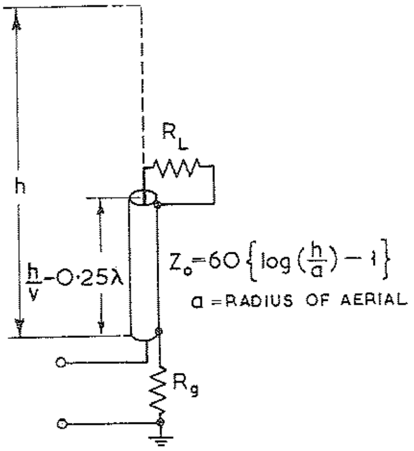
h
R_L
$\frac{h}{v}-0{\cdot}25\lambda$
$Z_0=60\left\{\log\left(\frac{h}{a}\right)-1\right\}$
a = RADIUS OF AERIAL
R_g

Fig. 2.16 - Approximate equivalent circuit of base-fed aerial

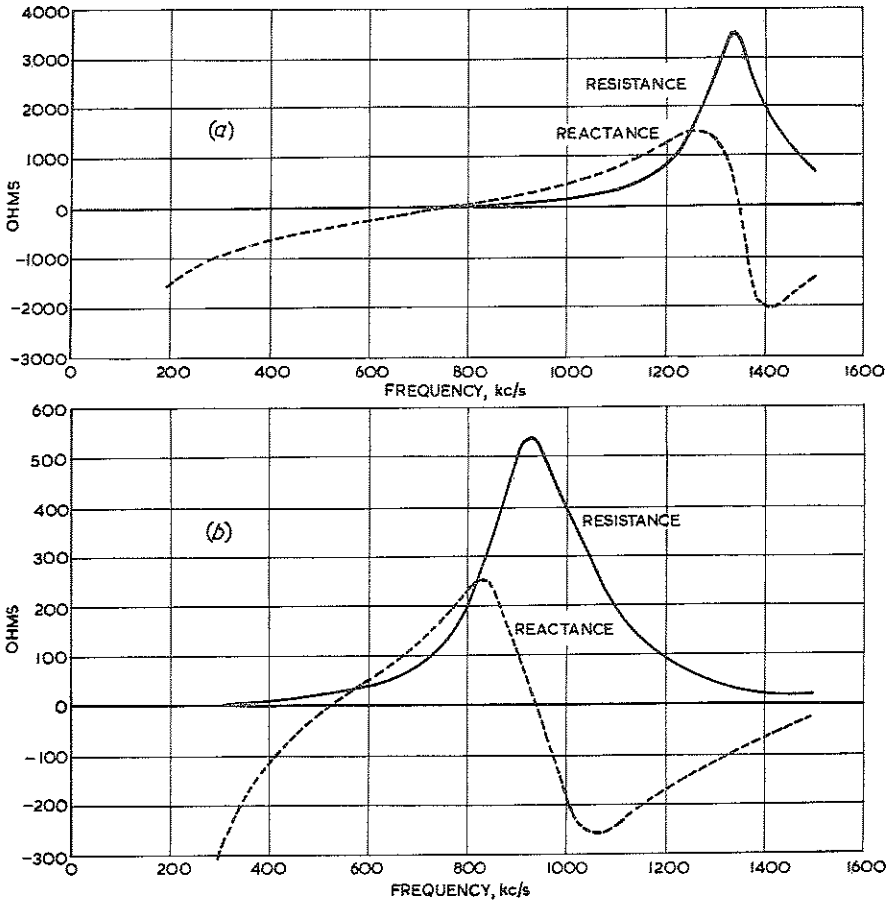

(a) Thin wire, h = 95 m, a = 0·35 mm, Z_0 = 690 ohms
(b) Mast radiator, h = 114 m, a = 0·95 m, Z_0 = 230 ohms

Fig. 2.17 - Impedance/frequency characteristics of base-fed aerials

reasons aerials of large diameter are sometimes simulated by using a number of wires in the form of a cage.

The measured impedance/frequency characteristics of two aerials are shown in Fig. 2.17; one is for a thin wire (much thinner than would be used in practice), and the other is for a mast radiator.

2.2.5. The Characteristic Impedance of a Vertical Cylindrical Aerial

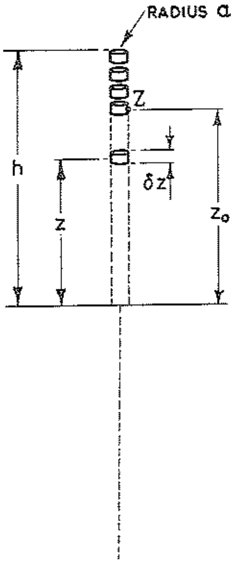

Fig. 2.18

The aerial (Fig. 2.18) is considered to be divided up into a large number of isolated elements, length δz, placed end to end. Each element is given unit positive charge per unit length; correspondingly, the image carries unit negative charge per unit length. The potential at any point on the surface of the cylinder is calculated by assuming the charge is distributed along a thin filament on the axis of the aerial; this assumption is justified later. The potential of a typical element at Z, height z_0, due to another element length δz, height z, is given by

$$\delta V = \frac{1}{4\pi\epsilon_0}\,\frac{\delta z}{\sqrt{\{(z_0-z)^2+a^2\}}}$$

where a is the radius of the aerial.

The potential at Z due to the complete aerial together with its image, V_z, is given by

$$V_z = \frac{1}{4\pi\epsilon_0}\left\{\left|\int_{z_0}^{0}\frac{dz}{\sqrt{\{(z_0-z)^2+a^2\}}}\right| + \left|\int_{z_0}^{h}\frac{dz}{\sqrt{\{(z_0-z)^2+a^2\}}}\right| - \left|\int_{0}^{-h}\frac{dz}{\sqrt{\{(z_0-z)^2+a^2\}}}\right|\right\}$$

$$= \frac{1}{4\pi\epsilon_0}\left\{2\sinh^{-1}\frac{z_0}{a} + \sinh^{-1}\frac{(h-z_0)}{a} - \sinh^{-1}\frac{(h+z_0)}{a}\right\}$$

This expression does not vary with z_0 by more than a factor of 2 except for points very near the top and the base. It is therefore permissible to average its value over the range $z_0 = 0 \to h$ in order to derive the potential of the complete aerial when the isolated elements are connected together, V. We obtain

$$V = \frac{1}{4\pi\epsilon_0}\left\{4\sinh^{-1}\left(\frac{h}{a}\right) - 2\sinh^{-1}\left(\frac{2h}{a}\right) - 4\sqrt{1+\frac{a^2}{h^2}} + 2\sqrt{1+\frac{a^2}{4h^2}} + 3\frac{a}{h}\right\}$$

If $h/a \gg 1$ this becomes

$$V = \frac{1}{2\pi\epsilon_0}\left\{\log\left(\frac{h}{a}\right) - 1\right\} \text{ since } \sinh^{-1} x \to \log 2x \text{ as } x \to \infty.$$

The average capacity of the aerial per unit length is therefore

$$\frac{2\pi\epsilon_0}{\left\{\log\left(\frac{h}{a}\right)-1\right\}}$$

By analogy with a uniform transmission line we write the characteristic impedance, Z_0, as

$$Z_0 = 60\left\{\log\left(\frac{h}{a}\right)-1\right\} \tag{2.12}$$

The expression for the potential of the complete aerial has been calculated assuming that the charge is distributed along the axis, rather than on the surface of the aerial. Since the result involves the radius only in the term $-\log a$ it follows from the footnote on p. 25 that this procedure is valid.

A different value for Z_0 has been proposed by Schelkunoff, based on the equivalent biconical transmission line (Fig. 2.19(a)). The characteristic impedance of an infinitely-long single cone above perfectly-conducting ground is given by[7]

$$Z_0 = 60\log\left(\cot\frac{\psi}{2}\right)$$

where ψ is the semi-angle of the cone.

If the cylindrical aerial is divided into short elements (Fig. 2.19(b)) each can be regarded as approximating to the frustum of a cone. The semi-angle for an element at a height z is $\tan^{-1} a/z$; for $z \gg a$ the characteristic impedance of the element is therefore $60 \log 2z/a$. The average value for the whole aerial is

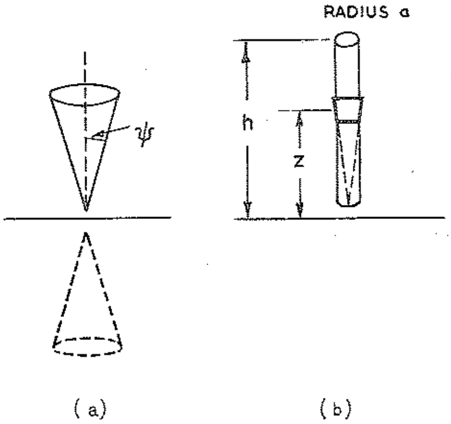

Fig. 2.19

$$Z_0 = 60\,\frac{1}{h}\int_0^h \log\frac{2z}{a}\,dz = 60\left\{\log\left(\frac{2h}{a}\right)-1\right\}$$

This value differs from that in Equation (2.12) because the increase in the capacitance of the elements near the top of the aerial (on account of its abrupt termination) is neglected. This method consequently gives a higher value of Z_0, although the difference is not large provided $h/a > 100$; that given by Equation (2.12) is in better agreement with measured results.

The value of Z_0 for an aerial of non-circular cross section can be derived by regarding it as the central conductor of a transmission line; the equivalent cylinder is that having the same capacitance per unit length. The diameter of the outer is immaterial provided the spacing to the inner is appreciably greater than the largest lateral dimension of the inner.

2.3. Radiation Coupling Between Spaced Aerials

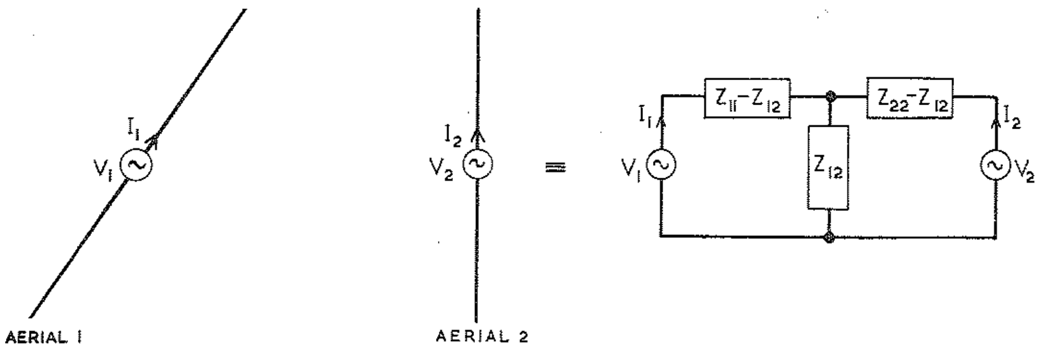

Fig. 2.20 - Equivalent circuit of coupled aerials

2.3.1. Definition of Mutual Impedance Between Aerials

The radiation coupling between spaced aerials can be expressed in terms of a parameter we will call the mutual impedance. Referring to Fig. 2.20, let the voltage and current at the input terminals of aerial 1 be V_1 and I_1 respectively; in the absence of aerial 2 the ratio of V_1 to I_1 is the self impedance of aerial 1, Z_{11}. Similarly, for aerial 2 the corresponding quantities are V_2, I_2 and Z_{22}. We will define the mutual impedance between aerial 1 and aerial 2 as minus the voltage induced at the open-circuited terminals of aerial 2 when unit current flows in aerial 1; correspondingly, let Z_{21} be minus the voltage induced at the open-circuited terminals of aerial 1 when unit current flows in aerial 2. From the reciprocity theorem it follows that $Z_{12} = Z_{21}$. The equivalent circuit is shown in Fig. 2.20,* and it follows that

$$V_1 = Z_{11}I_1 + Z_{12}I_2 \tag{2.13}$$

$$V_2 = Z_{22}I_2 + Z_{12}I_1 \tag{2.14}$$

We can define Z_{12} with reference to any two pairs of terminals, one pair on each aerial, but its value depends on the terminals chosen. It is most convenient to take these as being at the positions of the loop currents for the transmitting condition, and we will deal only with this case; the mutual impedance is then described as being "referred to the loop currents".

The effective impedances of aerials 1 and 2 are respectively

$$Z_1 = \frac{V_1}{I_1} = Z_{11} + Z_{12}\frac{I_2}{I_1} \tag{2.15}$$

$$Z_2 = \frac{V_2}{I_2} = Z_{22} + Z_{12}\frac{I_1}{I_2} \tag{2.16}$$

---

*In Fig. 2.20, Z_{11} is strictly the input impedance with the output terminals open-circuited, and Z_{22} is the output impedance with the input terminals open-circuited. However, we assume here that when one aerial is open-circuited at the reference terminals it has a negligible effect on the impedance of the other.

The corresponding powers supplied to aerials 1 and 2 are respectively

$$P_1 = I_1^2 \text{ Re} . \left(Z_{11} + Z_{12} \frac{I_2}{I_1} \right) \tag{2.17}$$

$$P_2 = I_2^2 \text{ Re} . \left(Z_{22} + Z_{12} \frac{I_1}{I_2} \right) \tag{2.18}$$

If aerial 2 is parasitic, i.e. energised only by radiation coupling from aerial 1, the ratio of the currents is found by putting $V_2 = 0$ in Equation (2.14)

$$\frac{I_2}{I_1} = - \frac{Z_{12}}{Z_{22}} \tag{2.19}$$

This ratio can be controlled by changing Z_{22}; it is maximum when Z_{22} is minimum, i.e. when the parasitic aerial is tuned for zero reactance. From Equations (2.15) and (2.19) the effective impedance of aerial 1 when aerial 2 is parasitic is

$$Z_1 = Z_{11} - \frac{Z_{12}^2}{Z_{22}} \tag{2.20}$$

It is evident that the mutual impedance concept is of great use in calculations on coupled aerials.

We will first derive a theoretical formula for Z_{12}, and then show how to use the result in practical cases.

2.3.2. Calculation of Mutual Impedance

In Fig. 2.21 the two aerials are shown as being over a ground plane, but this is merely by way of example; the method described is of quite general application. The z-axis is chosen to be parallel to aerial 2, and Z is a point on the position eventually to be taken up by this aerial. Let aerial 1 carry unity loop current and give rise to an electric force E_z at Z, in the absence of aerial 2. If we regard aerial 2 as broken into short isolated elements of length δz, its introduction does not affect E_z; the voltage between the ends of adjacent elements will therefore be $E_z \delta z$. When the elements are joined together the resultant current will be the same as if zero-impedance generators of voltage $E_z \delta z$ spaced δz apart were inserted in series along the length of aerial 2, as shown in the equivalent circuit in Fig. 2.21.

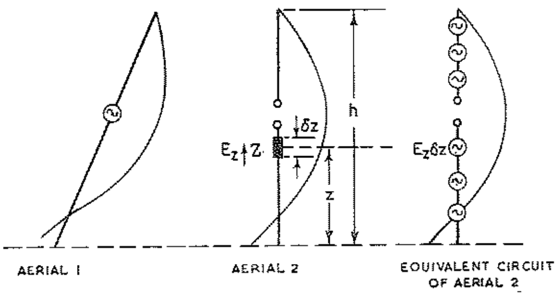

Fig. 2.21 - Calculation of mutual impedance between spaced aerials

Let a single generator of voltage $E_z \delta z$ at the loop of aerial 2 cause a loop current $E_z \delta z / Z_{22}$ to flow, where Z_{22} is the self impedance of aerial 2; the current at the point Z is $E_z \sin(\beta \overline{h-z}) \delta z / Z_{22}$ (the current distribution on aerial 2, when transmitting, is assumed to be sinusoidal). Applying the reciprocity theorem, a generator of voltage $E_z \delta z$ at the point Z causes a current $E_z \sin(\beta \overline{h-z}) \delta z / Z_{22}$ to flow at the loop, when the terminals are short circuited. The total loop current is therefore

$$\frac{1}{Z_{22}} \int_0^h E_z \sin(\beta \overline{h-z}) dz$$

It follows that the voltage at the loop when the terminals are open-circuited is

$$\int_0^h E_z \sin(\beta \overline{h-z}) dz$$

and that

$$Z_{12} = - \int_0^h E_z \sin(\beta \overline{h-z}) dz \qquad (2.21)$$

2.3.3. The Mutual Impedance Between Similar Parallel Aerials

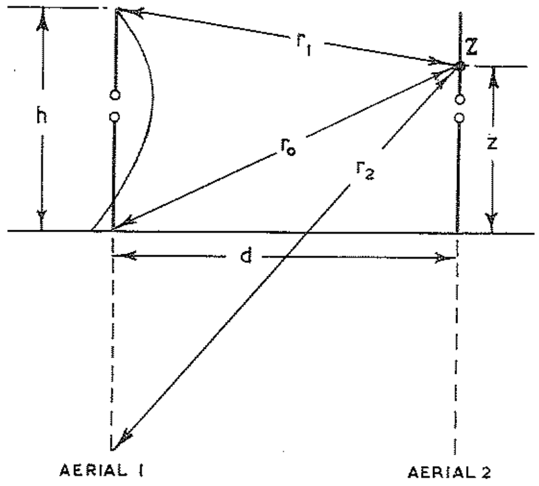

Fig. 2.22 - Calculation of mutual impedance between similar vertical aerials

Consider the two similar vertical aerials shown in Fig. 2.22, spaced a distance d apart over perfectly-conducting ground. If the loop current in aerial 1 is unity, E_z, the vertical component of electric force at the point Z in the absence of aerial 2, is given by Equation (2.6).

$$E_z = j30 \left\{ 2\cos(\beta h) \frac{e^{-j\beta r_0}}{r_0} - \frac{e^{-j\beta r_1}}{r_1} - \frac{e^{-j\beta r_2}}{r_2} \right\}$$

where r_0, r_1, r_2 are defined in Fig. 2.22. From Equation (2.21) we have

$$Z_{12} = -j30 \int_0^h \left\{ 2\cos(\beta h) \frac{e^{-j\beta r_0}}{r_0} - \frac{e^{-j\beta r_1}}{r_1} - \frac{e^{-j\beta r_2}}{r_2} \right\} \sin(\beta \overline{h-z}) dz \qquad (2.22)$$

This integral is evaluated in Section 7.2; the result is

$$
\begin{aligned}
Z_{12} = 15[&2\{1+2\cos^2(\beta h)\}Ei\{-j\beta d\} - \\
&-\{4\cos^2(\beta h) + j\,2\sin(2\beta h)\}Ei\{-j\beta(\sqrt{h^2+d^2}+h)\} - \\
&-\{4\cos^2(\beta h) - j\,2\sin(2\beta h)\}Ei\{-j\beta(\sqrt{h^2+d^2}-h)\} + \\
&+\{\cos(2\beta h) + j\sin(2\beta h)\}Ei\{-j\beta(\sqrt{4h^2+d^2}+2h)\} + \\
&+\{\cos(2\beta h) - j\sin(2\beta h)\}Ei\{-j\beta(\sqrt{4h^2+d^2}-2h)\}]
\end{aligned}
\qquad (2.23)
$$

where $Ei(-jx) = Ci(x) - j\,Si(x)$. If instead of aerials over a ground plane (as in Fig. 2.22) we had considered centre-fed aerials in free space, Equation (2.23) gives minus the voltage induced at *each* loop of aerial 2.

For the special case of $0{\cdot}25\lambda$ aerials over perfectly-conducting ground we obtain

$$
\begin{aligned}
Z_{12} = 15\Bigg[&2Ei\{-j\beta d\} - \\
&-Ei\left\{-j\beta\left(\sqrt{\left(\frac{\lambda}{2}\right)^2+d^2}+\frac{\lambda}{2}\right)\right\} - Ei\left\{-j\beta\left(\sqrt{\left(\frac{\lambda}{2}\right)^2+d^2}-\frac{\lambda}{2}\right)\right\}\Bigg]
\end{aligned}
\qquad (2.24)
$$

This expression when multiplied by 2 is also the mutual impedance between parallel $0{\cdot}5\lambda$ aerials d apart, in free space. Z_{12} for this case is shown graphically in Fig. 2.23 and values are listed in Table 2 (p. 36).

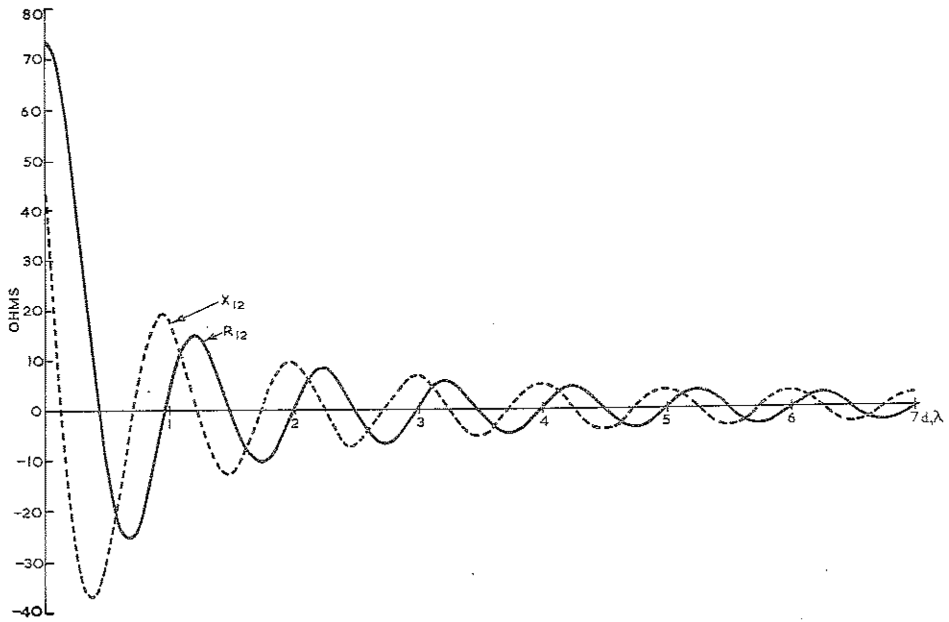

Fig. 2.23 - Mutual impedance, $Z_{12}(=R_{12}+jX_{12})$, between parallel $0{\cdot}5\lambda$ aerials in free space, distance d apart, referred to the loop currents

As $d \to 0$, $Z_{12} \to Z_{11}$; we can therefore use Equation (2.23) to derive Z_{11} for an aerial of small but finite radius. But in so doing the limit must be carefully examined, as in calculating Z_{12} we have assumed that the currents flow along thin filaments at the axes of the aerials; we must instead treat each aerial as if it consisted of a large number of filaments spaced round the periphery.

TABLE 2

Mutual Impedance, $Z_{12}(= R_{12} + jX_{12})$, Between Parallel 0·5 λ Aerials in Free Space, Distance d Apart Referred to Loop Currents

d	R_{12}	X_{12}	d	R_{12}	X_{12}
0	+73·1	+42·5	2·8 λ	−6·2	+2·6
0·05 λ	+71·6	+24·3	2·9 λ	−3·4	+5·6
0·10 λ	+67·3	+7·5	3·0 λ	+0·5	+6·3
0·15 λ	+60·5	−6·3	3·1 λ	+4·0	+4·7
0·20 λ	+51·4	−19·2	3·2 λ	+5·8	+1·4
0·25 λ	+40·8	−28·4	3·3 λ	+5·3	−2·2
0·30 λ	+29·3	−34·4	3·4 λ	+3·0	−4·7
0·35 λ	+17·5	−37·2	3·5 λ	−0·4	−5·4
0·40 λ	+6·2	−37·4	3·6 λ	−3·4	−4·1
0·45 λ	−3·8	−34·1	3·7 λ	−5·0	−1·3
0·50 λ	−12·5	−29·9	3·8 λ	−4·7	+1·8
0·6 λ	−23·3	−15·9	3·9 λ	−2·6	+4·1
0·7 λ	−24·9	−0·3	4·0 λ	+0·3	+4·7
0·8 λ	−18·5	+12·3	4·1 λ	+2·9	+3·6
0·9 λ	−7·5	+18·5	4·2 λ	+4·4	+1·2
1·0 λ	+4·0	+17·7	4·3 λ	+4·1	−1·6
1·1 λ	+12·3	+11·2	4·4 λ	+2·4	−3·6
1·2 λ	+15·3	+1·9	4·5 λ	−0·2	−4·2
1·3 λ	+12·6	−6·7	4·6 λ	−2·6	−3·2
1·4 λ	+6·0	−11·9	4·7 λ	−3·9	−1·1
1·5 λ	−1·9	−12·3	4·8 λ	−3·7	+1·4
1·6 λ	−8·2	−8·4	4·9 λ	−2·1	+3·3
1·7 λ	−10·9	−2·0	5·0 λ	+0·2	+3·8
1·8 λ	−9·4	+4·5	5·1 λ	+2·3	+2·9
1·9 λ	−4·8	+8·7	5·2 λ	+3·5	+1·0
2·0 λ	+1·1	+9·4	5·3 λ	+3·4	−1·3
2·1 λ	+6·0	+6·6	5·4 λ	+2·0	−2·9
2·2 λ	+8·4	+1·8	5·5 λ	+0·1	−3·5
2·3 λ	+7·5	−3·3	5·6 λ	−2·1	−2·7
2·4 λ	+4·0	−6·8	5·7 λ	−3·2	−0·9
2·5 λ	−0·7	−7·5	5·8 λ	−3·1	+1·1
2·6 λ	−4·8	−5·5	5·9 λ	−1·8	+2·7
2·7 λ	−6·8	−1·6	6·0 λ	+0·1	+3·1

It is shown in Section 7.2 that, when $d \to 0$ Re.Z_{12} is independent of d, so this term presents no difficulty, and also that Im.Z_{12} contains d only in the form log d; it follows from the footnote on p. 25 that Im.Z_{11} is Im.Z_{12} for two filaments spaced a distance apart equal to the radius of the aerial. Consequently, the self impedance of a cylindrical aerial of radius a is equal to the mutual impedance between two filaments spaced a apart.

It follows from Section 7.2, Equation (7.8), that for a 0·25 λ aerial over perfectly-conducting ground Im.Z_{11} is $15\,Si(2\pi)$ or 21·3 ohms, while for a 0·5 λ aerial it is $15\{4\,Si(2\pi)-Si(4\pi)\}$ or 62·7 ohms, both values being independent of the radius of the aerial. In both cases the loop reactance is positive, and this suggests that the *electrical* length of the aerial is slightly greater than its *physical* length; in other words, the apparent velocity of propagation is less than that of light. Moreover, for a given loop reactance the lower the characteristic impedance of the aerial the lower would we expect the apparent velocity of propagation to be. This is a tempting conclusion to draw from the theory, as it is consistent with practical experience. However, Section 7.2, Equation (7.8) shows also that Im.Z_{11} varies over wide limits (both positive and negative) at values of h other than 0·25λ and 0·5λ. It is therefore dangerous to interpret Im.Z_{11} as giving a reliable indication of the electrical length of the aerial.

The method we have described for calculating the mutual impedance between parallel aerials may be applied to other arrangements. Pistolkors[9] has given results for the mutual impedance between collinear and staggered 0·5λ aerials in free space.

2.3.4. Examples of Calculations on Coupled Aerials

Example 1

Two 0·25λ aerials spaced 0·375λ apart on perfectly-conducting ground carry currents of equal amplitude but differing in phase by 45°. If the total input power is 100 kW, how is it divided between the two aerials? How does the field strength in different horizontal directions compare with that for a single 0·25λ aerial radiating the same total power?

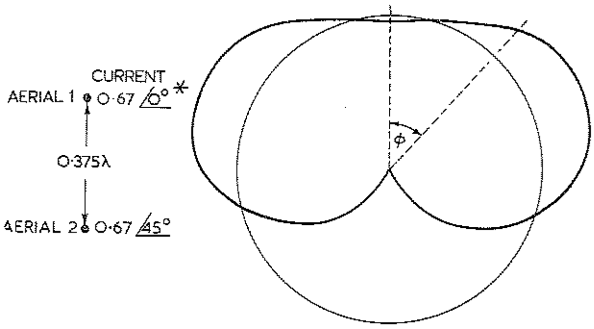

Fig. 2.24 - Horizontal radiation pattern of two 0·25λ aerials over perfectly-conducting ground, spaced 0·375λ; the currents are equal in amplitude and differ in phase by 45°. The circle shows the field strength to the same scale for a single 0·25λ aerial radiating the same power

Interpolating and halving the values of Z_{12} in Table 2, p. 36 (since we are dealing with 0·25λ aerials over perfectly-conducting ground)

$$Z_{11} = 36{\cdot}6 + j21{\cdot}3$$

$$Z_{12} = 5{\cdot}9 - j18{\cdot}7$$

For aerial 1,

$$\frac{V_1}{I_1} = Z_{11} + Z_{12}\frac{I_2}{I_1} = 36{\cdot}6 + j21{\cdot}3 + (5{\cdot}9 - j18{\cdot}7)(0{\cdot}71 + j0{\cdot}71) = 54{\cdot}0 + j12{\cdot}3$$

---

*The symbol ∠ is used to designate the phase angle of a complex quantity.

For aerial 2,

$$\frac{V_2}{I_2} = Z_{22} + Z_{12}\frac{I_1}{I_2} = 36{\cdot}6 + j21{\cdot}3 + (5{\cdot}9 - j18{\cdot}7)(0{\cdot}71 - j0{\cdot}71) = 27{\cdot}6 + j3{\cdot}9$$

The power supplied to aerial 1 is therefore

$$\frac{54{\cdot}0}{54{\cdot}0 + 27{\cdot}6} \,.\, 100\text{ kW i.e. } 66\text{ kW},$$

and the power supplied to aerial 2 is 34 kW. The total radiation resistance is $(54{\cdot}0 + 27{\cdot}6)$ ohms, i.e. 81·6 ohms. The current in each aerial is therefore

$$\sqrt{\frac{36{\cdot}6}{81{\cdot}6}}$$

or 0·67 times the current in a single aerial radiating the same power.

Taking the field strength for a single aerial radiating 100 kW as unity, the field strength for the two-element system is found by the vector addition of the contributions from the two aerials:

$$E_\phi = 1{\cdot}34\,\cos\pi(3\cos\phi - 1)/8$$

where ϕ is the bearing of the point considered, relative to the line joining the two aerials. This expression is plotted in Fig. 2.24; the circle represents the field strength for a single $0{\cdot}25\lambda$ aerial radiating the same power. In the directions of the maxima the field strength due to the directional aerial system is greater than that for the single aerial in the ratio 1·34:1.

Example 2

Two parallel $0{\cdot}5\lambda$ aerials are spaced $0{\cdot}25\lambda$ in free space; one is driven and the other is parasitic. How will the horizontal radiation pattern change as the parasitic aerial is tuned?

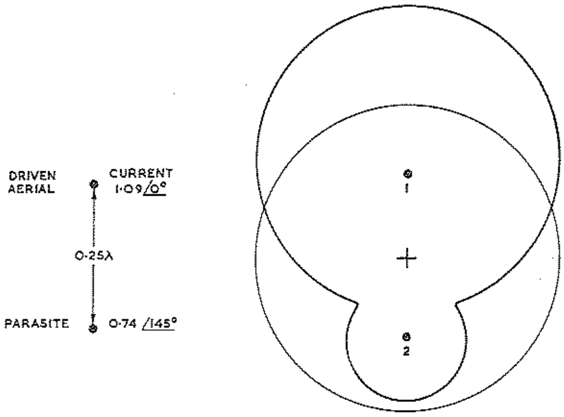

Fig. 2.25 - Horizontal radiation pattern of two parallel $0{\cdot}5\lambda$ aerials spaced $0{\cdot}25\lambda$; one is a parasite tuned for zero loop-reactance. The circle shows the field strength to the same scale for a single $0{\cdot}5\lambda$ aerial radiating the same power

Let the loop currents in aerials 1 and 2 be I_1 and I_2 respectively.

From Table 2, p. 36, $Z_{12} = (40{\cdot}8 - j28{\cdot}4)$

Let $Z_{22} = 73{\cdot}1(1 + j\tan\phi)$,

where $j73{\cdot}1\tan\phi$ is the sum of the self reactance of aerial 2 and any added series reactance. From Equation (2.19)

$$\frac{I_2}{I_1} = -\frac{(40{\cdot}8 - j28{\cdot}4)}{73{\cdot}1(1 + j\tan\phi)} = 0{\cdot}68\cos\phi\underline{/145^\circ - \phi}$$

The ratio I_2/I_1 is maximum when $\phi = 0$, i.e. when the aerial is tuned, and is then $0{\cdot}68\underline{/145^\circ}$. For this case, from Equation (2.20) the impedance of aerial 1 is given by

$$Z_1 = 73{\cdot}1 + j42{\cdot}5 - \frac{(40{\cdot}8 - j28{\cdot}4)^2}{73{\cdot}1} = 61{\cdot}4 + j74{\cdot}0$$

The loop current flowing in aerial 1, as a ratio of the current flowing in a single $0{\cdot}5\lambda$ aerial radiating the same power, is therefore

$$\sqrt{\frac{73{\cdot}1}{61{\cdot}4}} = 1{\cdot}09.$$

The horizontal radiation pattern can now be calculated as the sum of the contributions from two aerials, the driven aerial carrying a current $1{\cdot}09\underline{/0^\circ}$, and the parasitic aerial $0{\cdot}74\underline{/145^\circ}$. The resulting pattern is shown in Fig. 2.25, the circle corresponding to a single $0{\cdot}5\lambda$ aerial radiating the same power; the ratio of field strength in the forward direction to that for a single aerial is 1·7. The horizontal radiation patterns for different values of tuning reactance can be calculated in a similar manner by giving ϕ the appropriate values. The results for two values of aerial spacing ($0{\cdot}1\lambda$ and $0{\cdot}25\lambda$) are shown in Fig. 2.26.

It will be seen that the horizontal radiation pattern changes rapidly in shape as the tuning of the parasite is changed, particularly for the smaller spacing. Since a change of frequency causes a change in ϕ, another way of expressing this result is to say that the bandwidth of the system decreases with the spacing between the two aerials. When maximum radiation is in the direction of the driven aerial the parasite is called a reflector; when in the opposite direction the parasite is called a director.

We have assumed so far that the aerial system is adjusted to give the required directional radiation pattern by changing a series reactance inserted at the centre of the parasite; in practice it is more usual to change the length of the parasite. However, since the difference in length is usually a small fraction of the wavelength this does not affect the foregoing theory appreciably.

2.3.5. Receiving Aerials

The equivalent circuit of a receiving aerial is shown in Fig. 1.2(b). A method of calculating the base impedance (Z_a in Fig. 1.2(b)) is given in Section 2.2.4. We must also be able to calculate the open-circuit voltage (V in Fig. 1.2(b)) induced

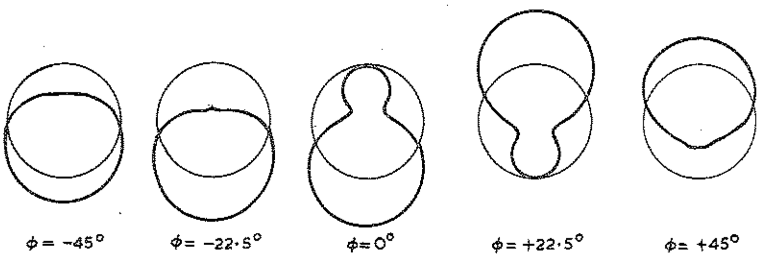

AERIAL SPACING 0·1λ

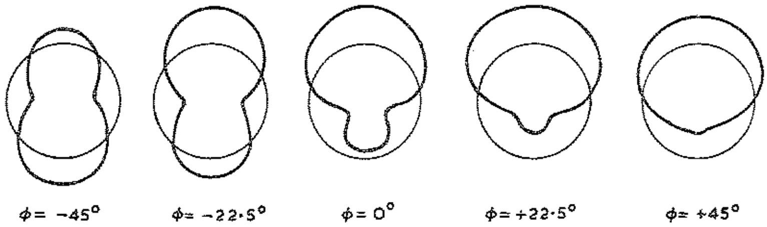

AERIAL SPACING 0·25λ

Fig. 2.26 - Horizontal radiation patterns for two parallel 0·5λ aerials in free space; one aerial is a parasite; the phase angle of the self impedance being ϕ. The circle shows the field strength to the same scale for a single 0·5λ aerial radiating the same power

by the incident wave. We could do so by considering the radiation coupling between the transmitting and receiving aerials, using the mutual impedance concept developed in Section 2.8. However, this would involve a complete knowledge of the propagation path between the two aerials. A different approach is therefore more convenient, bearing in mind that the receiving aerial is so weakly coupled to the transmitting aerial that the latter is not significantly affected by the former.

The field strength at the receiving aerial can be measured, or in idealised cases it may be calculated; knowing the incident field strength the voltage induced in the receiving aerial can also be calculated. If, for instance, the aerial is a simple vertical wire or mast of height h with the ground as one terminal, and the component of electric force in the incident wave in the direction of the aerial at a point height z is E_z, it follows from Section 2.3.2. that

$$V = \frac{1}{\sin(\beta h)} \int_0^h E_z \sin(\beta \overline{h - z})\, dz \qquad (2.25)$$

If E_z is constant in amplitude and phase over the length of the aerial (say E), as it would be for a plane wave arriving from a direction normal to the axis of the aerial, Equation (2.25) becomes

$$V = \frac{E(1 - \cos \beta h)}{\beta \sin \beta h} \qquad (2.26)$$

If $h \ll \lambda$, as is usual for low- and medium-frequency receiving aerials

$$V = E\,\frac{h}{2}$$

In other words, the length by which the field strength must be multiplied to give the open-circuit voltage (usually called the "effective length") is $h/2$. If the aerial has a capacitance top sufficiently large to make the current in the vertical portion (when transmitting) approximately constant, the effective length is then h.

If the receiving aerial is a centre-fed $0{\cdot}5\lambda$ dipole, Equation (2.26) becomes

$$V = E\,\frac{\lambda}{\pi}$$

and the effective length is therefore λ/π. The maximum power is abstracted from the aerial when it is connected to a matched load. For a $0{\cdot}5\lambda$ dipole having a loop radiation resistance R_L, the maximum power available is therefore

$$\frac{1}{R_L}\left(\frac{E\lambda}{2\pi}\right)^2 ;$$

in other words, the area by which the power density in the incident wave must be multiplied to give the maximum output power is $30\lambda^2/\pi R_L$, and this is sometimes described as the "absorbing area". For a $0{\cdot}5\lambda$ dipole in free space, for instance, $R_L = 73$ ohms and the absorbing area is $0{\cdot}13\lambda^2$. The corresponding result for a tuned doublet can be found using the value of the radiation resistance given by Equation (2.9). The absorbing area is $0{\cdot}12\lambda^2$, i.e. only slightly less than that of a $0{\cdot}5\lambda$ dipole. It should however be remembered that it is impracticable to realise this high value, because of the low radiation resistance of the doublet, and the consequently prohibitive losses in the doublet and tuning coil.

We have so far stressed the reciprocal properties of an aerial used for transmission or reception, insofar as the radiation pattern and impedance are concerned. The aerial *current*, on the other hand, may be very different in the two conditions. When immersed in a plane-wave of electric force E, arriving from a direction normal to the axis of the aerial, the equivalent circuit approximates to a transmission line in which there are inserted series generators of voltage $E\delta z$ spaced δz apart.

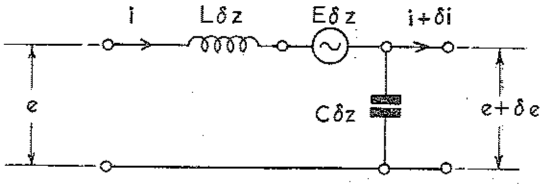

Fig. 2.27 - Equivalent circuit of element of receiving aerial

The differential equations satisfied by the element of the transmission line shown in Fig. 2.27 are

$$\frac{\partial e}{\partial z} = -j\,\omega L i + E$$

$$\frac{\partial i}{\partial z} = -j\,\omega C e$$

where L and C are the equivalent inductance and capacitance per unit length;

$$Z_0\left(=\sqrt{\frac{L}{C}}\right)$$

is the characteristic impedance of the aerial. We therefore have

$$\frac{\partial^2 i}{\partial z^2} + \beta^2 i = -j\beta\,\frac{E}{Z_0}$$

The general solution is $i = -\dfrac{jE}{\beta Z_0} + A\sin(\beta z) + B\cos(\beta z)$

where A and B are constants depending on the boundary conditions. For a vertical aerial of height h, open-circuited at the base

$$i = \frac{jE}{\beta Z_0}\left[\frac{\cos\left\{\beta\left(\frac{h}{2} - z\right)\right\} - \cos\left\{\beta\,\frac{h}{2}\right\}}{\cos\left\{\beta\,\frac{h}{2}\right\}}\right]$$

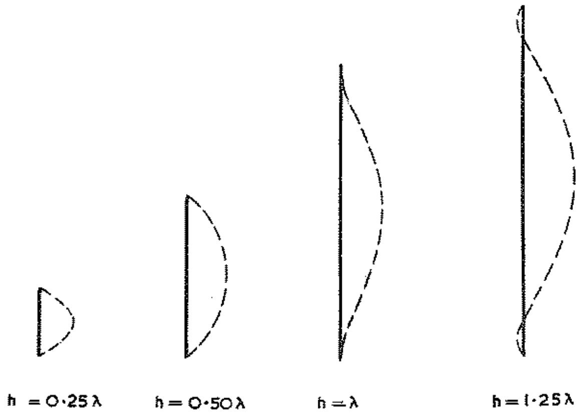

Fig. 2.28 - Approximate current distribution on open-circuited receiving aerial immersed in a plane-wave field

This is a "raised cosine" distribution; some cases are illustrated in Fig. 2.28, normalised to have the same maximum current.

The current for other terminations can be derived in a similar manner. If, for instance, the aerial is earthed at the base the current is like that in the upper half of an open-circuited aerial of twice the length. In general the current distribution depends not only on the terminating reactance but also on the angle of arrival of the incident wave.

In the above analysis we have considerably simplified the picture by disregarding the effect of re-radiation, merely to draw attention to the difference between the transmitting and receiving conditions. If the receiving aerial is terminated in a reactance the whole of the received power is re-radiated, and this limits the maximum current in the resonance condition.

3. HIGH-FREQUENCY AERIALS

3.1. General Considerations

The high-frequency band (3–30 Mc/s) is used mainly for communication systems depending on reflection of the propagated signal from the ionosphere. The lower frequencies are used for ranges up to about 4000 km, which involve a single reflection (or single hop); the higher frequencies are used for multi-hop circuits and give world-wide communication. Because of the high attenuation over such long paths, and the consequent degradation of the service by noise and other forms of interference, it is essential to concentrate the power available into a narrow beam projected in the direction of the area to be served.

For a broadcasting service the angular spread of the beam is determined by the size and location of this area. A near-by country, for instance, may require a beam covering a wide range of azimuthal and zenithal angles, projected at a large angle to the horizontal. On the other hand, a distant country generally requires a relatively narrow beam projected at a small angle to the horizontal.

For a point-to-point service, ideally the spread of the beam is determined only by the uncertainty regarding the ionospheric path. The ionosphere sometimes causes a lateral deviation of the beam; the variations in the height of the reflecting layer and the diffuse nature of the reflection also make it difficult to calculate the optimum projection angle precisely. Moreover, it is not always practicable to use a beam as sharp as theoretically desirable if this demands an unduly complicated aerial. Consequently the same types of aerials are often used both for broadcasting and for point-to-point circuits.

A directional aerial is achieved by using a number of radiating elements and energising them in such a way that the individual contributions reinforce each other in the desired directions, but substantially cancel in those directions in which no radiation is required; such an arrangement is often called an array. The degree of directivity is defined by comparing the array with a convenient reference aerial, and that usually adopted for the high-frequency band is the $0{\cdot}5\lambda$ dipole in free space. The gain, G, is defined as

$$G = \frac{\text{Power supplied to } 0{\cdot}5\lambda \text{ dipole in free space giving the same maximum field strength as array}}{\text{Power supplied to array}} \tag{3.1}$$

G can be found by considering the array and a $0{\cdot}5\lambda$ dipole in free space giving the same maximum field strength, and then integrating (either mathematically or graphically) to find the ratio of the radiated powers. From Equation (2.10) the product of maximum field strength and distance divided by the square root of the power

$$\left(\frac{Er}{\sqrt{P}}\right)$$

is $9{\cdot}9$ for a $0{\cdot}25\lambda$ aerial over perfectly-conducting ground; for a $0{\cdot}5\lambda$ aerial in free space

$$\frac{Er}{\sqrt{P}}$$

is therefore $$\frac{9{\cdot}9}{\sqrt{2}}$$

i.e. 7·0. It follows that, for the array

$$\frac{Er}{\sqrt{P}} = 7{\cdot}0\sqrt{G} \tag{3.2}$$

It is theoretically possible to obtain unlimited gain from an aerial system having overall dimensions as small as we please.* But the radiation resistance is then so low as to make such an arrangement quite impracticable; the currents in the elements would be excessive and the losses consequently prohibitive. In practice, therefore, a high gain necessarily means an extensive aerial, but there are many ways of arranging radiating elements to give a required radiation pattern. In some cases it may be necessary to compromise between the complexity of the aerial system and its performance; this may involve not only considerations of technical performance but also those relating to mechanical design, the area of land required, the cost, and other factors. There is therefore no "best" aerial for any application; the advantages and disadvantages of possible ways of meeting the requirements must be studied in relation to the particular case.

At the high frequencies under consideration the surface wave suffers rapid attenuation with distance; although this component may be used for communication over very short ranges, for the more important long-range services with which we are concerned here only the space wave is important. The effective field strength is therefore found by the vector addition of the direct wave and the ground-reflected wave; the latter is equal to the direct wave multiplied by the reflection coefficient of the ground for a plane wave of the appropriate polarisation, and delayed in time corresponding to the path difference between two components. The reflection coefficient is shown in Fig. 3.1 for two frequencies corresponding to the extremes of the band used for long-range communication. At normal incidence ($\theta = 0°$) there is of course no difference between horizontal and vertical polarisation; the difference in the sign of ρ_h and ρ_v at normal incidence arises from the definitions of these coefficients, which are illustrated in Fig. 3.1.

Looking first at the curves for horizontal polarisation, we see that over the whole of the frequency band the reflection coefficient is not very different from −1; particularly is this true for angles between 70° and 90° from the vertical, which are very important for long-range communication. In other words, for horizontally-polarised waves the ground behaves virtually as if perfectly-conducting. On the other hand, for vertically-polarised waves the reflection coefficient is substantially less than unity for angles between 70° and 90° from the vertical, except near grazing incidence. Generally speaking, although the radiated polarisation depends on the direction from the array, it is substantially the same in all directions corresponding to the main beam. We can therefore think of an array comprising *horizontal* elements as radiating predominantly *horizontally-polarised* waves in the direction of the main beam, and correspondingly for arrays of vertical elements. It follows that the array of horizontal elements will have a higher gain than the corresponding array of vertical elements, the difference being accounted for by loss in the ground; at the angle at which $|\rho_v|$ is minimum (corresponding to the Brewster angle in optics) this difference is about 4 dB. Arrays of horizontal elements are therefore preferred for high-frequency services, and only this type will be considered. In calculating their performance it will be assumed that the ground is perfectly-conducting. The effect of imperfectly-conducting ground can be taken into account using the information contained in Fig. 3.1, but this does not affect the results appreciably.

---

*An example is given on p. 12 of "Aerials for Metre and Decimetre Wavelengths", R.A. Smith, Cambridge University Press.

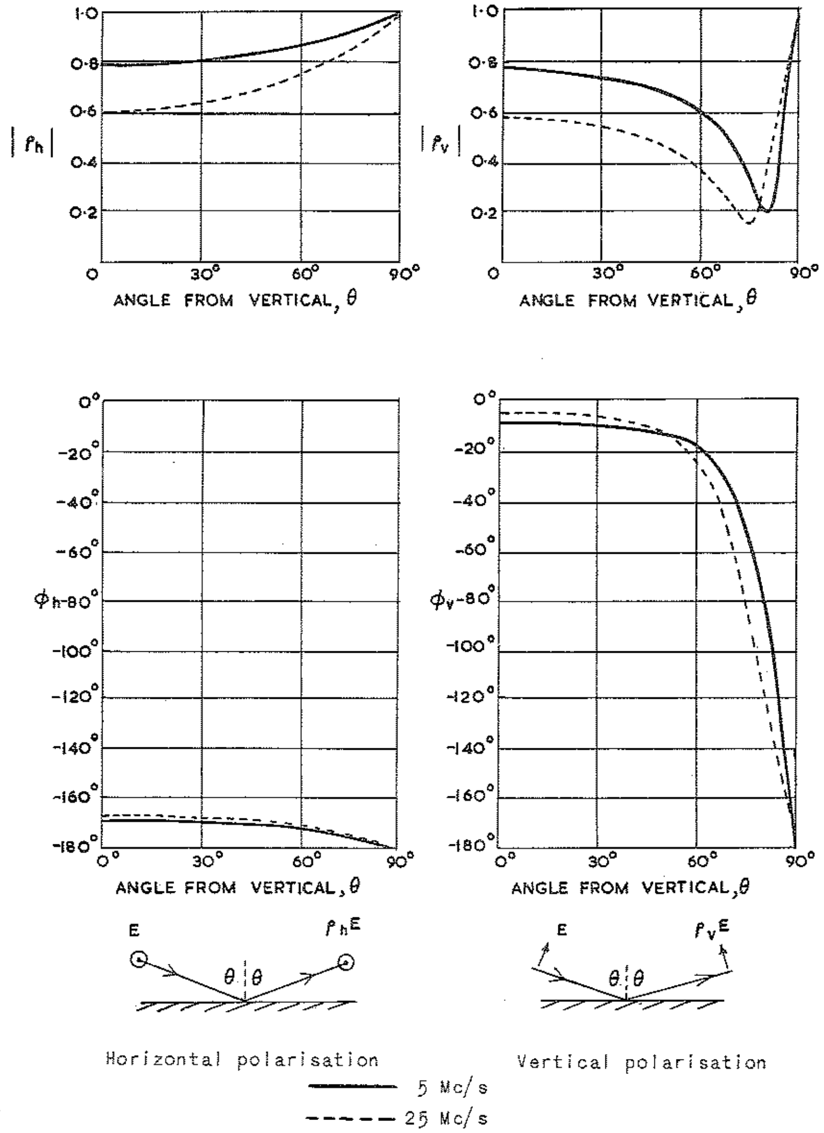

Fig. 3.1 - Reflection coefficient of ground, $\rho = |\rho|\angle\phi$;* $\sigma = 10^{-2}$ mhos/m, $\epsilon_r = 10$

*The symbol $\angle$ is used to designate the phase angle of a complex quantity.

Transmitting arrays are usually fed from balanced lines, to which they are matched in order to reduce both the maximum voltage across, and the losses in, the line. Matching is achieved by connecting a length of transmission line in parallel at an appropriate point, or by altering the characteristic impedance of a section of the line.

Receiving arrays can be connected in a similar manner, but the more usual arrangement is through an impedance-matching circuit or transformer to a co-axial line. This reduces the possibility of pick-up of local interference, which is important in the case of a receiving aerial.

3.2. The Curtain Array

In this type of array horizontal radiating elements are arranged in the form of a vertical curtain which is suspended from guys between the supporting masts. The elements carry equal co-phased currents, so that their contributions reinforce each other in the two directions normal to the curtain; by adding a reflecting curtain the array is made to produce a single beam.

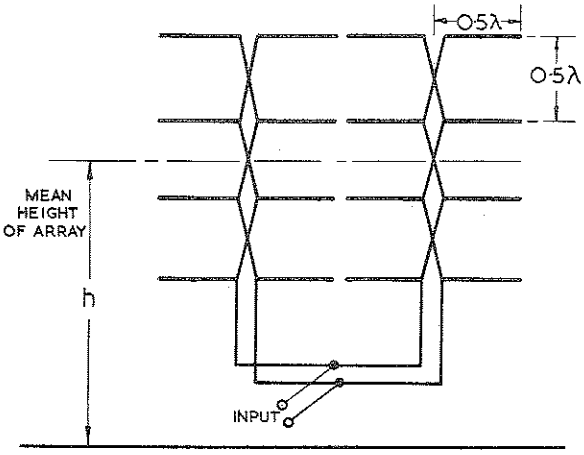

Fig. 3.2 - Typical curtain array

A typical curtain is shown in Fig. 3.2; it consists of four tiers spaced 0·5λ apart, each tier comprising four collinear 0·5λ elements placed end to end. The transmission line is transposed between tiers, so that the voltages applied to each 0·5λ + 0·5λ dipole are of the same amplitude and phase. Now the ratio of the voltage on a transmission line to the current at a point 0·25λ away is independent of the terminating impedance; and since we can regard each aerial element as approximating to a transmission line, it follows that the loop currents will be of the same amplitude and phase, independent of the radiation resistances of individual elements. The arrangement of Fig. 3.2 therefore automatically achieves the required equality of currents in the elements.

By way of example we will calculate the radiation pattern of the array shown in Fig. 3.2, using the co-ordinate system of Fig. 3.3(a). The collinear dipoles lie along the y-axis and the tiers are stacked vertically along the z-axis.

At the point P, co-ordinates (r, θ, ϕ), the field strength due to each 0·5λ element in free space is found by putting $h = 0{\cdot}25\lambda$ in Equation (2.1). We have

$$E_\psi = \frac{60 I_L}{r \sin\psi} \cos\left(\frac{\pi}{2}\cos\psi\right)$$

where I_L is the loop current and ψ is the angle between OP and OR; this contribution is in phase with that for a doublet carrying a co-phasal current placed at the centre

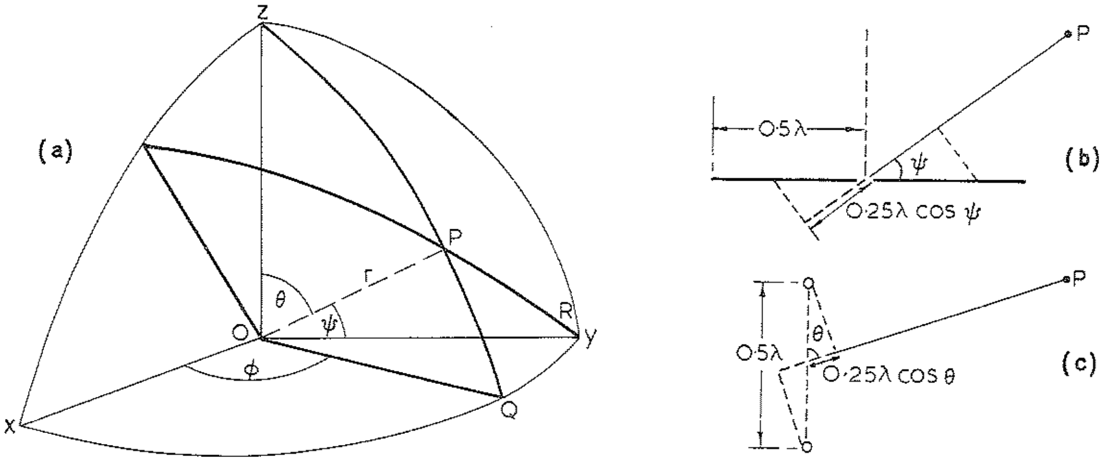

Fig. 3.3 - Co-ordinates of P

of the 0·5λ element. For two such 0·5λ elements placed end to end as in Fig. 3.3(b), relative to a source at the mid-point the contribution from one element leads and the other lags by a path difference 0·25λ cos ψ, i.e. by a phase angle

$$\frac{\pi}{2}\cos\psi\,;$$

the field strength is therefore

$$2\,E_\psi \cos\left(\frac{\pi}{2}\cos\psi\right),$$

the phase reference now being the mid-point of the two elements. Similarly the field strength due to four collinear elements is

$$E'_\psi = 2\,E_\psi\left\{\cos\left(\frac{\pi}{2}\cos\psi\right) + \cos\left(\frac{3\pi}{2}\cos\psi\right)\right\}$$

Proceeding in a similar manner, for two such tiers carrying co-phasal currents spaced 0·5λ apart as in Fig. 3.3(c), the field strength is

$$2\,E'_\psi \cos\left(\frac{\pi}{2}\cos\theta\right).$$

For four such tiers

$$E''_\psi = 2\,E'_\psi\left\{\cos\left(\frac{\pi}{2}\cos\theta\right) + \cos\left(\frac{3\pi}{2}\cos\theta\right)\right\}$$

Finally, we must take into account the effect of the ground; for horizontal polarisation this may be taken as perfectly conducting, and therefore equivalent to an image aerial carrying equal currents of opposite sign. If the mean height of the array above ground level is h, the effect of this image is to modify the radiation pattern by a factor $2\sin(\beta h\cos\theta)$. The complete radiation pattern is therefore given by combining the results given above; we obtain

$$E_{\psi,\,\theta} = \frac{480 I_L}{r\sin\psi}\cos\left(\frac{\pi}{2}\cos\psi\right)\left\{\cos\left(\frac{\pi}{2}\cos\psi\right)+\cos\left(\frac{3\pi}{2}\cos\psi\right)\right\}$$

$$\left\{\cos\left(\frac{\pi}{2}\cos\theta\right)+\cos\left(\frac{3\pi}{2}\cos\theta\right)\right\}\sin(\beta h\cos\theta) \qquad (3.3)$$

In passing it should be noted that the result is expressed as the product of two *independent* functions, one of ψ and the other of θ. Calculations of this kind can be greatly simplified, as in this case, by choosing the most suitable variables.

Inspection of Equation (3.3) shows that the effect of the in-line arrangement of elements is to narrow the radiation pattern in the ψ plane; this particular array, for instance, has zeros at ±30° to the normal to the elements. The number of tiers affects the sharpness of the beam in the θ plane and also the magnitude of the subsidiary higher-angle lobes; but if there are more than two tiers the term involving h largely determines both the projection angle and width of the main lobe in the θ plane. If, for instance, the lowest tier of the array shown in Fig. 3.2 is λ above ground level, h is then $1{\cdot}75\lambda$, and the last term in Equation (3.3) is maximum when $\theta = 82{\cdot}5^\circ$. In the θ plane the main lobe is therefore substantially sinusoidal in shape, with a maximum at 7·5° and zeros at 0° and 17° to the horizontal. Similarly, if the lowest tier were 2λ above ground level the maximum would be at 5° and the zeros at 0° and 10° to the horizontal.

In visualising the radiation pattern it is convenient to imagine the array as being at the centre of a sphere, on the surface of which points of equal field strength are joined by "contour" lines. For this purpose Equation (3.3) is expressed in terms of the latitude and longitude of P, rather than in terms of θ and ψ; the latitude is the complement of θ and the longitude ϕ is found by solving the spherical triangle PQR in Fig. 3.3(a) giving

$$\cos\psi = \sin\phi\sin\theta \qquad (3.4)$$

For plotting purposes the onion-shaped chart shown in Fig. 3.4 can be used. The length of the lines of latitude are proportional to the sine of the latitude; as a result, areas on this chart are equal to the corresponding areas on the surface of the sphere.

If the contours are designated according to *power* flow rather than field strength, the gain of the array can be derived graphically in a very simple manner. The contours are first normalised with respect to a maximum of say 100 units; the area between adjacent contours is then measured by means of a planimeter and multiplied by the average of the two extreme values of power flow, the contributions from all parts of the chart being added. A similar graphical integration is then carried out for the reference aerial, and the ratio of the two totals gives the gain of the array. For instance, the gain of the array whose radiation pattern is shown in Fig. 3.4 is 49, or 16·9 dB. From Equation (3.2) $Er/\sqrt{P}$ in the direction of maximum radiation is therefore 49.

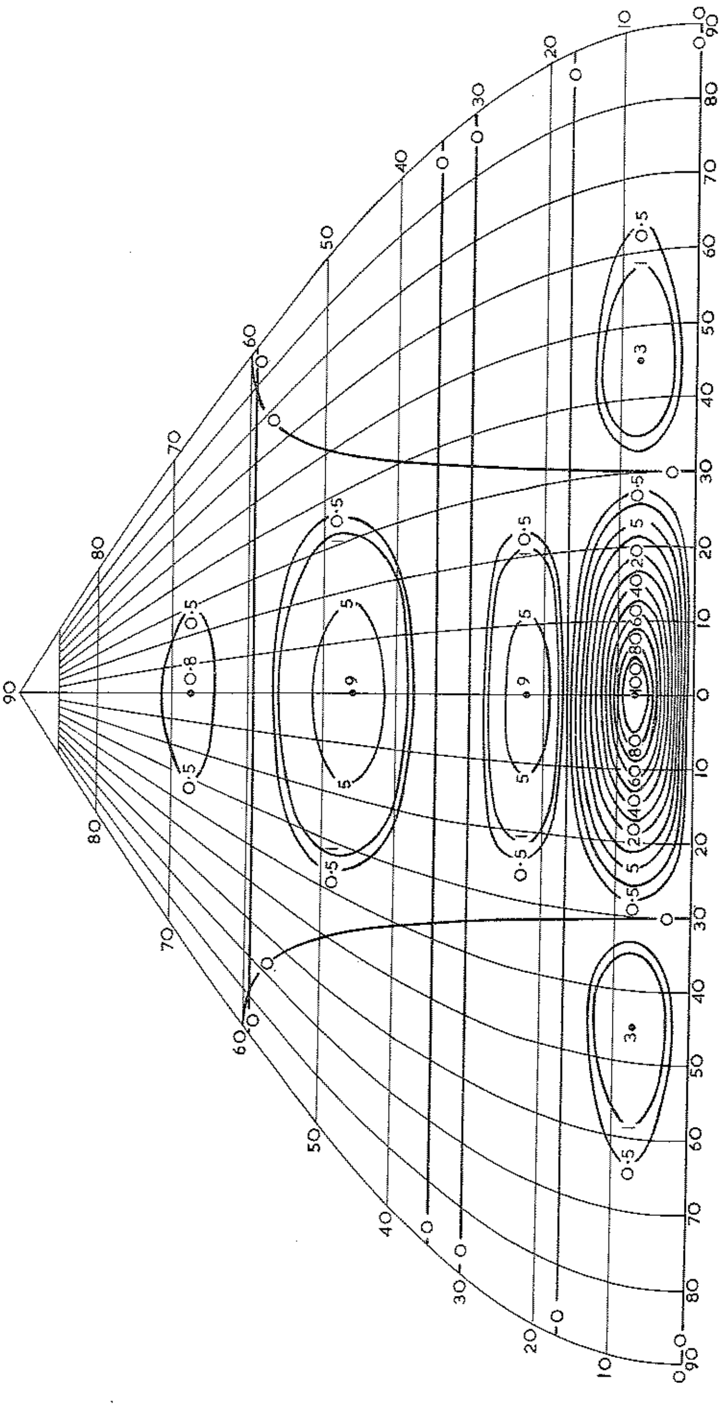

Fig. 3.4 - Power distribution pattern of curtain array comprising four tiers 0·5λ apart, each of four collinear 0·5λ elements placed end to end, the lowest row being λ above ground level

The corresponding pattern for a single 0·5λ aerial 0·5λ above ground level is shown in Fig. 3.5. The power gain in this case is 4·24 or 6·3 dB; $Er/\sqrt{P}$ is therefore 14.4. Note that the reference aerial is a hypothetical standard, since radiation into free space is specified; the benefit from using an array, rather than a single 0·5λ aerial having maximum radiation at the same projection angle, is less than the gain as defined by approximately 6 dB.

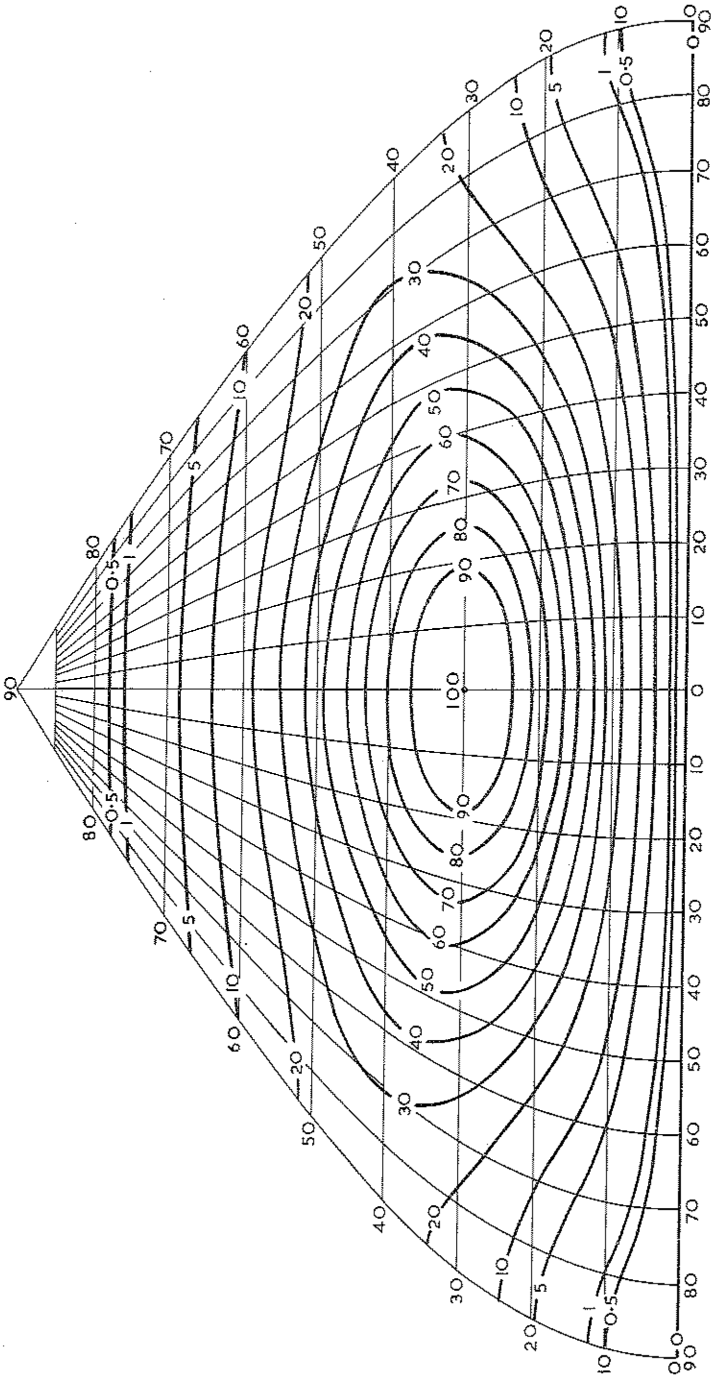

Fig. 3.5 - Power distribution pattern for 0·5λ aerial 0·5λ above ground level

The gain has so far been calculated using the Poynting-vector method.* An alternative method is to use the mutual impedance concept dealt with in Section 2.3, this being equivalent to calculating the gain by the induced-EMF method.*

---

*See Section 2.1.2.

For example, in the case of the 0·5λ aerial 0·5λ above ground level the effect of the perfectly-conducting ground is equivalent to that of a parallel 0·5λ aerial, spaced λ, carrying an equal current of opposite sign. Using Table 2, page 36, we find that the radiation resistance is 69·1 ohms. For the same loop current, the power in the reference aerial is therefore greater in the ratio 73·1/69·1, or 1·06; the maximum field strength for the aerial 0·5λ above ground level is double that for the reference aerial carrying the same current, since in this direction the direct and reflected waves add in phase. The gain is therefore 4 × 1·06, or 4·24. The gain of the more complicated arrays, for instance that shown in Fig. 3.2 can be calculated in a similar manner. A limited range of mutual resistance values suitable for such calculations has been published.[9]

The ability independently to control the horizontal beam width by the number of elements in each tier, and the vertical beam width and projection angle by the number of tiers and height above ground level, makes the curtain array particularly suitable in the planning of overseas broadcasting services.

The method we have used for deriving the radiation pattern can be applied to any form of curtain aerial. If there is an *odd* number of elements in each tier (or an odd number of tiers) the contribution from the central element (or tier) is considered first, the contributions from the adjacent elements (or tiers) added, and so on.

Single curtains are bi-directional; they radiate a beam in the direction of each of the two normals, whereas the usual requirement at any one time is a single beam. The power that would otherwise be wasted can be saved by providing a similar curtain of 0·5λ elements spaced 0·25λ behind the main curtain, as shown in Fig. 3.6. The additional curtain is tuned to act as a parasitic reflector by adjusting the position of a short circuit on the feeding line to which the generator would normally be connected. For typical multi-element arrays it is thus possible to reduce the

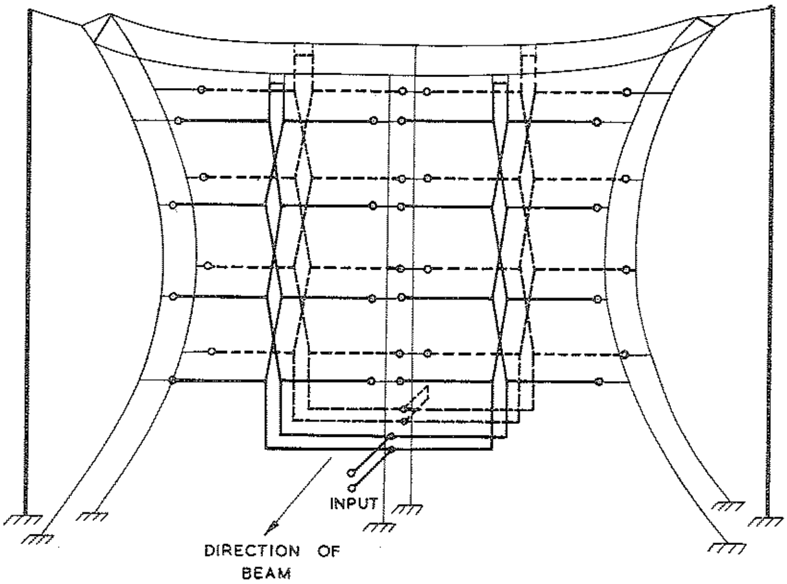

Fig. 3.6 - Unidirectional curtain array

field strength in the "back" direction to about 5% of that in the "forward" direction; in other words, the front-to-back ratio is 26 dB. This is greater than might be expected from the radiation pattern of a 0·5λ aerial and a similar parasitic element. However, the mutual impedance between two similar curtains is higher than that for two constituent elements spaced the same distance apart, and this accounts for the high front-to-back ratio achieved. The amount of power lost in the back direction is therefore negligible, and the increase in gain due to using a reflector curtain is 3 dB. As the two curtains are identical, by interchanging their functions the direction of the beam can be reversed.

It is possible to slew the beam over a small range of horizontal angles by off-setting the feeds to the two halves of the curtain, as shown in Fig. 3.7(a).

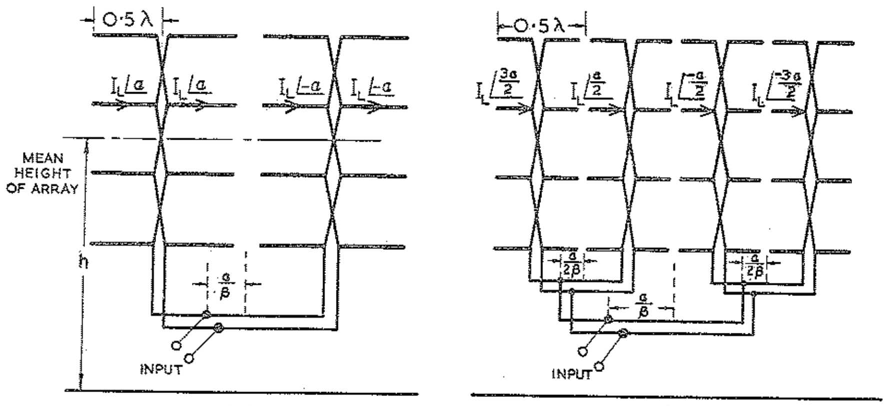

(a) (b)

Fig. 3.7 - Methods of slewing the beam of a curtain array

The currents in one half are advanced in phase relative to those in the other half, and the beam is therefore slewed in the direction of the lagging half. Here we assume that both halves of the curtain are individually matched to the transmission line, and that the mutual impedance between them is small so that the matching is unaffected when the array is slewed.

For the array shown in Fig. 3.7(a) for instance, where the tapping point is displaced from the mid-point by a length α/β corresponding to a phase difference of α radians, the radiation pattern is given by

$$E_{\psi,\,\theta} = \frac{480 I_L}{r \sin\psi} \cos\left(\frac{\pi}{2}\cos\psi\right) \left\{ \cos\left(\frac{\pi}{2}\cos\psi - \alpha\right) + \cos\left(\frac{3\pi}{2}\cos\psi - \alpha\right) \right\}$$

$$\left\{ \cos\left(\frac{\pi}{2}\cos\theta\right) + \cos\left(\frac{3\pi}{2}\cos\theta\right) \right\} \sin(\beta h \cos\theta) \qquad (3.5)$$

As α increases the main beam is slewed to an increasing extent, but a subsidiary lobe (or side lobe) develops in another direction; the amplitude of this side lobe increases and the gain of the array decreases with slew angle as shown in Fig. 3.8. To avoid an undue reduction in gain, arrays of the type shown in Fig. 3.7(a) are not slewed over a range greater than about ± 12°.

The permissible slewing range can be increased by the progressive phasing system shown in Fig. 3.7(b); for a progressive phase change of α radians between columns the radiation pattern is given by

$$E_{\psi,\,\theta} = \frac{480 I_L}{r \sin\psi} \cos\left(\frac{\pi}{2}\cos\psi\right) \left\{ \cos\left(\frac{\pi}{2}\cos\psi - \frac{\alpha}{2}\right) + \cos\left(\frac{3\pi}{2}\cos\psi - \frac{3\alpha}{2}\right) \right\}$$

$$\left\{ \cos\left(\frac{\pi}{2}\cos\theta\right) + \cos\left(\frac{3\pi}{2}\cos\theta\right) \right\} \sin(\beta h \cos\theta) \qquad (3.6)$$

Though more complicated than that shown in Fig. 3.7(a), we see from Fig. 3.8 that this arrangement permits a slewing range up to about ±30° before there is an appreciable reduction in the gain.

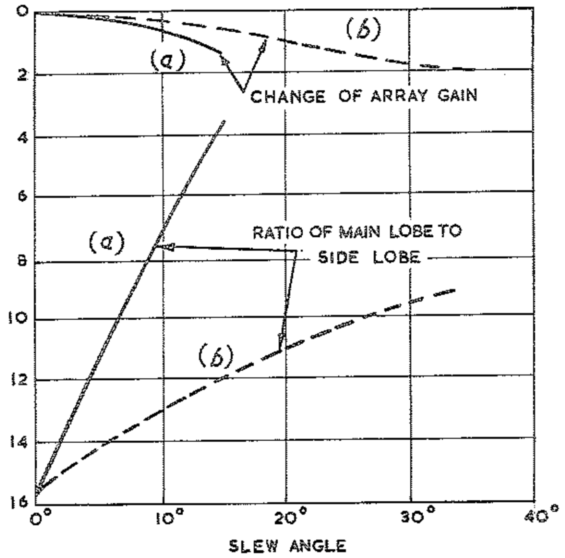

(a) Slewing method shown in Fig. 3.7(a)
(b) Slewing method shown in Fig. 3.7(b)

Fig. 3.8 - Performance of curtain array of the type shown in Fig. 3.7 as a function of slew angle

Curtain arrays of the type described are satisfactory over a frequency band of a few per cent, but beyond this range the gain falls rapidly due both to radiation in the back direction and to the change in the current distribution between elements; in addition, mismatching reduces the power handling-capacity. By using the branch-feeding arrangement shown in Fig. 3.9 these difficulties are largely overcome; the desired current distribution is achieved, and the matching is improved by using cages instead of relatively thin wires for the radiating elements. The bandwidth of arrays comprising such units is limited only by the change of the radiation pattern with frequency, or by power handling problems; in practice arrays can be designed to cover a frequency range equal to about 25% of the mid-band frequency.

An adaptation of the curtain array is shown in Fig. 3.10. The 0·5 λ elements are energised in the way already described, but the curtain is arranged *parallel* to the ground, and at a height of about 0·25λ. The contributions from the curtain and its image therefore reinforce each other in the vertical direction, and produce a beam directed vertically upwards. For this reason aerials of this type

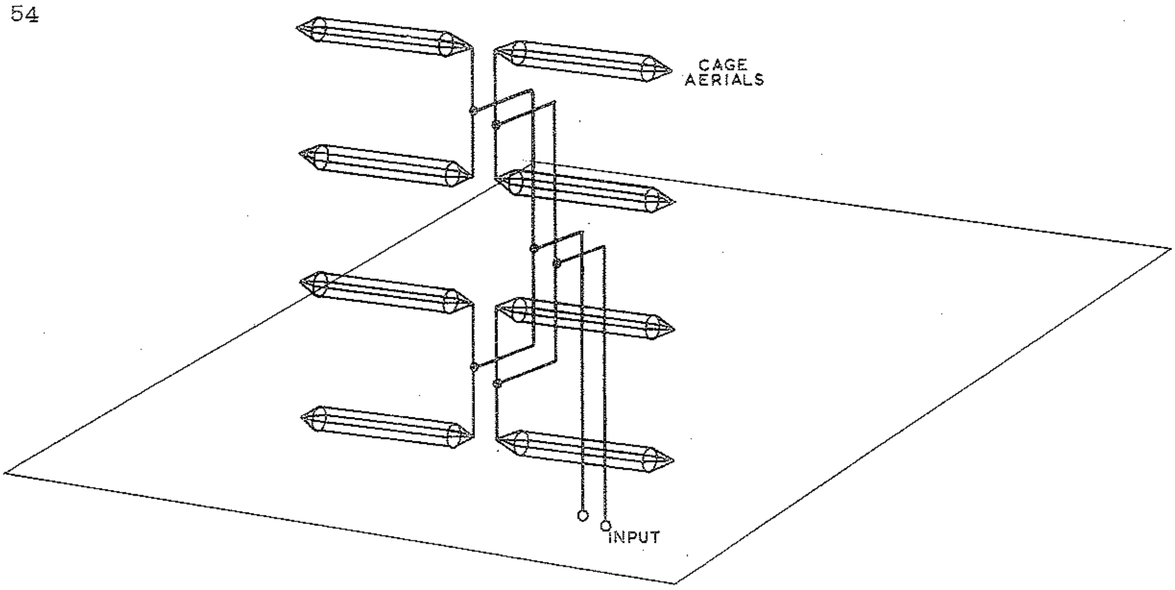

Fig. 3.9 - Branch feeding of curtain array

are sometimes called vertical-incidence arrays. They are used on frequencies for which the radiation is reflected from the ionosphere, and give coverage over a large area using a relatively cheap system. They are therefore employed for broadcasting to large sparsely-populated regions. The angular spread of the beam is determined by the number of elements in each row, and the number of rows in the array; the radiation pattern and gain can be calculated in the same way as for the conventional curtain array.

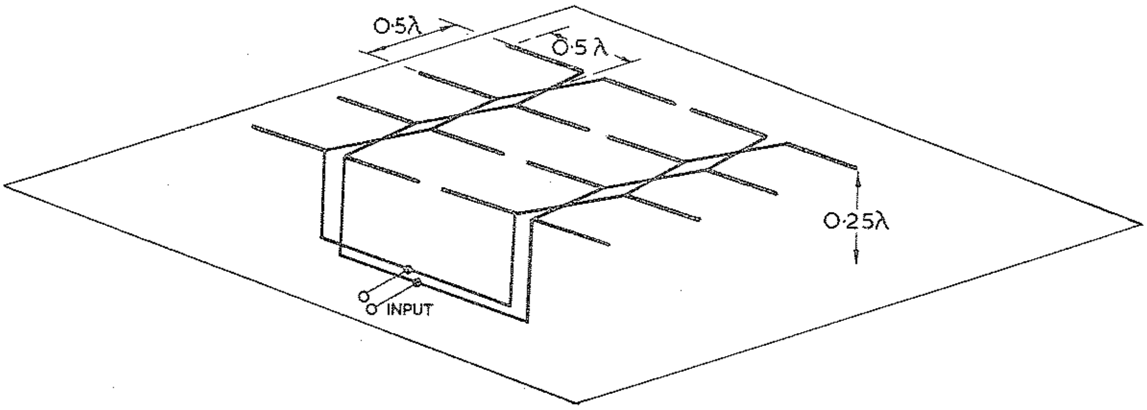

Fig. 3.10 - Vertical-incidence array

3.3. The End-Fire Array

The radiating elements in an end-fire array are arranged in line parallel to the ground, spaced at equal intervals of not less than 0·25λ; the currents are equal and in progressive phase as shown in Fig. 3.11. The contributions from individual elements at a great distance from the array are in phase in the direction in which the elements are spaced. The radiation pattern therefore takes the form of a single main lobe in this direction, together with a number of smaller side lobes;

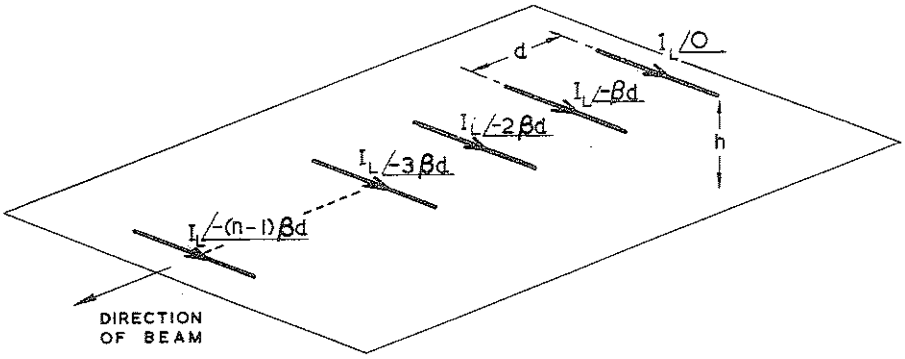

Fig. 3.11 - End-fire array

the angular spread of the main beam depends on the length, and the projection angle on both the length and height of the array. An advantage of this arrangement is that the height of the masts required to give a specified projection angle is less than for a curtain array. On the other hand, the lobe widths in the ϕ and θ planes are not independent, and this may sometimes be a disadvantage.

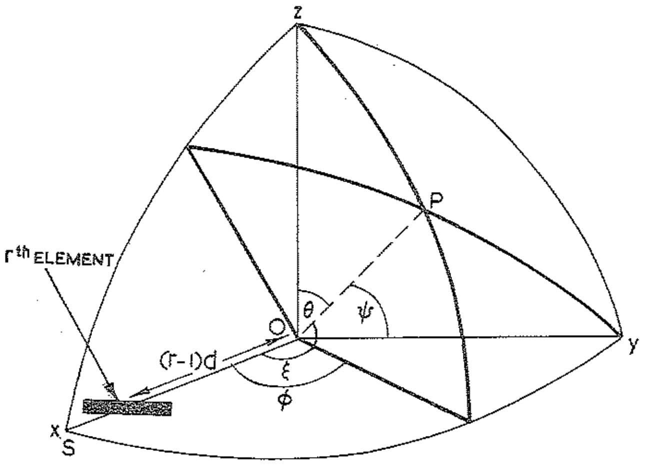

Fig. 3.12 - Co-ordinates of P

We will use the co-ordinate system shown in Fig. 3.12 to calculate the radiation pattern for an array of n elements, height h above ground level and spaced d apart in the direction of the x-axis.

Compared with the element at the origin the current in the rth element lags by a phase angle $(r-1)\beta d$, but the path to P is shorter by a length corresponding to a phase angle $(r-1)\beta d \cos\xi$, where ξ is the angle POS. If the field at P due to a single element located at the origin is $f(\psi)$, that due to the array over perfectly-conducting ground is given by

$$E = 2f(\psi)\left\{\sum_{r=1}^{n} e^{-j(r-1)\beta d(1-\cos\xi)}\right\}\sin(\beta h\cos\theta)$$

$$\left.\begin{array}{ll}
\text{or} & E = 2f(\psi)e^{-j\frac{(n-1)\beta d(1-\cos\xi)}{2}} \\
 & \qquad \left\{2\sum_{r=1,\,3,\,5\ldots}^{(n-1)} \cos\frac{(n-r)\beta d(1-\cos\xi)}{2}\right\}\sin(\beta h\cos\theta) \\
\text{if } n \text{ is even,} & \\
\text{and} & E = 2f(\psi)e^{-j\frac{(n-1)\beta d(1-\cos\xi)}{2}} \\
 & \qquad \left\{1+2\sum_{r=1,\,3,\,5\ldots}^{(n-2)} \cos\frac{(n-r)\beta d(1-\cos\xi)}{2}\right\}\sin(\beta h\cos\theta) \\
\text{if } n \text{ is odd.} &
\end{array}\right\} \quad (3.7)$$

If, for instance, each element is $0{\cdot}5\lambda$ long and carries a loop current I_L, if follows from Equation (2.1) that

$$f(\psi) = \frac{60 I_L}{r\sin\psi}\cos\left(\frac{\pi}{2}\cos\psi\right) \quad ;$$

ψ is given in terms of the co-latitude and longitude of P by Equation (3.4). Similarly ξ is given by

$$\cos\xi = \cos\phi\sin\theta \qquad (3.8)$$

The exponential term in Equation (3.7) affects only the *phase* of the field at P, and is left in merely to link up with the corresponding result for the rhombic aerial given later.

The progressive phasing requirement is usually achieved by terminating a transmission line in its characteristic impedance, and then coupling the radiating elements very weakly so as not to affect the matching of the transmission line appreciably. This is a convenient but necessarily a very inefficient arrangement, since the greater part of the power is then dissipated in the terminating resistor. One arrangement of this type is shown in Fig. 3.13, in which the weak coupling is achieved by connecting each radiating element through a small capacitance. In another arrangement very thin $0{\cdot}5\lambda + 0{\cdot}5\lambda$ dipoles (which consequently have a high driving-point impedance) are connected directly across the transmission line. These forms of end-fire array are sometimes used for reception in those cases where it is more important to discriminate against interference than to supply the maximum voltage to the input of the receiver.

The Yagi aerial (named after its inventor) is a type of end-fire array in which only one of the $0{\cdot}5\lambda$ elements is energised, the others being parasitic. The single reflector is spaced between $0{\cdot}15\lambda$ and $0{\cdot}25\lambda$ behind the energised aerial; the directors are spaced in front of the energised aerial at equal intervals of between $0{\cdot}1\lambda$ and $0{\cdot}15\lambda$. To achieve the correct phase relationship between the

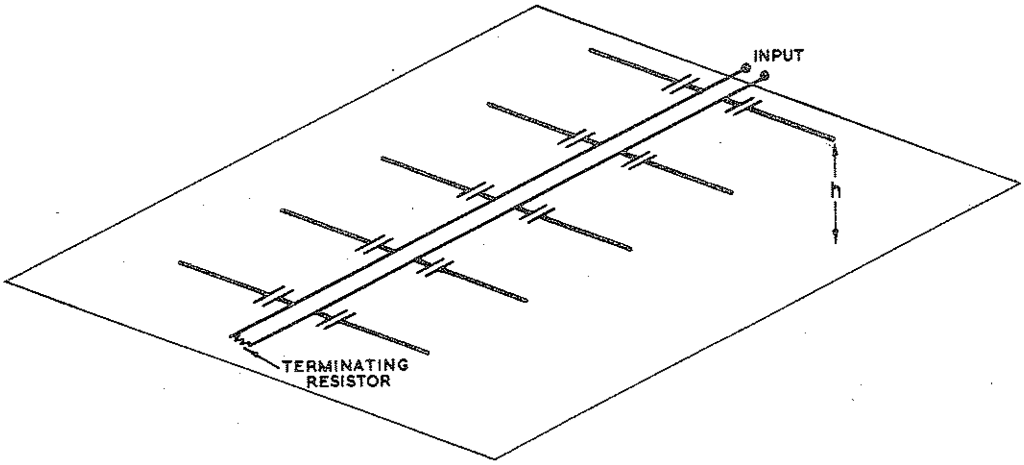

Fig. 3.13 - A practical form of end-fire array

currents, the reflector is made a little longer and the directors a little shorter than 0·5λ, by an amount depending on the radius of the elements. Since the current in the directors decreases with distance from the energised aerial there is a limit to the number it is worthwhile using; the maximum is usually four but ten or more are occasionally used if a high gain is required. The reflector and directors can be mounted on a central metallic boom. A 4-element Yagi aerial is shown in Fig. 3.14 together with its radiation pattern in the plane of the elements.

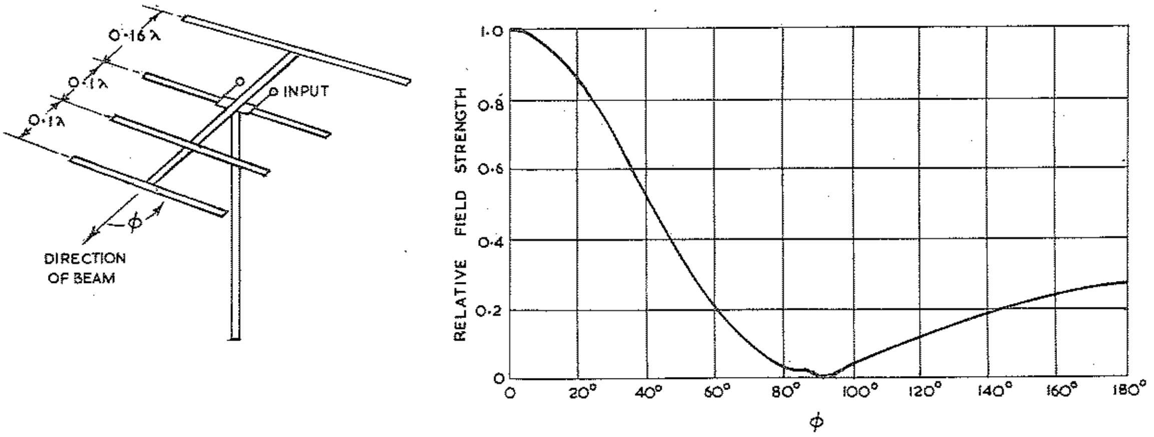

Fig. 3.14 - Measured radiation pattern of 4-element Yagi aerial

Although sometimes used in the high-frequency band the Yagi aerial is more commonly used for reception in the very-high-frequency band, for which the size of the elements is more convenient. The aerial has the advantage of having a relatively high gain for its size, but the gain falls and the impedance changes rapidly as the frequency deviates from the mid-band value; the percentage bandwidth is consequently small. This also means that small errors in the length of the parasitic elements appreciably affect both the radiation pattern and the impedance.

3.4. The Rhombic Aerial

This aerial, shown in Fig. 3.15 consists of a wire in the form of a horizontal rhombus, terminated in a resistance which matches the effective "transmission line" comprising the sides of the aerial. It may be regarded as a transmission line which has been "opened-out" to allow it to radiate.

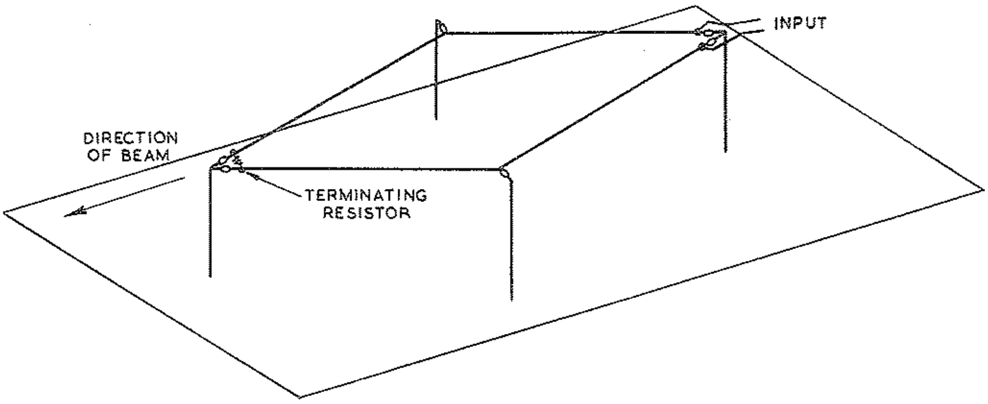

Fig. 3.15 - Horizontal rhombic aerial

The current distribution in each side of the rhombus approximates to a travelling wave; in other words, the amplitude is constant along the wire and the phase changes by 2π radians per wavelength. Before dealing with the radiation characteristics of the rhombic aerial it will be helpful to consider first the case of a wire in free space carrying a travelling wave; the co-ordinate system is shown in Fig. 3.16.

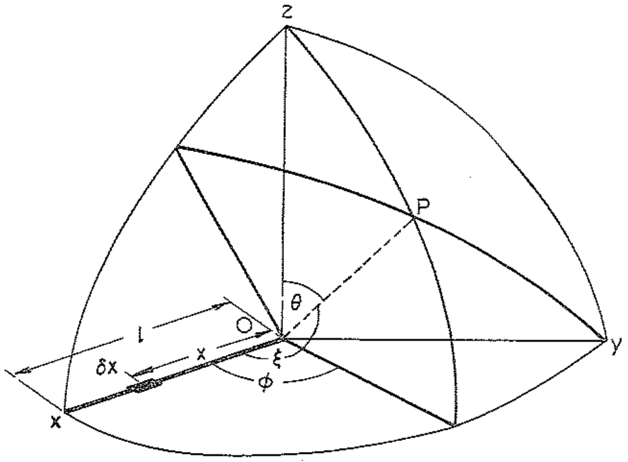

Fig. 3.16 - Co-ordinates of P

Let the wire, length l, lie along the x-axis with its input end at the origin; if the current here is I, at a point distance x from the origin the current is $Ie^{-j\beta x}$. The contribution to the field at P from the element δx therefore lags on that from a similar element at the origin by a phase angle βx on account of the phase of the current in the element, but it leads by an angle $\beta x \cos\xi$ on account of the shorter path length to P. Equation (1.19) gives the contribution from one element and the sum of all such contributions, E_ξ, can then be found. We will take as the reference for phase that of the field due to the element at the origin. For the horizontal wire in free space we therefore have

$$E_\xi = \frac{30I\beta\sin\xi}{r}\int_0^l e^{-j\beta x(1-\cos\xi)}\,dx$$

$$= \frac{60I}{r}\,e^{-j\frac{\beta l}{2}(1-\cos\xi)}\,\frac{\sin\xi}{(1-\cos\xi)}\,\sin\left\{\frac{\beta l}{2}(1-\cos\xi)\right\} \tag{3.9}$$

We can regard the wire carrying a travelling wave as equivalent to an end-fire aerial with a continuous distribution of radiating elements, each element having a radiation pattern proportional to sin ξ. The radiation is therefore concentrated round the surface of a cone whose axis lies along the wire. Since l is usually large compared with λ, the last term in Equation (3.9) largely controls the shape of the radiation pattern. The direction of maximum radiation is therefore at an angle given by

$$\beta l(1-\cos\xi) = \pi \tag{3.10}$$

If we feed two such wires in the form of a V from a balanced source, their contributions will reinforce each other in the plane of symmetry in a direction at an angle ξ to each wire, the value of ξ being given by Equation (3.10). This leads to the idea of an aerial in the form of a rhombus as providing a *practical* way of securing the required travelling wave on the radiating wires.

We will next calculate the radiation pattern for the general case of a rhombus of semi-angle γ; the aerial and co-ordinate system are shown in Fig. 3.17. We will take as the reference for phase that of the field due to an element at the origin, carrying a current in phase with that at the input of side (1). The contribution to the field at P from side (1), E_1, follows from Equation (3.9)

$$E_1 = \frac{60I}{r}\,e^{-j\frac{\beta l}{2}(1-\cos\xi_1)}\,\frac{\sin\xi_1}{(1-\cos\xi_1)}\,\sin\left\{\frac{\beta l}{2}(1-\cos\xi_1)\right\} \tag{3.11}$$

where, from Equation (3.8)

$$\cos\xi_1 = \cos(\phi-\gamma)\sin\theta \tag{3.12}$$

Since side (3) is parallel to side (1) its contribution, E_3, is similar in form, but the input current is $-Ie^{-j\beta l}$ instead of I, and the phase of the contribution is advanced by an angle $\beta l\cos(\phi+\gamma)\sin\theta$. Moreover, the two contributions are in the same direction, namely perpendicular to OP in the plane OPQ.

$$E_1+E_3 = \frac{60I}{r}\,e^{-j\frac{\beta l}{2}(1-\cos\xi_1)}\,\frac{\sin\xi_1}{(1-\cos\xi_1)}\,\sin\left\{\frac{\beta l}{2}(1-\cos\xi_1)\right\}$$

$$\left\{1-e^{-j\beta l(1-\cos\overline{\phi+\gamma}\sin\theta)}\right\} \tag{3.13}$$

Similarly, the contributions from sides (2) and (4) are perpendicular to OP in the plane OPQ′ and are given by replacing $(\phi-\gamma)$ by $(\phi+\gamma)$ and vice versa in Equations (3.12) and (3.13). The currents in sides (4) and (2) are opposite to those in

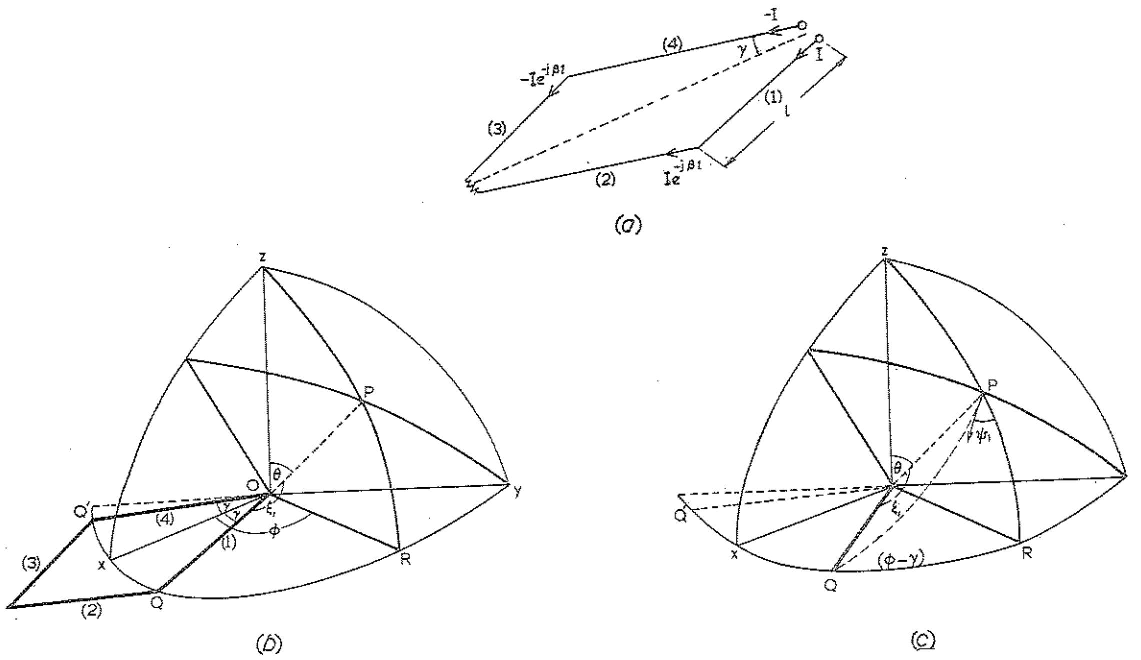

Fig. 3.17 - Co-ordinates of P

sides (1) and (3) respectively; we therefore obtain for the combined contribution

$$E_2+E_4 = -\frac{60I}{r}\, e^{-j\frac{\beta l}{2}(1-\cos\xi_2)}\, \frac{\sin\xi_2}{(1-\cos\xi_2)} \sin\left\{\frac{\beta l}{2}(1-\cos\xi_2)\right\}$$

$$\left\{1-e^{-j\beta l(1-\cos\overline{\phi-\gamma}\sin\theta)}\right\}$$

where ξ_2 is the angle POQ′ and

$$\cos\xi_2 = \cos(\phi+\gamma)\sin\theta \qquad (3.14)$$

To sum the contributions from the two pairs of sides we resolve them into E_θ and E_ϕ components. We have

$$E_\theta = (E_1+E_3)\cos\psi_1 + (E_2+E_4)\cos\psi_2$$

where ψ_1, ψ_2 are the spherical angles RPQ and RPQ′ respectively in Fig. 3.17(c).

Also $$E_\phi = (E_1+E_3)\sin\psi_1 + (E_2+E_4)\sin\psi_2$$

and the total field is $\sqrt{E_\theta^2+E_\phi^2}$. From the relationship between the sides and angles of the spherical triangle PQR, Fig. 3.17(c)

$$\sin\psi_1 = \frac{\sin(\phi-\gamma)}{\sin\xi_1}\,; \qquad \cos\psi_1 = \frac{\cos(\phi-\gamma)\cos\theta}{\sin\xi_1}$$

Similarly $$\sin\psi_2 = \frac{\sin(\phi+\gamma)}{\sin\xi_2}\,; \qquad \cos\psi_2 = \frac{\cos(\phi+\gamma)\cos\theta}{\sin\xi_2}$$

After some manipulation the modulus of the field at P can be expressed in the form

$$E = 240\,\frac{I\sin\gamma\sin\left\{\dfrac{\beta l}{2}\,(1-\cos\xi_1)\right\}\sin\left\{\dfrac{\beta l}{2}\,(1-\cos\xi_2)\right\}}{r\qquad\sqrt{1-\cos\xi_1}\qquad\qquad\sqrt{1-\cos\xi_2}} \tag{3.15}$$

where ξ_1, ξ_2 are given in terms of the co-latitude and longitude of P by Equations (3.12) and (3.14).

For the rhombic aerial at a height h above perfectly-conducting ground the corresponding expression is *

$$E = 480\,\frac{I\sin\gamma\sin\left\{\dfrac{\beta l}{2}\,(1-\cos\xi_1)\right\}\sin\left\{\dfrac{\beta l}{2}\,(1-\cos\xi_2)\right\}\sin(\beta h\cos\theta)}{r\qquad\sqrt{1-\cos\xi_1}\qquad\qquad\sqrt{1-\cos\xi_2}} \tag{3.16}$$

The optimum value of γ is found by making the maximum of the radiation pattern coincide with the required direction; in other words, the partial differentials with respect to θ and ϕ of the expression on the right-hand side of Equation (3.16) must be zero simultaneously. For maximum radiation in the direction of the rhombic ($\phi = 0$) and at an angle θ to the vertical we find that

$$\beta l(1-\cos\gamma\sin\theta) = 0{\cdot}74\,\pi \tag{3.17}$$

This differs from the condition given by Equation (3.10), which corresponds to the contributions from only *two* of the sides being in phase in the required direction. For any given values of l and θ Equation (3.17) determines γ; h is then chosen to make the last term in the numerator of Equation (3.16) maximum at the desired value of θ. The radiation pattern becomes sharper in both the horizontal and vertical planes, and the gain consequently increases, as the length of the side of the rhombus increases; in practice there must therefore be a compromise between the size of the aerial and its performance. A typical design for a point-to-point service is a rhombus having a side of 8λ and a semi-angle of 15°; for a broadcasting service a typical design is a rhombus having a side of 5λ and a semi-angle of 20°. The calculated radiation pattern for this latter aerial is shown in Fig. 3.18.

The pattern is characterised by a large number of subsidiary side lobes of appreciable amplitude. This means that a rhombic transmitting aerial is more likely to cause interference with other services working on the same frequency, or be subject to interference if used for reception, than if these side lobes were absent. Another disadvantage is that the widths of the main lobe in the ϕ and θ planes are inter-dependent, and also change with frequency. Fig. 3.19 shows the change of gain and

*The result could be simplified by expressing $(1-\cos\xi)$ in terms of the half-angle, but the form given in Equation (3.16) is more suitable for computation.

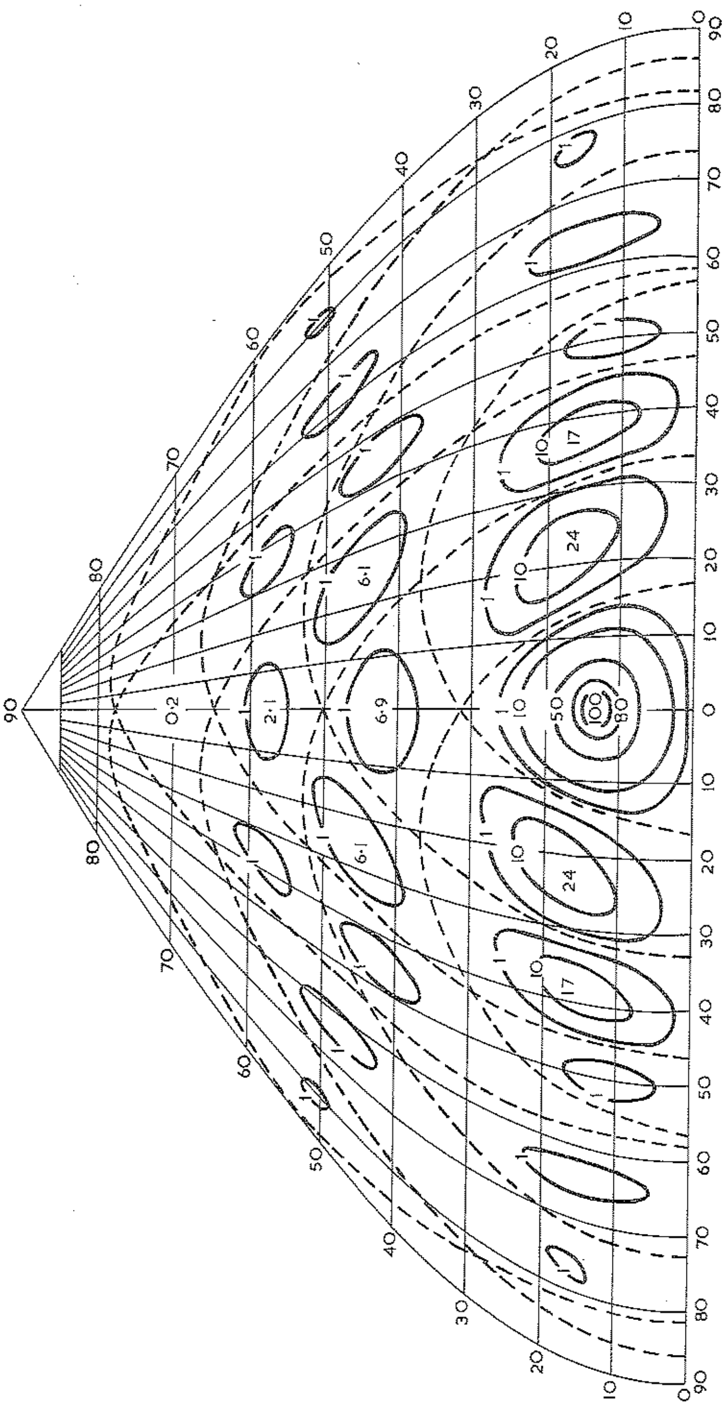

Fig. 3.18(a) - Power distribution pattern for rhombic aerial, $l = 5\lambda$, $\gamma = 20°$, $h = \lambda$ (forward direction)

beam width with frequency for a rhombic aerial typical of those used for point-to-point services.[10]

Power is dissipated in the resistor which terminates the rhombic aerial, so that the gain is less than that for the curtain array having a similar radiation

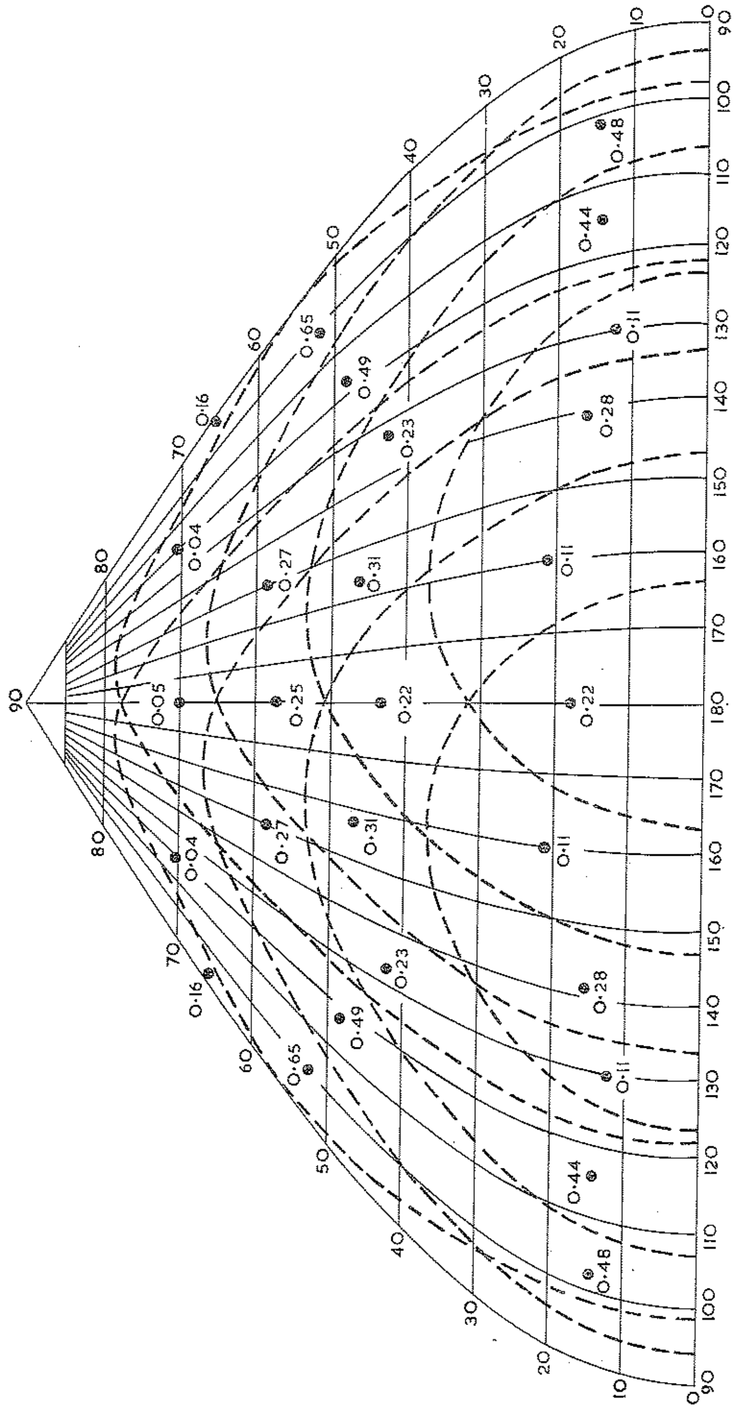

Fig. 3.18(b) - Power distribution pattern for rhombic aerial, $l = 5\lambda$, $\gamma = 20°$, $h = \lambda$ (backward direction)

pattern. The loss can be reduced by using two or three spaced wires in parallel; the characteristic impedance of the radiating wires is thereby reduced, and the attenuation of the current due to radiation is consequently increased. By this means it is possible to limit the power lost in the termination to about 30% of the input power. The resistor which terminates the rhombus is usually a balanced

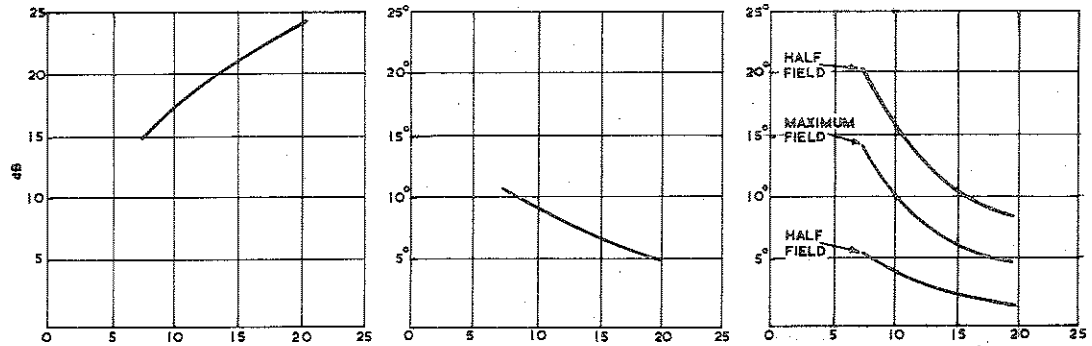

(a) Gain

(b) Horizontal beamwidth to half-field points

(c) Vertical beamwidth to half-field points

Fig. 3.19 - Characteristics of rhombic aerial, $l = 8\lambda$, $\gamma = 15^\circ$, $h = 2{\cdot}3\lambda$ at 15 Mc/s

transmission-line made of iron or steel. A resistance of about 800 ohms is required for the single-wire aerial, and about 500 ohms for the three-wire aerial. By interchanging the input and termination the direction of the beam can be reversed. The rhombic aerial is widely used for both transmission and reception in point-to-point services, and to a lesser extent for broadcast transmissions. The aerial is mechanically simple, and has both a good performance and a relatively constant input impedance over a frequency band of about one octave.

In the above analysis the radiation pattern has been calculated for an idealised case in which the current along the wires is assumed to be constant, whereas in practice the current decreases towards the termination as the result of the radiation of power. Although this affects the fine structure of the radiation pattern, measurements show that the practical performance does not differ appreciably from that of the idealised case. It does mean, however, that there is a limit to the length of the rhombus it is worthwhile using; in practice a side-length of about 8λ is rarely exceeded.

4. VERY-HIGH AND ULTRA-HIGH FREQUENCY AERIALS

4.1. General Considerations

The very-high and ultra-high frequency bands (30-300 and 300-3000 Mc/s respectively) are used mainly for purposes involving ranges up to the "radio horizon", i.e. a little beyond the optical range; these include point-to-point communications, broadcasting services, radio navigation and telemetering. A more restricted application, but one which is becoming increasingly important, is to services which rely on the "scatter" of energy from the ionosphere or troposphere; these are relatively inefficient, but offer the advantage of communication over long distances.

The design methods applying in the lower frequency bands are of course applicable in the higher bands; assemblies of elements can be arranged to give the required radiation characteristics, and their impedance calculated. However, the constituent $0{\cdot}5\lambda$ elements generally used are so small in these higher bands that new techniques become practicable, so much so that in the higher part of the ultra-high frequency band methods similar to those used in optics are much more convenient for shaping the beam of radiation; this change in technique occurs at roughly 1000 Mc/s. It is therefore convenient to consider in this section only those aerials involving assemblies of discrete radiating elements; the aerials involving techniques akin to those used in optics are outside the scope of this report.

The aerials under consideration will usually be at least one wavelength above ground level; in these circumstances, in most applications the surface wave is negligible compared with the space wave, and we need therefore to consider only the latter component. In many practical problems we are concerned with propagation along, or nearly along, the ground. We can approximate to this case as shown in Fig. 4.1, by considering a flat site, with a transmitting aerial T at a height h_1 and a receiving aerial R at a height h_2, spaced a distance d apart such that $d \gg h_1$, h_2. T$'$ is the image of T in the ground plane.

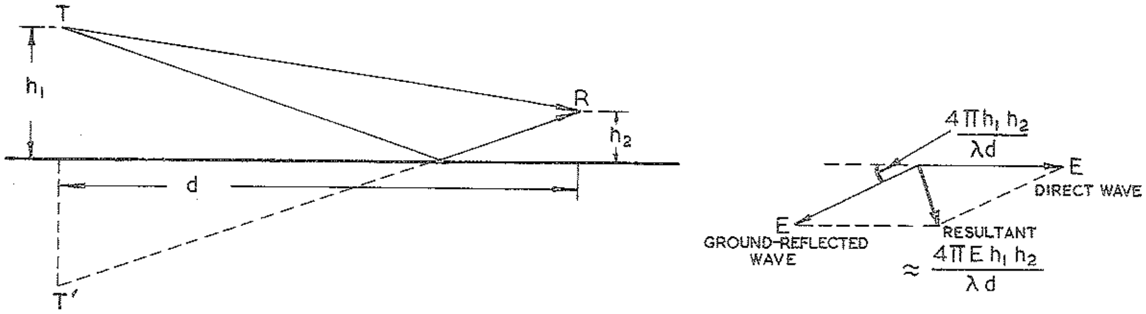

Fig. 4.1 - Transmission from T to R at nearly grazing incidence

The field at R is the resultant of the direct wave, path length

$$\mathrm{TR} = \sqrt{d^2 + (h_1 - h_2)^2} \approx d\left\{1 + \frac{(h_1 - h_2)^2}{2d^2}\right\}$$

and the ground-reflected wave, path length

$$\mathrm{T'R} = \sqrt{d^2 + (h_1 + h_2)^2} \approx d\left\{1 + \frac{(h_1 + h_2)^2}{2d^2}\right\}$$

The path difference is therefore $2h_1h_2/d$, and the corresponding phase difference is $4\pi h_1h_2/\lambda d$. Since the plane-wave reflection coefficient at grazing incidence is −1, independent of the characteristics of the ground (for both horizontally- and vertically-polarised waves), the phase difference between the direct wave and the ground-reflected wave is

$$\left(\pi + \frac{4\pi h_1 h_2}{\lambda d}\right).$$

If the field strength of the direct wave is E, the resultant field is therefore $4\pi E h_1 h_2/\lambda d$, since $d \gg h_1$, h_2. Now E is inversely proportional to the distance, d, so the resultant field strength varies inversely as the square of the distance. To achieve a high field for a given radiated power it is therefore necessary to make h_1 and h_2 as large as possible. It is often impracticable to make h_2 large, for instance in the case of broadcasting, or of reception in a vehicle. It is therefore desirable to build the transmitting station on a high site, and also to use a high aerial. The mast height is therefore determined by economic rather than technical considerations; in some cases regulations for the safety of aircraft may impose an upper limit.

We can look at this in another way. The radiated beam is elevated at a small angle to the ground. By increasing the height of the transmitting aerial we can depress the beam, and so increase the received field; but we are always at the disadvantage of working on the "skirt" of the vertical radiation pattern, whereas in the bands previously considered we endeavour to work in the direction of the *maximum* of the radiation pattern.

The propagation characteristics of the space wave are virtually the same for both horizontal and vertical polarisation, and both are used in practice. In the lower bands, on the other hand, we have seen that there is a preferred polarisation depending on the application.

The form of the performance specification over the working band depends on the purpose for which the aerial is used. The change in the shape of the radiation pattern may limit the bandwidth. In other cases the change of impedance is more important. If, for instance, we are transmitting a signal covering a relatively wide band of frequencies, such as that required for a television picture, small impedance mismatches between the aerial and the transmission line which feeds it will result in the signal being partially reflected. The signal reflected from the aerial will pass back to the transmitter where it will again be partially reflected, return to the aerial and be radiated as a "ghost" signal, delayed in time by two traversals of the transmission line. A small impairment of the shape of the transmitted signal may seriously affect the accuracy of a navigational aid or the quality of a television picture. In these cases only small deviations of the aerial impedance from the ideal are permissible, but this restriction applies over a band which is only a small percentage of the carrier frequency. The transmission lines used for feeding such arrays must also be substantially free from discontinuities. For multichannel communications services, on the other hand, although the working frequency band is very wide larger deviations of impedance from the ideal are usually permissible.

In some cases, for instance reception of broadcasting, the aerial must be a relatively simple mechanical structure such as a $0{\cdot}5\lambda$ dipole, an H aerial consisting of a $0{\cdot}5\lambda$ dipole and reflector (see Section 2.3.4) or a Yagi aerial comprising a $0{\cdot}5\lambda$ dipole, reflector and one or more directors (see Section 3.3). In cases where a greater degree of mechanical complexity is permissible, since the wavelengths involved are relatively short, highly directional arrays can be designed which are suitable for mounting on a single mast. The usual radiating element is a horizontal or vertical $0{\cdot}5\lambda$ dipole, because it is easy to support, it can be designed to have good bandwidth, and the impedance is convenient for matching to a co-axial transmission line.

A common arrangement is a number of tiers, each tier incorporating $0{\cdot}5\lambda$ elements, the tiers being energised in phase through coaxial lines in branch formation, similar to that shown in Fig. 3.9. If the array is required to radiate uniformly in all horizontal directions, the problem is to obtain a reasonable approximation to the requirement, taking into account the effect of the supporting mast. If a directional horizontal radiation pattern is required the supporting mast may be used as an aperiodic reflector. Alternatively, a reflecting screen can be incorporated into the array and attached to the mast; if the screen is sufficiently large the mast has little effect on the radiation characteristics.

There is an optimum spacing between tiers which gives the maximum gain. For two parallel $0{\cdot}5\lambda$ dipoles carrying equal co-phased currents the gain is maximum when the spacing is about $0{\cdot}7\lambda$; from Table 2 (p. 36) we see that the mutual resistance then has a maximum negative value. The spacing of $0{\cdot}5\lambda$ used for the high-frequency arrays described in Section 3.2 is for convenience in feeding the tiers, rather than to maximise the gain. The spacing giving the maximum gain depends on the number of tiers and the vertical variation pattern of individual tiers; a spacing of $0{\cdot}7\lambda$ between parallel elements, and λ between the centres of collinear elements, is near to the optimum for most arrangements.

4.2. The Folded Dipole

We have seen previously that the current distribution along a dipole is approximately the same as that along an open-circuited transmission line of the same length; the case of elements $0{\cdot}5\lambda$ long is illustrated in Fig. 4.2(a) and (b), the current distribution being shown dotted.

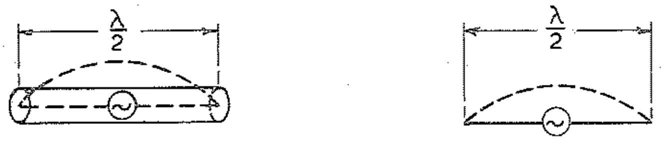

(a) Transmission line (b) Dipole

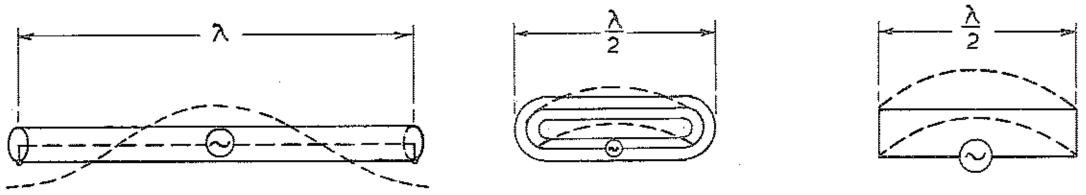

(c) Transmission line (d) Folded transmission line (e) Folded dipole

Fig. 4.2 - Current distribution along transmission line and equivalent dipole

Continuing this analogy, if we have a transmission line of length λ short-circuited at each end and energised at the centre, the current distribution is as shown in Fig. 4.2(c). Suppose that the line is hinged at the points where the current is zero, and that the outer portions are folded back on the inner portion, corresponding conductors of the folded portions being connected together at the junction, as in Fig. 4.2(d). No current then flows in the short circuit between the inner and outer conductors of the line, and it can therefore be omitted. The corresponding aerial is the "folded dipole" shown in Fig. 4.2(e), the spacing between the branches being a small fraction of the wavelength.

The general case of a folded dipole of length $2h$ is illustrated in Fig. 4.3. The single zero-impedance generator of voltage V in Fig. 4.3(a) can be replaced by two

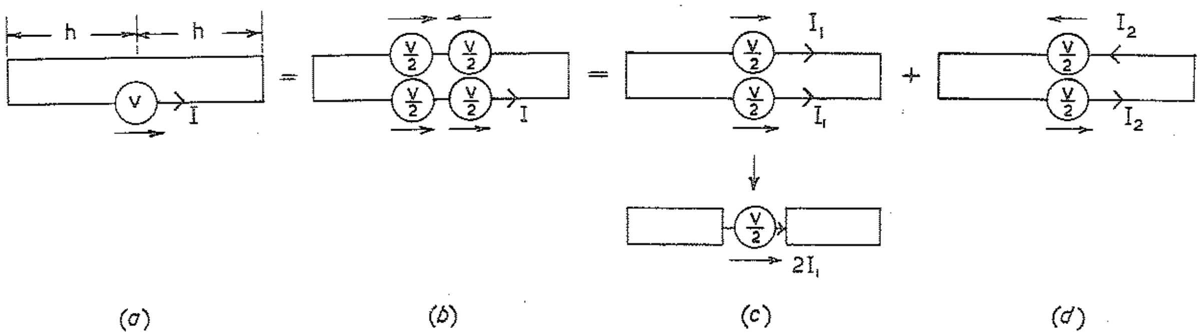

Fig. 4.3 - Equivalent circuit of folded dipole

zero-impedance generators of voltage $V/2$ in series in the lower branch; it is also permissible to insert two zero-impedance generators of voltage $V/2$ in opposition in the upper branch of the folded dipole, as in Fig. 4.3(b). By the superposition theorem we are allowed to consider the effect of these generators separately, as in Fig. 4.3(c) and (d). From considerations of symmetry, the currents in the upper and lower branches in Fig. 4.3(c), I_1, are equal and in the same direction; this circuit is equivalent to a centre-fed dipole comprising both branches in parallel, with a generator of voltage $V/2$ supplying a current $2I_1$. Similarly, the currents in the upper and lower branches of Fig. 4.3(d), I_2, are equal and opposite. The circuit of Fig. 4.3(d) therefore comprises two short-circuited transmission lines in series, with a generator of voltage V supplying a current I_2.

In Fig. 4.3, $I = I_1 + I_2$

i.e.
$$\frac{I}{V} = \frac{1}{4}\,\frac{2I_1}{V/2} + \frac{I_2}{V}$$

This can be written
$$A_{\text{folded dipole}} = \frac{1}{4} A_{\text{simple dipole}} - \frac{jY_0 \cot(\beta h)}{2} \qquad (4.1)$$

where $A_{\text{folded dipole}}$ is the admittance of the folded dipole, $A_{\text{simple dipole}}$ is the admittance of the centre-fed dipole in Fig. 4.3(c), and Y_0 is the characteristic admittance of the transmission lines in Fig. 4.3(d). A thin resonant 0·5λ dipole, for instance, has a purely resistive input impedance of 73 ohms; the corresponding folded dipole has a purely resistive input impedance of 292 ohms.

The conductance and susceptance of the simple dipole in the neighbourhood of 0·5λ resonance have the general form shown in Fig. 4.4, curves (a) and (b) respectively; these characteristics can be derived from the equivalent circuit of an aerial above perfectly-conducting ground (see Section 2.2.4). The susceptance of the folded dipole is found by adding to curve (b) curve (c), the susceptance of the transmission line system of Fig. 4.3(d), giving curve (d) in Fig. 4.4.

The conductance of the folded dipole therefore has a rather flat maximum in the neighbourhood of the 0·5λ resonance frequency, and the susceptance is small over a band of frequencies. The susceptance can in fact be made zero at two

(a) $\frac{1}{4}$ Conductance of simple dipole

(b) $\frac{1}{4}$ Susceptance of simple dipole

(c) Susceptance of transmission line system of Fig. 4.3(d)

(d) Susceptance of folded dipole

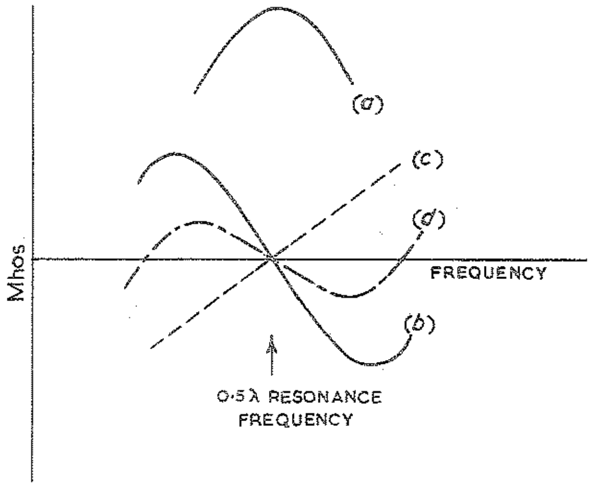

Fig. 4.4 - Admittance characteristics of simple and folded dipoles

frequencies, one on either side of the 0·5λ resonance frequency, provided Y_0 is sufficiently high. This means that to achieve an appreciable improvement in the bandwidth the branches must have relatively large dimensions; one such arrangement is shown in Fig. 4.5(a). Of course, as we have seen previously, an increase in the lateral dimensions has a beneficial effect on the bandwidth quite apart from the improvement due to folding.

In the foregoing analysis we have tacitly assumed that the resonance frequencies of the simple 0·5λ dipole and of the transmission line system are the same, whereas the former will be lower by an amount which increases with the lateral dimensions of the aerial (see Section 2.2.2). This merely means that a small susceptance may be required at the driving point to achieve the optimum bandwidth.

If the lateral dimensions of the folded branch are larger than those of the energised branch, the conductance at resonance will be less than one quarter of that of the simple dipole. This follows from the transmission line analogue in Fig. 4.2(c); it is equivalent to increasing the characteristic admittance of the folded branch, so that the maximum current flowing in it is greater than that in the energised branch. Conversely, if the lateral dimensions of the folded branch are smaller than those of the energised branch the input conductance is greater than one quarter of that of the simple dipole. Folding a 0·5λ dipole can therefore be used to increase the bandwidth, or to decrease the input conductance to any desired value, or both. An alternative form of folded dipole is shown in Fig. 4.5(b). Here the folded branch does not radiate; as a result, folding increases the bandwidth without affecting the input conductance. The folded dipole has the advantage that it can be conveniently supported by an arm attached at the mid-

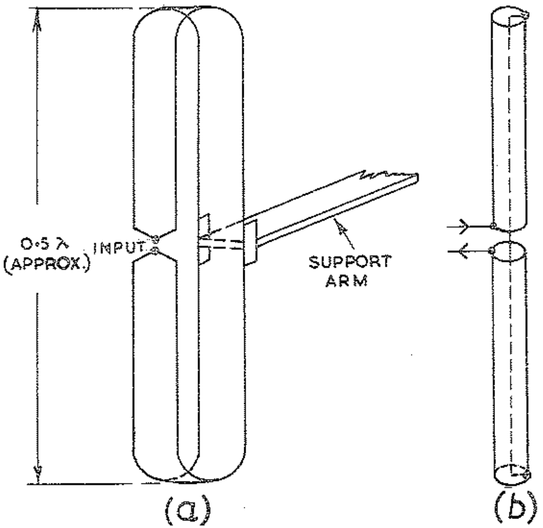

Fig. 4.5 - Two forms of 0·5λ folded dipoles

point of the folded branch, an arrangement which is only practicable in the higher frequency bands.

4.3. The Concept of Equivalent Generators

In the analysis of the folded dipole in Section 4.2 we found it useful to introduce the intermediate step of replacing the single generator by a number of generators having an equivalent effect. By grouping these generators into two sets and calculating their effects separately, we were enabled to derive a simple equivalent circuit. In such problems we are allowed to replace a short circuit by two zero-impedance constant-voltage generators in opposition, and an open circuit by two infinite-impedance constant-current generators of opposite sign in parallel. This concept of "equivalent generators" greatly simplifies calculations on certain types of aerial, and examples of its use are given in Sections 4.4 and 4.7.

4.4. Balanced-to-Unbalanced Impedance Transformations

If a balanced impedance, such as a centre-fed 0·5λ dipole, is fed from a balanced transmission line, as shown in Fig. 4.6(a), from considerations of symmetry the currents in the two wires of the line are equal and opposite. The transmission line therefore does not radiate, and the currents in the two halves of the dipole are equal. The system behaves as if the transmission line did not exist, and there were an isolated generator connected in series at the centre of the dipole; this is the arrangement we have envisaged throughout in calculating the radiation characteristics of such an aerial.

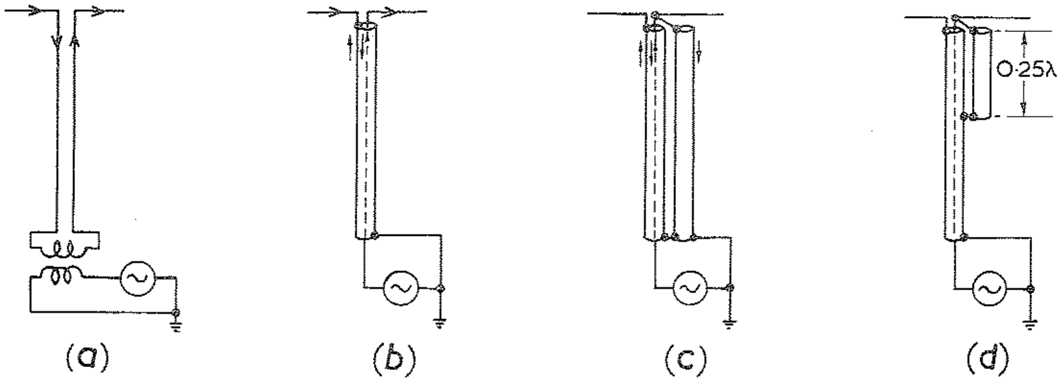

Fig. 4.6 - Methods of connecting a balanced aerial to a generator

It is often convenient to use a coaxial line for connecting the generator to the aerial; if the line is perfectly screened the currents on the inner conductor and the inner surface of the screen must be equal and opposite.

In the arrangement shown in Fig. 4.6(b) the current on the inner surface of the screen divides at the junction with the aerial, part flowing into one half of the dipole and part down the outer surface of the screen. This means that the screen acts as an aerial and radiates, and also that the currents in the two halves of the dipole are unequal. Both the radiation pattern and the impedance are therefore affected, in a manner determined by the length and disposition of the line with respect to earth. This unsatisfactory state of affairs can be corrected by using a length of "balancing" line, as shown in Fig. 4.6(c), thus restoring symmetry. The length of the "balancing" line is unimportant except insofar as it affects the impedance presented to the coaxial line at the aerial driving point. This impedance is equal to that of the dipole, in parallel with that of a short-circuited transmission line formed by the two lengths of coaxial-line outer screens. By making this length 0·25λ, as shown in Fig. 4.6(d), a balanced-to-unbalanced transformation is achieved without change of impedance. The balance of the aerial is maintained at all frequencies; but the impedance, and hence the bandwidth, is affected by the balancing system. If the characteristic impedance of the short-circuited 0·25λ line is appropriately chosen it can in fact appreciably increase the bandwidth, in the same way that folding can increase the bandwidth of a 0·5λ dipole.

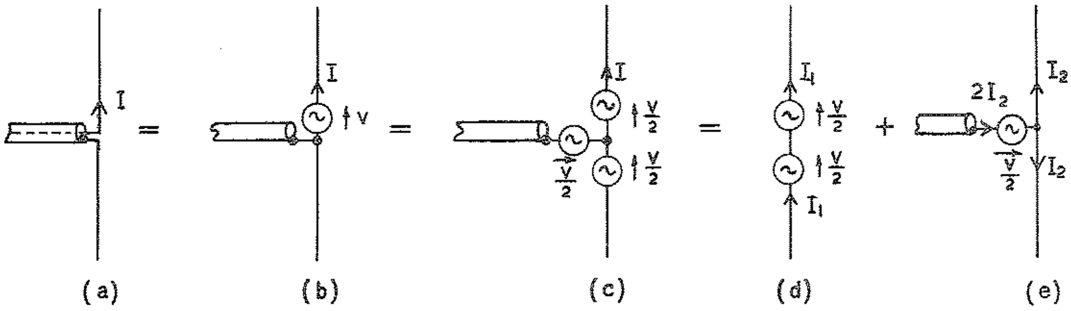

Fig. 4.7 - Equivalent circuit of balanced dipole connected to unbalanced source

The performance of the balanced dipole energised from a coaxial line is best visualised using the equivalent generator concept (see Section 4.3) in the manner shown in Fig. 4.7. The current flowing in the system is the sum of that in a dipole fed from an isolated generator of voltage V, I_1, and that through the circuit of Fig. 4.7(e), I_2; if the dipole is resonant I_1 will tend to be large compared with I_2. The effect of the current flowing on the outer of the coaxial line will therefore be least harmful at or near the resonance frequency of the dipole; it could be calculated taking into account the disposition of the coaxial feeding line.

In Fig. 4.7, $I = I_1 + I_2$

i.e. $$\frac{I}{V} = \frac{I_1}{V} + \frac{1}{4}\,\frac{2I_2}{V/2}$$

The admittance of the arrangement of Fig. 4.7(a) is therefore that of a centre-fed dipole fed from an isolated generator, plus one quarter of the admittance of the circuit shown in Fig. 4.7(e).

In Fig. 4.7 we have shown the coaxial line as perpendicular to the aerial; this means there is no radiation coupling between them. If there is any departure from this disposition (if, for instance, any part of the line is parallel to the aerial) an *additional* current will flow on the screen as a result of radiation coupling. But provided the coaxial line is arranged symmetrically with respect to the aerial up to a distance of at least 0·5λ from it, this effect will be small.

Some typical balanced-to-unbalanced transformations are shown in Fig. 4.8. In Fig. 4.8(a) the arrangement of Fig. 4.6(d) is simulated by cutting a slot 0·25λ

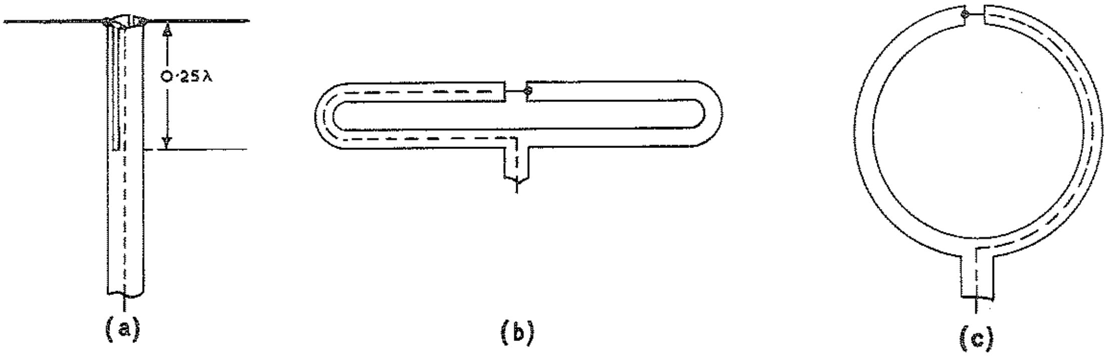

Fig. 4.8 - Typical balanced-to-unbalanced transformations

long in the outer of the transmission line. Fig. 4.8(b) shows a method of connecting an unbalanced source to a folded dipole, and Fig. 4.8(c) to a loop aerial, without affecting the balance of the aerials.

The methods so far described of transforming from balanced to unbalanced impedances are independent of the frequency as far as the *radiation characteristics* are concerned, although as stated earlier in this section they may affect the variation with frequency of the *impedance* presented to the coaxial line.

Methods of transforming from balanced to unbalanced impedance are sometimes used in which the transformation is ideal only at the design frequency. One method used in association with a vertical 0·5λ aerial is shown in Fig. 4.9(a). The lower half of the aerial takes the form of a "sleeve" 0·25λ long short-circuited to the outer of the feeding line at the driving point. The equivalent circuit is shown in Fig. 4.9(b); here X is the reactance of the short-circuited 0·25λ line formed by the outer of the coaxial line and the sleeve. Since X is infinite at the design frequency the lower half of the dipole is effectively isolated from the feeding system; however, at other frequencies X falls rapidly, since the lateral dimensions of the two portions of the short-circuited 0·25λ line are usually comparable, and the characteristic impedance of the combination is therefore low. Another disadvantage is that there is appreciable radiation coupling between the aerial and the nearer part of the outer of the coaxial line. Its effect can be minimised by adding another sleeve at an appropriate point as shown in Fig. 4.9(c); the equivalent circuit of this arrangement is shown in Fig. 4.9(d).

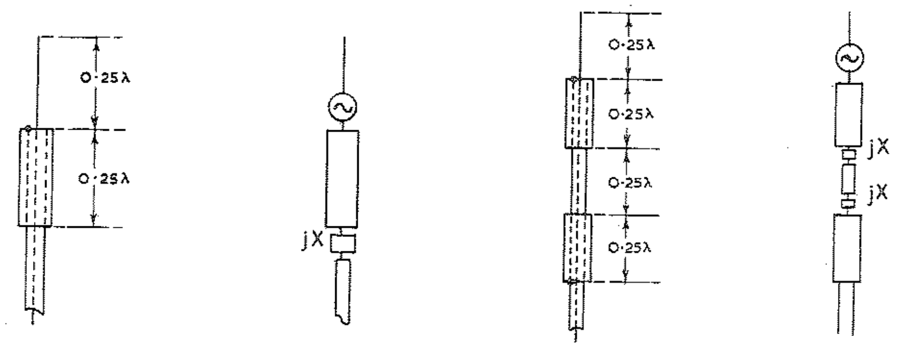

(a) Mechanical arrangement

(b) Equivalent circuit of (a)

(c) Aerial with double "sleeve"

(d) Equivalent circuit of (c)

Fig. 4.9 - Balanced-to-unbalanced transformation using a "sleeve"

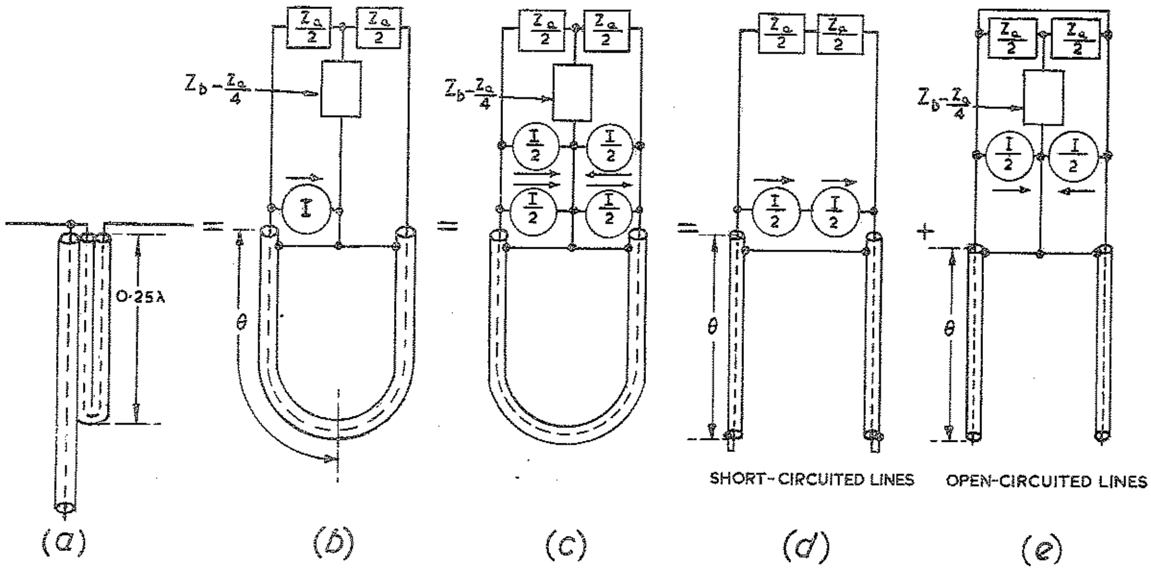

Fig. 4.10 - Balanced-to-unbalanced transformation using 0·5λ line

Another method of transforming from balanced to unbalanced impedance is shown in Fig. 4.10(a). One half of the balanced dipole is connected to the inner of the coaxial feeding line, and the other half to the same point through an additional line 0·5λ long. In order to calculate the performance over a frequency band we will consider the more general case, where the additional line has an equivalent electrical length of 2θ radians. The operation of this circuit is most easily visualised by using the concept of infinite-impedance constant-current generators. Let the impedance of the balanced aerial in the absence of the feeding line be Z_a and the impedance between the aerial terminals, when commoned, and the screen of the coaxial line be Z_b. The equivalent circuit is then as shown in Fig. 4.10(b), where I is the current supplied by a constant-current generator located at the point where the main line is connected to the aerial. An equivalent arrangement is shown in Fig. 4.10(c), which can be regarded as the sum of the two systems shown in Fig. 4.10(d) and (e). The voltage applied by the original generator is the sum of the voltages supplied by these two systems, i.e.

$$\frac{1}{2}\,\frac{I}{2}\,\frac{j2Z_aZ_0\tan\theta}{Z_a+j2Z_0\tan\theta}-\frac{I}{2}\,\frac{j2Z_bZ_0\cot\theta}{2Z_b-jZ_0\cot\theta}$$

The impedance presented to the original generator is therefore

$$\frac{1}{4}\,\frac{Z_a}{1-j\dfrac{Z_a}{2Z_0}\cot\theta}-j\,\frac{\frac{1}{2}Z_0\cot\theta}{1-j\dfrac{Z_a}{2Z_b}\cot\theta}$$

At the design frequency $\cot\theta = 0$, and the input impedance is $Z_a/4$; the currents flowing in the two halves of Z_a are then equal. At other frequencies they are unequal to an extent which can be calculated from the equivalent circuit, provided Z_a and Z_b are known.

4.5. The Radiation Pattern of an Aerial Mounted on a Cylindrical Mast

A mast supporting an aerial reflects some of the incident radiation and consequently affects the radiation pattern of the aerial. A solution has been obtained for a doublet mounted on an infinitely-long cylindrical mast,[11] and the derivation is given in Section 7.3. We will consider here only the principle of the method, and the results in some typical cases.

In previous problems we have found it convenient to regard the aerial under investigation as transmitting; however, in the present case the analysis is simplified by considering the aerial as receiving. We assume a transmitting doublet at a large distance from the cylinder, and calculate the electric force it produces at any specified point near to the cylinder. This electric force is proportional to the voltage that would be induced in a receiving doublet located at the point in question; its variation with direction from the transmitting doublet gives the required radiation pattern. Depending on whether we require the performance of a vertical,* tangential or radial element mounted on the cylinder, the corresponding field component is calculated.

In problems involving cylinders, insertion of the boundary conditions is facilitated by expressing Maxwell's equations in cylindrical co-ordinates. The field in the vicinity of the cylinder due to the transmitting doublet alone can then be expressed in the form of an infinite series of Bessel functions of the first kind having known coefficients. The field associated with the currents flowing on the cylinder can be expressed in the form of an infinite series of Hankel functions of the second kind having arbitrary coefficients. The sum of these two components must satisfy the boundary condition that the tangential component of electric force is zero at the surface of the perfectly-conducting cylinder. The coefficients of the Hankel functions are thus determined, and an expression can be obtained for the field at any point in space; from this we can derive the magnitude and phase of the voltage induced in the receiving doublet, and hence the radiation pattern of the doublet.

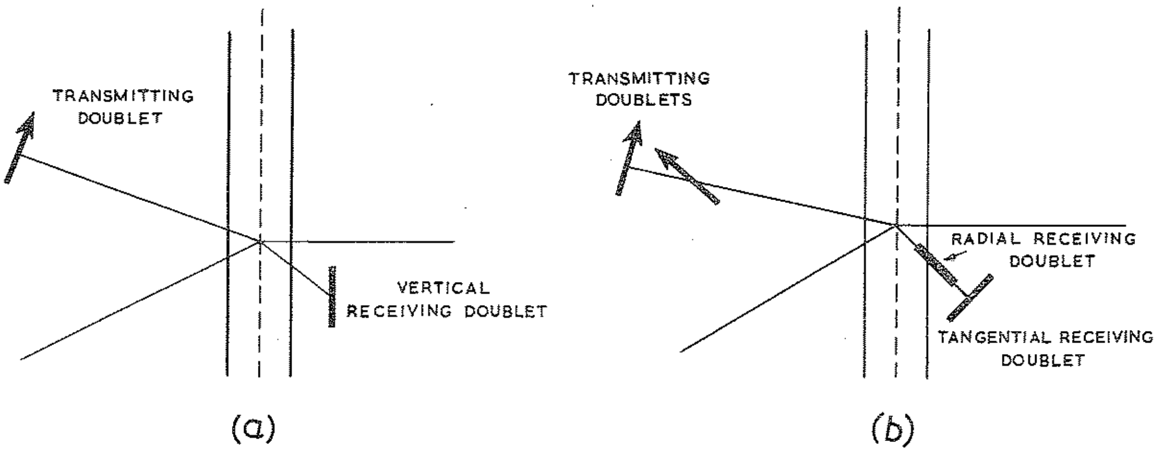

Fig. 4.11 - Transmitting doublets giving rise to fields in the direction of vertical, tangential and radial receiving doublets mounted on a cylindrical mast

---

*The axis of the cylinder is taken to be vertical.

The only field component in the direction of a vertical receiving doublet is that due to a transmitting doublet perpendicular to the radius vector in the plane of incidence, as shown in Fig. 4.11(a). For a tangential or radial receiving doublet there are field components due to the two transmitting doublets shown in Fig. 4.11(b). Both are perpendicular to the radius vector, one being in and the other normal to the plane of incidence. In the horizontal plane containing the receiving doublet, and also in the vertical plane of symmetry, one or the other of these components is zero.

The polarisation of the waves radiated by an aerial mounted on a cylindrical mast is found by interchanging the transmitting and receiving doublets in Fig. 4.11. Thus a vertical doublet radiates only vertically-polarised waves. A tangential or radial doublet in general radiates a combination of horizontally-polarised and vertically-polarised waves; but in the horizontal plane containing the doublet both radiate only horizontally-polarised waves, and in the vertical plane of symmetry the tangential doublet radiates only horizontally-polarised waves and the radial doublet radiates only vertically-polarised waves.

Reverting to the case shown in Fig. 4.11, the field can be considered as the sum of two components, the primary field due to the distant transmitting doublet and the secondary field due to the waves reflected by the cylinder. When the distance of the receiving doublet from the surface of the cylinder is comparable with or greater than the cylinder radius, the infinite series for the primary field converges much more slowly than that for the secondary field. In such cases it is less laborious to calculate the primary field due to the incident plane-wave directly, without using the series expansion. The secondary field is then calculated from the infinite series of Hankel functions, and the two components combined.

By way of example, Fig. 4.12 shows the horizontal radiation patterns of a vertical doublet mounted at a distance of 0·24λ from the axis of a cylindrical mast, for three different values of mast radius; for comparison purposes the curves have been normalised to the same maximum field strength. The smaller the radius of the mast the less its effect on the radiation pattern; however, Fig. 4.12 shows that a mast of surprisingly small radius alters the shape of the pattern appreciably.

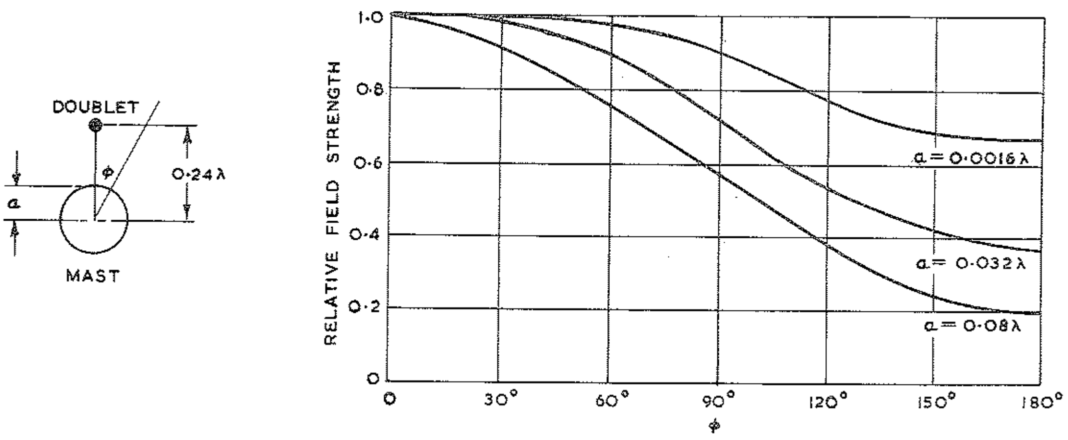

Fig. 4.12 - Horizontal radiation patterns of vertical doublet spaced 0·24λ from axis of cylindrical mast

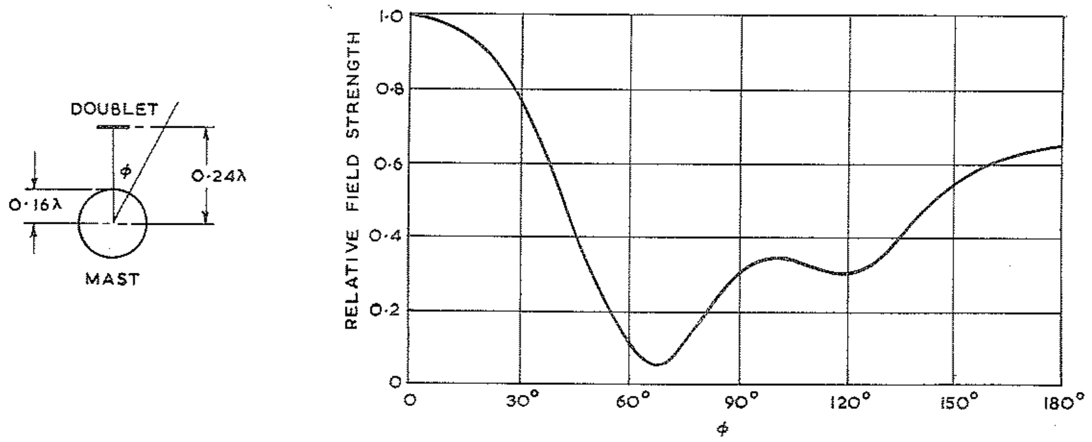

Fig. 4.13 - Horizontal radiation pattern of tangential doublet spaced 0·24λ from axis of cylindrical mast, radius 0·16λ

Fig. 4.13 shows the horizontal radiation pattern of a tangential doublet spaced 0·24λ from the axis of a cylindrical mast of radius 0·16λ. Here the main effect of the mast is to blur the zeros in directions end-on to the doublet, and to introduce a partial "shadow" behind the mast.

Fig. 4.14 shows the horizontal radiation pattern of a radial doublet on a mast of radius 0·15λ. From considerations of symmetry, the radiation pattern of any radial aerial on a cylindrical mast will have zeros in line with the aerial.

The foregoing discussion has been concerned with the radiation patterns of doublets mounted on a cylindrical mast, whereas the usual radiating element is a 0·5λ dipole; the results are not very different in this case, because the radiation patterns of both elements in free space are similar. A dipole is equivalent to a series of collinear doublets. For a vertical 0·5λ dipole it follows that the horizontal radiation pattern is the same as for a doublet spaced the same distance

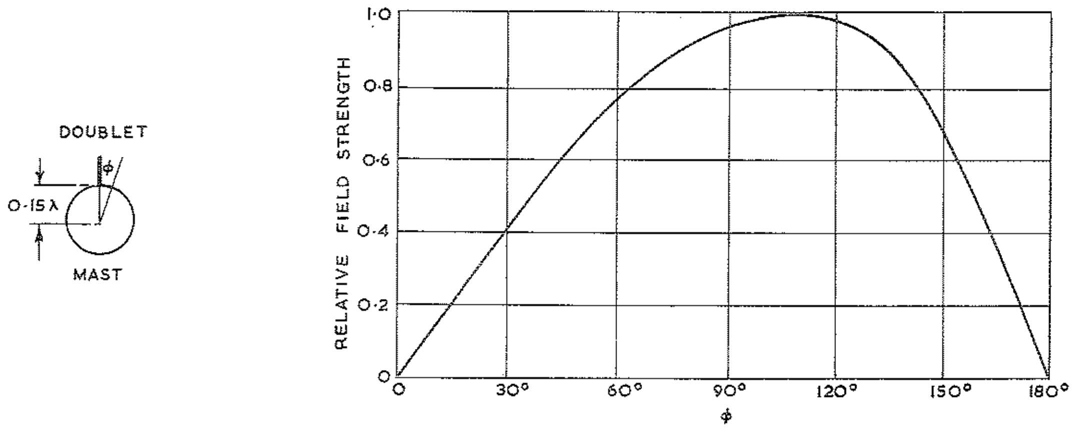

Fig. 4.14 - Horizontal radiation pattern of radial doublet on cylindrical mast, radius 0·15λ

from the axis, while the vertical pattern is modified in the same ratio as for a $0{\cdot}5\lambda$ dipole and a doublet in free space. No such simple modification applies in the case of tangential or radial $0{\cdot}5\lambda$ dipoles, because the spacing of the component doublets from the axis is not constant. The foregoing theoretical method can of course be applied, but its application is very laborious. A method which is sufficiently accurate for the tangential $0{\cdot}5\lambda$ dipole is to calculate the primary field directly, as described earlier in this Section, and then to approximate to the secondary field by assuming the dipole takes the form of an arc of a circle concentric with the cylinder.

The theoretical results discussed above apply for an infinitely-long cylindrical mast; in practice a mast behaves substantially like one infinitely long if it extends at least one half-wavelength above and below the radiating elements.

The performance of an array mounted on a cylindrical mast can be found by adding the contributions of individual elements;[11*] arrangements giving the required shape of radiation pattern can then be devised. The performance of such arrays can also be determined experimentally. The usual method is to make a small-scale model of the array, and then to measure the variation in the pick-up from a distant transmitting aerial as the model is rotated; such tests are carried out at a wavelength bearing the same ratio to the working wavelength as the ratio of the dimensions of the model and the full-scale aerial.

Experimental methods are essential if the performance of an array mounted on a mast of non-circular cross section must be known accurately. An approximate theoretical method which is satisfactory if the cross sectional dimensions are small compared with the wavelength is to take as the equivalent cylindrical mast one having the same capacitance per unit length. A method for dealing with larger masts of triangular and square cross-section has been published,[12] but it involves laborious computation.

4.6. Aerials Having a Uniform Horizontal Radiation Pattern

For some purposes aerials are required to have a substantially uniform horizontal radiation pattern; a typical case is a transmitting aerial for a broadcasting service. A method of meeting this requirement is illustrated in idealised form in Fig. 4.15. A continuous distribution of radiating elements (vertical, tangential or radial) is arranged in the form of a ring round a cylindrical mast. The elements carry equal currents which in one arrangement are in-phase, and in the other are in progressive-phase, i.e. the phase changes uniformly round the ring, the total phase change being an integral multiple of 2π radians. From considerations of symmetry the radiation is uniform in all horizontal directions for either arrangement. In practice a continuous distribution of radiating elements is impracticable, and a compromise must be sought between the number of elements and the uniformity of the radiation pattern.

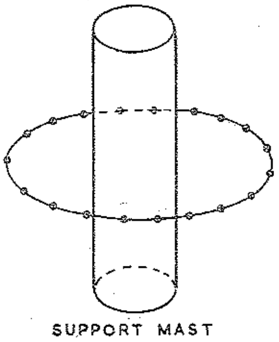

Fig. 4.15 - One tier of ring aerial

---

*There are some errors on pp. 686 and 687 of Reference 11.

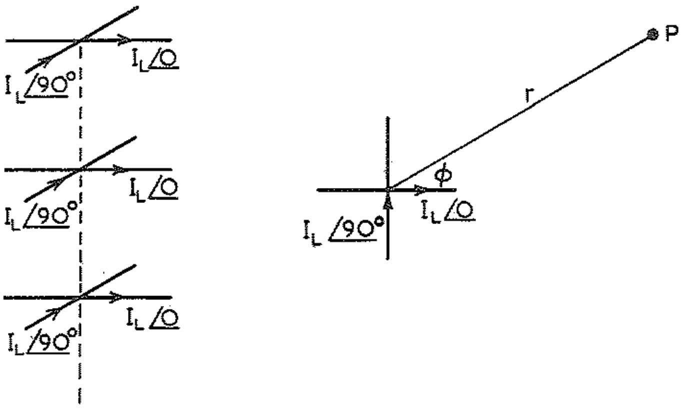

Fig. 4.16 - The "turnstile" aerial

The most suitable arrangement depends on the particular case. Generally speaking the in-phase system is used for masts having a radius (or equivalent radius) greater than about 0·05λ; the elements are then usually energised from a common point through lines of equal length.

A progressive-phase system is often used if the mast has a relatively small cross-section, for instance a thin pole mounted on top of the main supporting structure. Fig. 4.16 shows a horizontally-polarised aerial of this type; each tier consists of two horizontal 0·5λ dipoles at right angles (which we can regard as four 0·25λ radial elements) carrying equal currents in phase quadrature. If the pole were infinitesimally thin no current would be induced in it by such an array; provided its cross-sectional dimensions are small compared with the wavelength it will have little effect on the radiation characteristics. If the loop current of each dipole is I_L, it follows from Equation (2.1) that the field at a distance r and at an angle ϕ in the plane containing the dipoles is given by

$$E_\phi = \frac{60 I_L}{r}\left\{\frac{\cos\left(\frac{\pi}{2}\cos\phi\right)}{\sin\phi} + j\,\frac{\cos\left(\frac{\pi}{2}\sin\phi\right)}{\cos\phi}\right\} \qquad (4.2)$$

As ϕ changes, the modulus of the expression for E_ϕ given by Equation (4.2) is constant within ±0·5 dB. Since there is no coupling between the two dipoles the gain of a single tier in a plane containing the dipoles, relative to a 0·5λ dipole, is 0·5 (i.e. −3 dB).

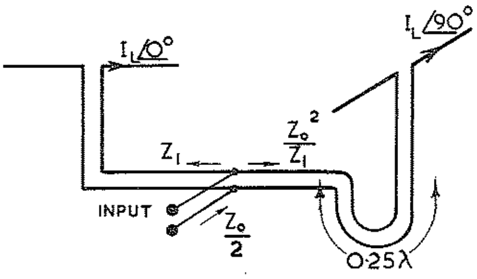

Fig. 4.17 - Method of feeding a progressive-phase aerial system

This type of aerial is known as a "turnstile". The usual method of connection is shown schematically in Fig. 4.17. We consider the dipoles in each tier (or the combined dipoles in each vertical plane) as constituting two groups, and endeavour to match each group to the transmission line which feeds it. An additional 0·25λ length of line is included in the feed to one group, in order to give the required phase difference between the currents in the two groups. If the impedance of one group at the paralleling point is Z_1 the reflection coefficient at that point is

$$\left(\frac{Z_1 - Z_0}{Z_1 + Z_0} \right) ,$$

where Z_0 is the characteristic impedance of the transmission line. The impedance of the other group at the mid-band frequency is Z_0^2/Z_1; if the two groups are connected in series to a transmission line of characteristic impedance $2Z_0$, or in parallel to a line of characteristic impedance $Z_0/2$, the reflection coefficient of the combination is

$$\mp \left(\frac{Z_1 - Z_0}{Z_1 + Z_0} \right)^2 ,$$

i.e. the square of the reflection coefficient for each group along. This result will apply approximately over a limited band of frequencies, since the change with frequency of the electrical length of the 0·25λ phasing line will in general have a negligible effect. The impedance of the complete aerial is therefore much more constant over a small frequency band than that of either group separately, particularly if the reflection coefficient for each group is small.

This compensation applies to all arrays in which the radiating elements can be divided into two groups, fed in phase quadrature by the method shown in Fig. 4.17. However, one consequence of a departure of the impedance of an individual group from the ideal is that the power is unequally divided between the two groups; the horizontal radiation pattern consequently changes over the frequency band.

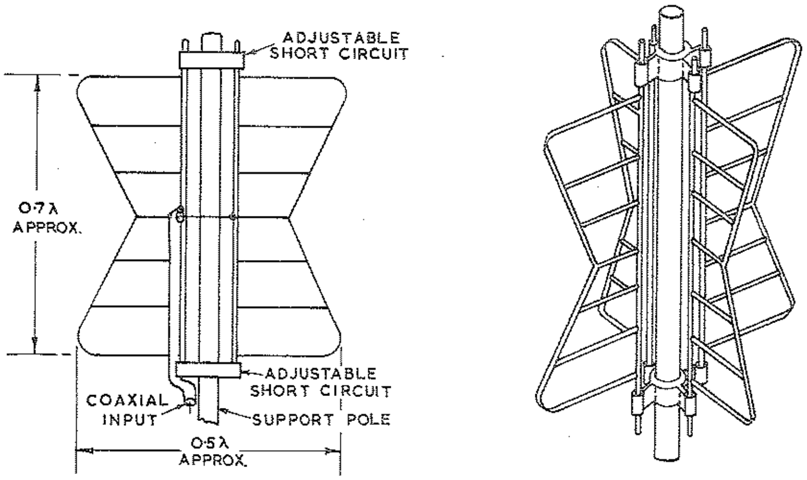

(a) Batwing element (b) Single tier

Fig. 4.18 - The Batwing aerial

A modification of the turnstile aerial is shown in Fig. 4.18. The radiating element consists of a skeletonised "batwing"; this can be regarded as a transmission line (or slot) across which radiating elements are tapped, the lengths being graded to "spread" the current distribution. As a result one tier has approximately the same gain as two tiers of the turnstile aerial. By suitably choosing the length and width of the slot and the shape of the batwing, the impedance can be made much less frequency-dependent than that of a simple dipole. The batwing aerial is commonly used in the very-high-frequency band for television transmissions, being then mounted on relatively thin pole at the top of a support mast.

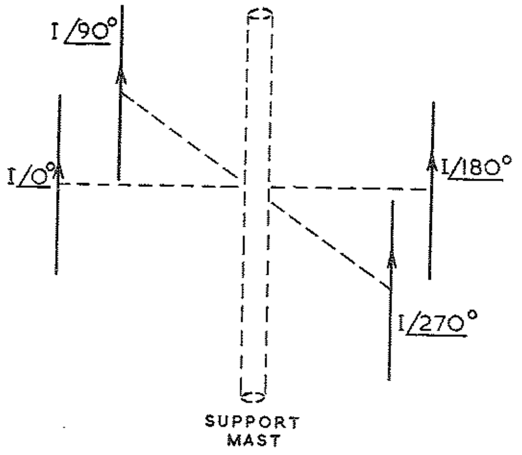

Fig. 4.19 - Progressive-phase ring of vertical aerials

A progressive-phase ring of vertical elements is shown in Fig. 4.19. Four 0·5λ dipoles carry equal currents, the phase being advanced by 90° between adjacent elements. The uniformity of the horizontal radiation pattern depends on the radius of the ring; for a radius of 0·2λ, for instance, the deviations from the mean are ±1 dB. As in the case of the turnstile aerial, if the supporting pole were infinitesimally thin it would have no effect, since there would then be no component of electric force along it; similarly, provided the cross-sectional dimensions of the pole are small compared with the wavelength its effect is small.

Special problems arise in the design of transmitting aerials for broadcasting if a large number of tiers is used in order to achieve a high gain. If all tiers are energised in phase the vertical radiation pattern takes the form of a main lobe and a number of minor lobes, with intermediate zeros; the larger the number of tiers the greater the number of these lobes and zeros. As the aim of a broadcasting service is to "illuminate" the whole of the service area, zeros in the vertical pattern must be "filled-in", otherwise areas near to the transmitting aerial would not be served. This is achieved by adjustments to the relative amplitude and/or phase of the currents in some of the tiers; the gain of the aerial is consequently reduced, but generally by only a small amount. A further consequence is that, even if there were no practical limit to the number of tiers, there is an upper limit to the useful aerial gain; this corresponds to the vertical radiation pattern giving the same field strength at all points in the service area.

4.7. Slot in Infinite Perfectly-Conducting Flat Sheet

The symmetry of the equations relating the electric force (E) and the magnetic force (H) in free space suggests that, corresponding to any reference radiating system, there exists another for which the electric force is proportional to the magnetic force in the reference system, and vice versa; the two systems are then said to be *complementary*. Let the electric and magnetic forces for the reference system be E_1 and H_1 respectively, and for the complementary system E_2, H_2; since E_1 and H_1 satisfy Maxwell's equations in free space, E_2, H_2 do so also if

$$H_2 = \sqrt{\frac{\epsilon_0}{\mu_0}}\, E_1 = \frac{E_1}{\eta} \tag{4.3}$$

and

$$E_2 = -\sqrt{\frac{\mu_0}{\epsilon_0}}\, H_1 = -\eta H_1 \tag{4.4}$$

where η is the intrinsic impedance of the medium, i.e. 120π ohms for free space. Moreover, the values given by Equations (4.3) and (4.4) correspond also to the radiation of the same power by the two systems.

Consider a dipole in the form of a thin strip of metal, energised across a gap at the centre, as shown in Fig. 4.20(a); the complementary aerial is a slot of the same dimensions cut in an infinite flat sheet of thin perfectly-conducting material, energised across the mid-points of the longer sides. Following Booker[13] this relationship can be demonstrated as follows.

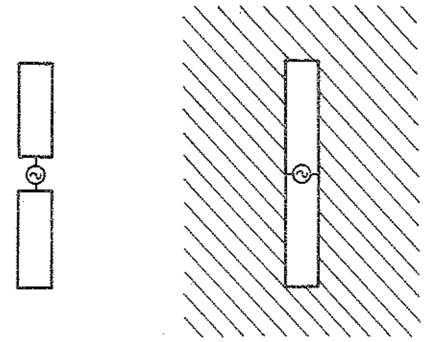
(a) Electric dipole

(b) Complementary slot

Fig. 4.20 - Dipole and complementary slot

The *electric* dipole we have so far considered, is a perfect conductor of electricity. The full lines in Fig. 4.21(a) show the current flow along the dipole and the lines of electric force in space; the lines of magnetic force are shown dotted. The corresponding *magnetic* dipole, in which electric and magnetic quantities are interchanged is shown in Fig. 4.21(b). The strip is now a perfect conductor of magnetism (for instance iron dust having an infinite permeability), and a "magnetic current" is maintained in it by surrounding it with a circuit containing a series generator;* for reasons that will appear later two generators of equal voltage connected in series are shown. The lines of electric and magnetic force are interchanged compared with those for the electric dipole.

If we introduce a perfectly-conducting flat sheet containing a slot into which the magnetic dipole just fits, as in Fig. 4.21(c), the field is not disturbed in any way, since the electric force is everywhere normal to the sheet. The sheet carries equal electric currents of opposite sign at corresponding points on opposite sides. It is permissible to connect the junctions of the generators to the mid-points of the longer sides of the slot; no current flows in this connecting lead. We have now effectively divided the space into two halves which are screened from each other, and it is therefore permissible to reverse the polarity of the generator on one side of the sheet, thus reversing the associated field. The magnetic field is now continuous across the magnetic dipole, as shown in Fig. 4.21(d), and the magnetic material can be removed without affecting the field in any way. The electric

*The Ferrite-rod aerial used in domestic medium-frequency receivers is an example of a magnetic dipole.

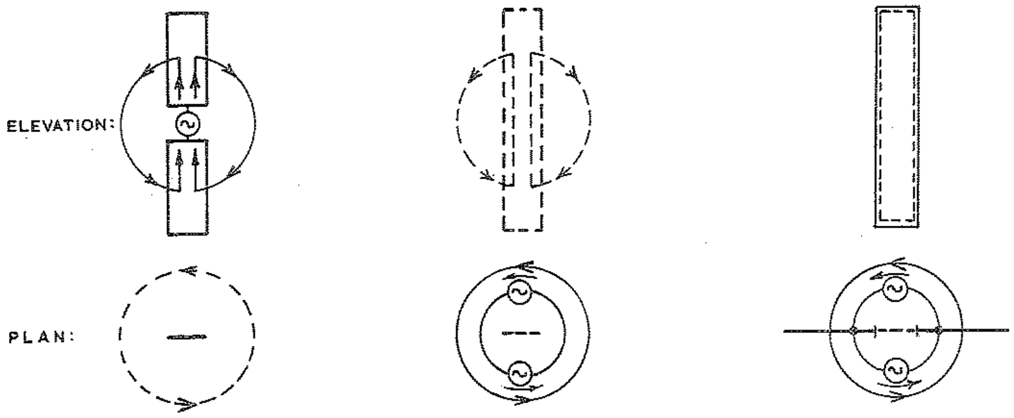

(a) Electric dipole

(b) Magnetic dipole

(c) Magnetic dipole in perfectly-conducting sheet

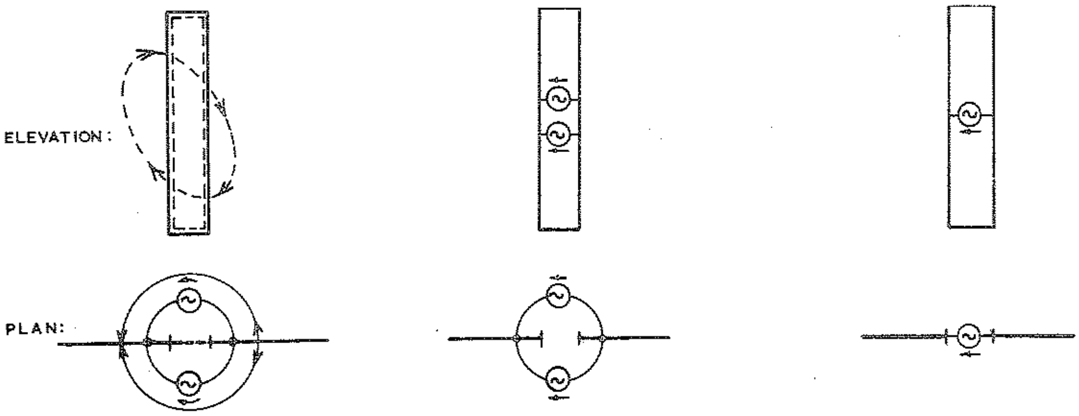

(d) As (c), with one generator reversed

(e) As (d), with magnetic material removed

(f) Slot in infinite sheet

Fig. 4.21 - Correspondence between electric dipole, magnetic dipole, and slot aerial

currents on the two sides of the sheet are of the same sign at corresponding points, and the sheet has become an essential part of the radiating system. A current also flows in the connection between the generators and the sheet. The two generators in parallel in Fig. 4.21(e) can be replaced by a single generator; we then have an empty slot energised across the mid-points of the longer sides, as in Fig. 4.21(f).

The complementary slot is therefore equivalent to a magnetic dipole, and hence to an electric dipole with electric and magnetic quantities interchanged; the only anomaly in the analogy is that the phase of the field on one side of the sheet is reversed. This is of no practical importance.

A vertical dipole, for instance, radiates vertically-polarised waves, while a vertical slot radiates horizontally-polarised waves, and vice versa. Both the 0·5λ vertical dipole and the complementary slot have a uniform horizontal radiation pattern and a figure-of-eight vertical radiation pattern.

In addition to the relationship between the radiation patterns of complementary aerials there is a corresponding relationship between their impedances. Fig. 4.22 shows the associated fields at the driving points. The voltage applied to the electric dipole is minus the line integral of the electric force across the gap, i.e.

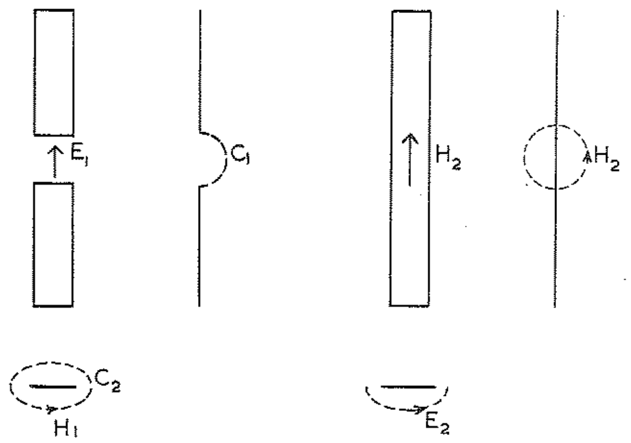

(a) Electric dipole, impedance Z_1

(b) Complementary slot, impedance Z_2

Fig. 4.22 - Relationship between impedances of complementary aerials

$$-\int_{c_1} E_1 ds$$

where C_1 is the contour shown. The current flowing is the line integral of the magnetic force round the contour C_2, i.e.

$$\int_{c_2} H_1 ds$$

Hence

$$Z_1 = \frac{-\int_{c_1} E_1 ds}{\int_{c_2} H_1 ds} \tag{4.5}$$

Correspondingly,

$$Z_2 = \frac{-\frac{1}{2}\int_{c_2} E_2 ds}{-2\int_{c_1} H_2 ds} \tag{4.6}$$

From Equations (4.3) to (4.6)

$$Z_1 Z_2 = -\tfrac{1}{4}\,\frac{\displaystyle\int_{c_1} E_1 ds \int_{c_2} E_2 ds}{\displaystyle\int_{c_2} H_1 ds \int_{c_1} H_2 ds} = \tfrac{1}{4}\,\eta^2 \qquad (4.7)$$

For instance, for a thin resonant 0·5λ dipole $Z_1 = 73$ ohms, and for the complementary slot $Z_2 = 485$ ohms. It also follows from Equation (4.7) that the impedance-frequency characteristic of the dipole has the same form as the admittance-frequency characteristic of the slot, and vice versa. The bandwidth of the dipole can be increased by making it wider, without appreciably affecting the 0·5λ resonance impedance of 73 ohms; correspondingly, the bandwidth of the slot can be increased by making it wider, without appreciably affecting the 0·5λ resonance impedance of 485 ohms.

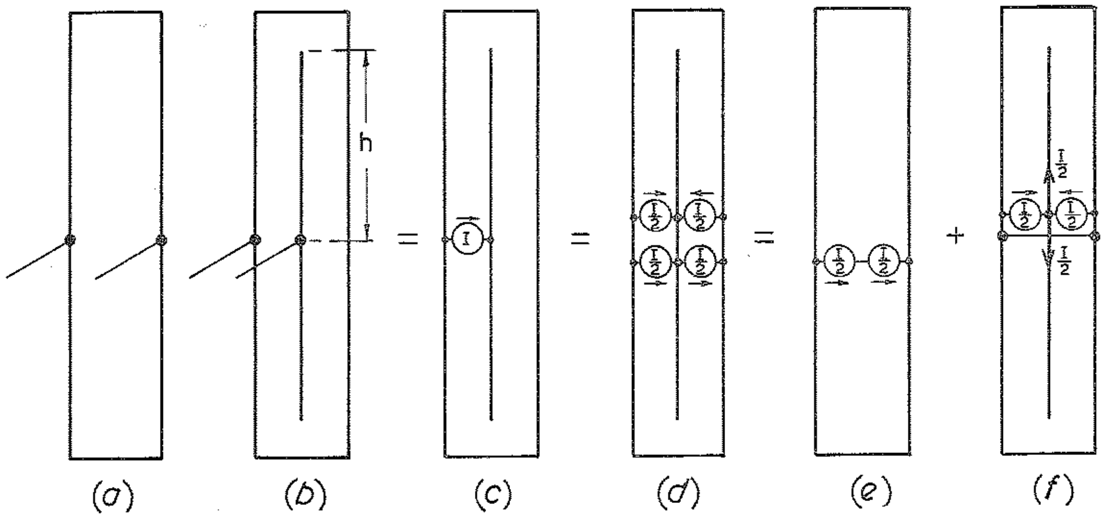

Fig. 4.23 - Relationship between the impedances of the slot and folded slot

Fig. 4.23 shows two methods of energising a slot aerial. In Fig. 4.23(a) the generator is connected directly across the mid-points of the longer sides; this is the case already treated. In Fig. 4.23(b) the generator is applied between one side of the slot and the mid-point of an open-circuited rod lying along the axis. This arrangement is complementary to the folded dipole and will therefore be called a folded slot. Fig. 4.23(b) is redrawn in (c), the constant-current generator supplying a current I. An equivalent circuit is shown in Fig. 4.23(d), in which an open circuit has been replaced by two infinite-impedance constant-current generators of opposite sign in parallel; this equivalent circuit can be regarded as the sum of the two systems shown in Fig. 4.23(e) and (f). The voltage applied across the driving point by the original generator is the sum of the voltages applied by the two left-hand generators of the sets shown in Fig. 4.23(e) and (f). It follows that

$$Z_{\text{folded slot}} = \tfrac{1}{4}\,Z_{\text{slot}} + j\tfrac{1}{2}Z_0 \cot(\beta h) \qquad (4.8)$$

where Z_{slot} is the impedance of the slot energised as shown in Fig. 4.23(a), $Z_{\text{folded slot}}$ is the impedance of the slot energised as shown in Fig. 4.23(b), and Z_0, h are the characteristic impedance and half-length respectively of the non-radiating transmission line shown in Fig. 4.23(f).

The impedance of the folded slot is thus one quarter of that of the simple slot, in series with a reactance given by the last term in Equation (4.8); if $h = 0{\cdot}25\lambda$ this reactance is zero. The driving point impedance of a $0{\cdot}5\lambda$ folded slot is then 121 ohms, a value suitable for matching to a coaxial line. At other frequencies the central rod is equivalent to a series reactance whose variation with frequency is opposite in sign to that of the slot; it therefore partially compensates for the change in reactance of the slot with frequency. However, in practice it is difficult to make Z_0 high enough (i.e. to make the open-circuited rod sufficiently thin) to achieve adequate compensation.

One way of mitigating this difficulty is to remove one half of the central rod shown in Fig. 4.23(b); the final term in Equation (4.8), and hence the degree of reactance compensation, is then doubled. Moreover, slight asymmetries between the upper and lower halves of the rod, which would introduce an irregular change of reactance with frequency, are eliminated. Another way of increasing the degree of reactance compensation is to make h an integral number of quarter-wavelengths at the mid-band frequency, leaving the rod open-circuited if the integer is odd, and short-circuited to the sheet if the integer is even. By displacing the rod from its central position the impedance transformation due to folding can be made to take any value between zero and unity.[14] This is analogous to controlling the admittance of a folded dipole by the relative lateral dimensions of the two branches.

The slot aerials so far described radiate symmetrically on each side of the sheet, whereas the usual requirement is to radiate on only one side. This is accomplished by "boxing" the slot, as shown in Fig. 4.24, thus confining the radiation to the unboxed side of the sheet. The conductance at the driving point is consequently halved, and the susceptance is modified by an amount depending on the physical dimensions of the box. For a hemispherical box having a radius of $0{\cdot}25\lambda$ the susceptance is not greatly changed, but many other shapes of box can be used. Boxed slot aerials are used in the skins of aeroplanes to provide dragless radiators.

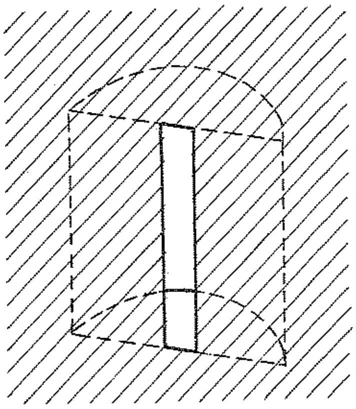

Fig. 4.24 - The "boxed" slot

The correspondence between the dipole and slot aerial is a special case of a general relationship between complementary systems. This is analogous to what is known in optics as Babinet's principle, which may be stated as follows. Consider a thin plane screen which is non-reflecting, pierced by holes; the complementary screen is that in which holes and obstructing screen are interchanged. If first one screen and then the other are placed in front of a light source, Babinet's principle states that the sum of the disturbances behind the two screens is the same as that produced if no screen were present. This is obviously true on the basis of ray theory, but it is also true when diffraction is taken into account. The extension of this principle to electromagnetic problems was formulated by Booker;[13] it involves interchanging electric and magnetic quantities in passing from one system to the complementary system, and also using conjugate sources, i.e. replacing electric dipoles by magnetic dipoles and vice-versa.

4.8. Slot in Finite Perfectly-Conducting Flat Sheet

For the electric dipole the lines of magnetic force lie in circles perpendicular to, and with their centres on the axis, as shown in Fig. 4.25(a). The amplitude as a function of θ (the angle to the vertical) depends on the length of the dipole; for a doublet, for instance, the magnetic force is proportional to $\sin\theta$.

For the complementary slot shown in Fig. 4.25(b) the *electric* force is proportional in magnitude and direction to that of the *magnetic* force for the electric dipole, except that its direction is reversed on one side of the sheet. This reversal of direction means that there is a discontinuity in the electric force in passing through the sheet; to satisfy the boundary condition equal currents must flow in the same direction on each side of the sheet at corresponding points.

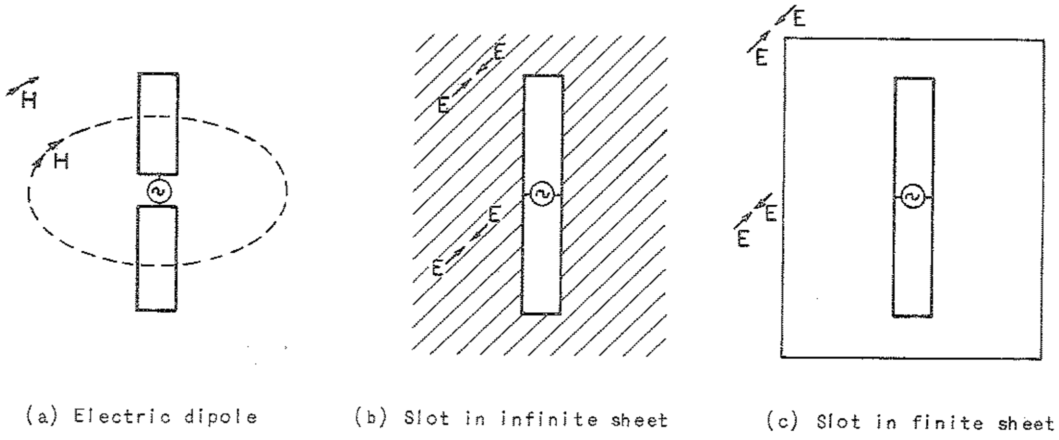

(a) Electric dipole (b) Slot in infinite sheet (c) Slot in finite sheet

Fig. 4.25 - Slot in infinite and finite sheets

If the sheet is of finite size, from considerations of symmetry the electric force on one side of the plane containing the sheet must be equal and opposite to that on the other side. This is true for points *beyond* the edges of the sheet as well as for points on it. But since there cannot be a discontinuity in the electric force at a point in free space, in the plane containing the sheet the electric force must be zero beyond its edges. This means that, whereas the slot in an *infinite* sheet has a zero in the radiation pattern only along the axis of the slot, the slot in a *finite* sheet has a zero in all directions in the plane of the sheet.

4.9. Longitudinal Slot in Infinitely-Long Cylinder

The radiation pattern of a longitudinal slot in a cylinder is most conveniently calculated by considering it as a receiving aerial immersed in a plane-wave field. General expressions for the field components in such a case are derived in Section 7.3 in a form directly applicable to the present problem.

Consider a vertical cylinder (Fig. 4.26) containing an infinitesimal slot of length δl and of width small compared with its length, the slot being at an angle ϕ to the x axis. From the boundary condition at a perfectly-conducting surface it follows that the current flowing in a short-circuit bridging the mid-points of the longer sides is $H_z\delta l$, where H_z is the z-component of the magnetic force at the surface of the cylinder. The variation of H_z with the angle of incidence, θ, of the plane wave, and the angular position of the slot therefore gives the radiation pattern. It is shown in Section 7.3 that a horizontally-polarised* transmitting doublet gives an H_z component at the surface of the cylinder, whereas a vertically-polarised transmitting doublet does not. It follows that the slot aerial receives (or radiates when transmitting) only horizontally-polarised waves.

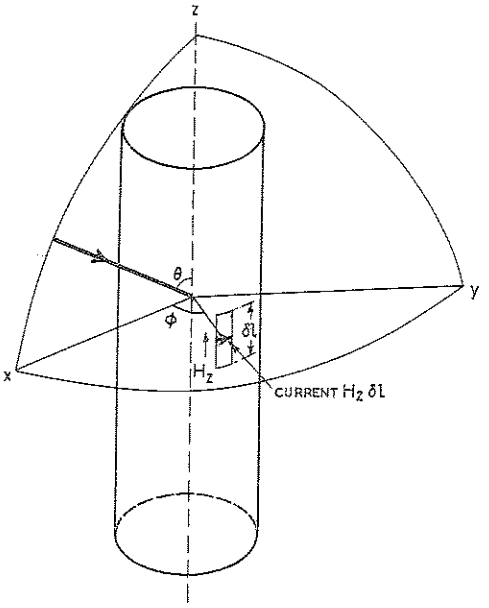

Fig. 4.26 - Longitudinal slot in infinitely-long cylinder

The current flowing in the short-circuit across the slot ($H_z\delta l$) is given by Section 7.3, Equation (7.34), where the incident field is that in Section 7.3, Equation (7.21). The latter can be related to the current flowing in a distant transmitting doublet. We can then apply the reciprocity theorem to find the electric force, E, at a distant point having spherical co-ordinates (r, θ, ϕ) when a voltage V is applied to the slot. We obtain

$$E = -\frac{V\delta l}{2\pi^2 a}\,\frac{e^{-j\beta r}}{r}\sum_{0}^{\infty}\epsilon_n j^n\,\frac{1}{H_n^{(2)\prime}(\beta a\sin\theta)}\,\cos(n\phi) \qquad (4.9)$$

where a is the radius of the cylinder, ϵ_n is Neumann's number ($\epsilon_n = 1$ for $n = 0$, $\epsilon_n = 2$ for $n \neq 0$) and $H_n^{(2)\prime}(z)$ denotes the derivative of $H_n^{(2)}(z)$ with respect to z. $H_n^{(2)}(z)$ is the Hankel function of the second kind of order n, and is defined by

$$H_n^{(2)}(z) = J_n(z) - jY_n(z)$$

where $J_n(z)$ and $Y_n(z)$ are Bessel functions of order n of the first and second kinds respectively. Furthermore

$$H_n^{(2)\prime}(z) = \tfrac{1}{2}\,\{H_{n-1}^{(2)}(z) - H_{n+1}^{(2)}(z)\}$$

The term in Equation (4.9) involving θ and ϕ is the radiation pattern of the slot. The modulus of this expression gives the amplitude, and the argument the phase, of the field at an angle ϕ from the line joining the axis of the cylinder to that of the slot. The first term in the series ($n = 0$) is a constant, the succeeding terms corresponding to sinusoidal deviations from this constant value. By putting $\theta = 90°$ in Equation (4.9) we obtain the horizontal radiation pattern of the longitudinal slot.

---

*A horizontally-polarised doublet is one with its axis normal to the plane of incidence, and a vertically-polarised doublet is one with its axis in the plane of incidence and perpendicular to the radius vector.

A slot of finite length is equivalent to a number of collinear separately-energised infinitesimal slots. It follows that the horizontal radiation pattern is independent of the length of the slot, or the manner in which it is energised.

The vertical radiation pattern is the product of the vertical pattern of an infinitesimal slot, given by Equation (4.9), and that for a linear distribution of point sources occupying the same length, and energised in the same manner, as the slot. As in the case of arrays of dipoles, the maximum gain for a slot of given length is achieved when the voltage distribution along the slot is uniform in amplitude and of the same phase.

Equation (4.9) applies rigorously to a slot of infinitesimal width in an infinitely-long cylinder. But it is also substantially correct for a slot of finite width in a cylinder of finite length, provided the slot width is a small fraction of the wavelength, and the cylinder extends appreciably beyond the ends of the slot.

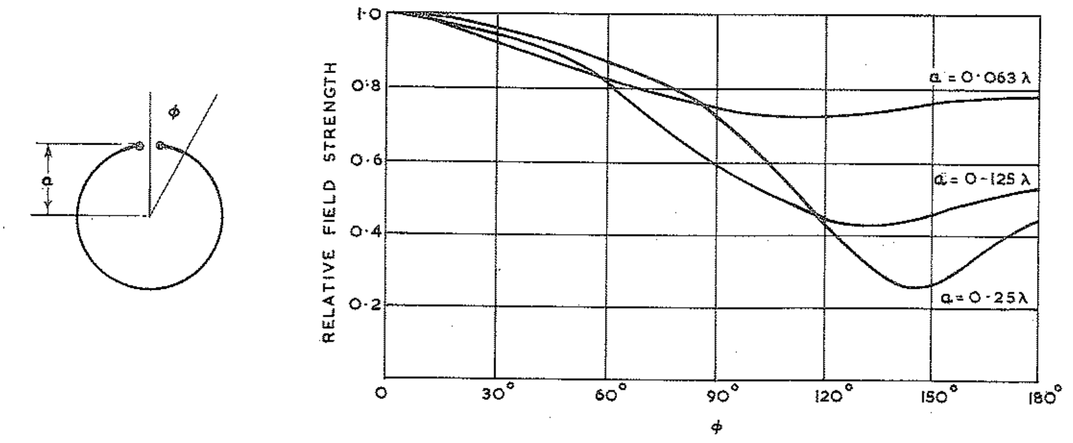

Fig. 4.27 - Horizontal radiation pattern of longitudinal slot in cylinder

Fig. 4.27 shows the horizontal radiation pattern of a longitudinal slot for three values of cylinder radius. When the radius is small the circumferential currents are substantially uniform in amplitude and phase, and the horizontal radiation pattern is therefore approximately uniform. As the cylinder radius increases the pattern becomes much more directional, the ratio of maximum to minimum being shown by the curve for one slot in Fig. 4.28.[15]

The radiation pattern of two or more longitudinal slots can be calculated by the vector addition of the contributions from individual slots using Equation (4.9).

It is sometimes desirable for structural reasons to use a cylinder of large diameter, and at the same time to achieve a substantially uniform horizontal radiation pattern. In this case it is necessary to use a number of slots, energised in phase when regarded as magnetic dipoles, as shown in Fig. 4.29. If we have, say, N equally spaced slots it follows from Equation (4.9) that the horizontally radiation pattern is given by

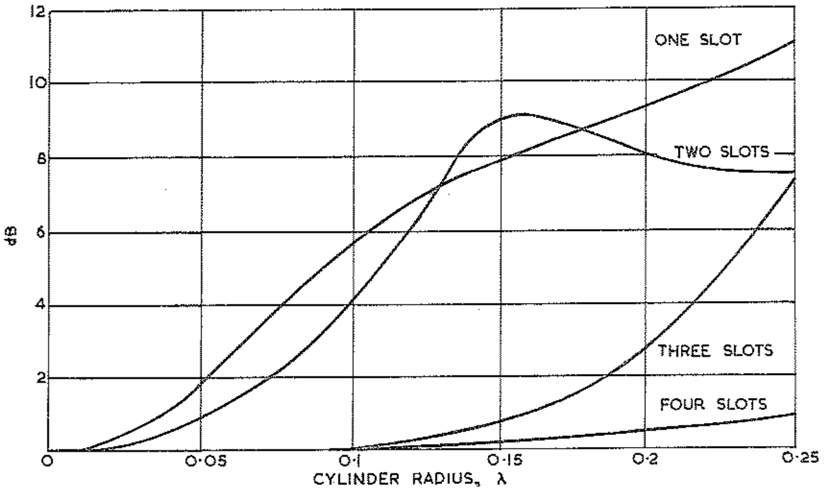

Fig. 4.28 - Ratio of the horizontal radiation pattern maximum and minimum values, for equally-spaced longitudinal slots in a cylinder, energised in phase

$$E \propto \sum_{0}^{\infty} \epsilon_n j^n \frac{1}{H_n^{(2)'}(\beta a)} \left\{ \cos(n\phi) + \cos\left(n\phi + \frac{2\pi}{N}\right) + \right.$$
$$\left. + \cos\left(n\phi + \frac{4\pi}{N}\right) + \ldots + \cos\left(n\phi + \frac{N-1}{N}\, 2\pi\right) \right\} \qquad (4.10)$$

The only non-zero terms in Equation (4.10) are when $n = 0, N, 2N \ldots$; as N increases the coefficient of all terms except the first decrease, and the pattern consequently becomes more uniform. We can compare this arrangement with that of a horizontal loop aerial of large radius; if the loop is energised at a number of equally spaced points the current distribution (and hence the horizontal radiation pattern) is much more uniform than if a single driving-point were used. The ratio of maximum to minimum in the horizontal radiation pattern is shown in Fig. 4.28 as a function of cylinder radius, for different numbers of slots.

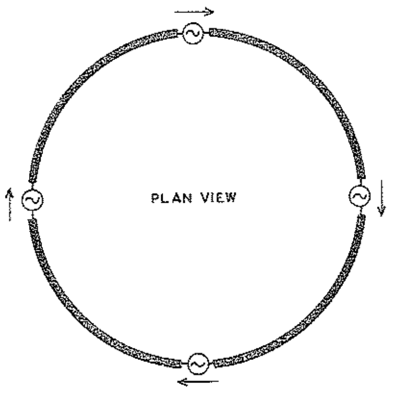

Fig. 4.29 - Four longitudinal slots in cylinder, energised in phase

One method of energising a slot aerial is shown in Fig. 4.23(a). For a 0·5λ slot in an infinite flat sheet the distribution along the slot of the voltage across the slot is the same as the current distribution for the complementary strip dipole. The amplitude is approximately sinusoidal, being maximum at the centre and zero at the ends, and the phase is substantially the same along the slot. The input impedance in this case has been shown in Section 4.7 to be about 485 ohms; the impedance can be reduced to a value convenient for connection to a coaxial line by the method shown in Fig. 4.23(b).

For a longitudinal slot which is energised at one point the phase velocity of the wave inside the leaky cylindrical waveguide may be greater than that of light; provided the periphery is a small fraction of the wavelength the arrangement may be thought of as a transmission line continuously loaded with parallel inductance. If the radius is too small the wave is not propagated far along the slotted cylinder; as the radius increases the wave is propagated further but the phase velocity falls. There is therefore an optimum radius giving maximum directivity in the vertical plane; this corresponds to the maximum length of slot for which the voltage distribution is substantially uniform and co-phasal. An aerial having a higher gain than a 0·5λ slot, but requiring only a single feed-point, is thus achieved. However, the gain is not as great as could be achieved by using separately-fed collinear 0·5λ slots occupying the same overall length, since the voltage distribution along the single slot is not so favourable.

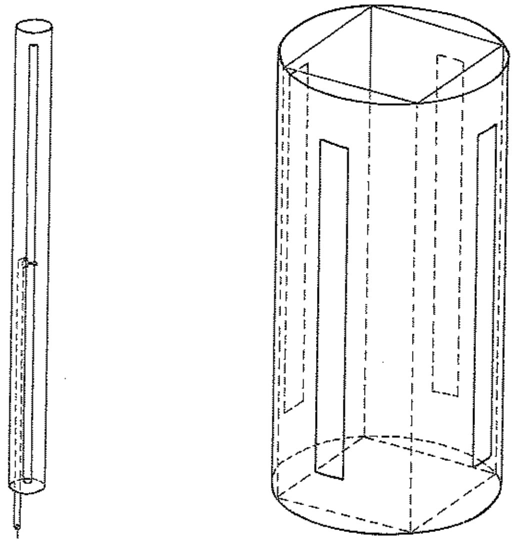

(a) Single-slot aerial (b) Four-slot aerial

Typical dimensions

	(a)	(b)
Cylinder radius	0·08λ	0·31λ
Cylinder length	1·1λ	1·0λ
Slot length	1·0λ	0·75λ
Slot width	0·03λ	0·1λ

Fig. 4.30 - Single tier of two types of slot aerials used for sound broadcasting in the 90 Mc/s band

Fig. 4.30(a) shows a slot aerial of this type, which is used for sound broadcasting in the 90 Mc/s band; the horizontal radiation pattern is substantially uniform (see Fig. 4.28) and the impedance is suitable for matching to a co-axial line.

In the case of slots in a cylinder of much larger diameter undesirable wave modes may be propagated within the cylinder, thus adversely affecting both the voltage distribution along the slot (and hence the gain), and the impedance. These disadvantages may be avoided by "boxing-in" individual slots as shown in Fig. 4.30(b), the dimensions of the box being chosen to give a suitable phase velocity along the slot. This arrangement, which is also used for sound broadcasting in the 90 Mc/s band, is mechanically convenient as it leaves an electrically "dead" space in the centre of the mast for the installation of transmission lines and climbing ladders.

A number of tiers of the type shown in Fig. 4.30 energised in phase, can be mounted one above the other to increase the gain of the aerial.

5. ACKNOWLEDGEMENTS

This report is based on a course of lectures given by the author to post-graduate students at the City & Guilds College of the Imperial Institute, London. He wishes to thank Sir Willis Jackson, Head of the Electrical Engineering Department of the City & Guilds College, for his advice in planning the lectures, and also Mr. W. Proctor Wilson, Head of the B.B.C. Research Department, for the encouragement and help which resulted in the lectures appearing in report form.

The author also wishes to acknowledge the great benefits he has derived from discussions with his colleagues in the Aerial Section of the B.B.C. Research Department; many of their suggestions concerning the presentation of the theory were adopted, both in the course of lectures and in the report.

6 REFERENCES

1. Jahnke, E. and Emde, F., Tables of Functions, Dover Publications, 1943.
2. Tani, K., Tables of $Si(x)$ and $Ci(x)$ for the range $x = 0$ to $x = 50$, Tokyo, 1931.
3. Page, H. and Monteath, G.D., "The Vertical Radiation Patterns of Medium-Wave Broadcasting Aerials", Proc. I.E.E., Vol. 102, Part B, No. 3, p. 279, 1955.
4. Hallén, E., "Theoretical Investigations into the Transmitting and Receiving Qualities of Antennae", Nova Acta (Uppsala), Series 4, Vol. 11, p. 1, 1938.
5. Gray, M.C., "A Modification of Hallén's Solution of the Antenna Problem", Journal of Applied Physics, Vol. 15, p. 54, 1944.
6. Wells, N., "Aerial Characteristics", J.I.E.E., Vol. 89, p. 76, 1942.
7. Schelkunoff, S.A., Advanced Antenna Theory, Wiley & Sons, Chapters 1 and 2.
8. Howe, W.G.O.H., "On the Capacity of Radio-Telegraphic Antennae", Electrician, Vol. 73, pp. 829, 859, 906, 1914.
9. Pistolkors, A.A., "The Radiation Resistance of Beam Antennas", Proc. I.R.E., Vol. 17, p. 562, 1929.
10. Booth, C.F. and MacLarty, B.N., "The New High-Frequency Transmitting Station at Rugby", Proc. I.E.E., Vol. 103, Part B, No. 9, p. 263, May 1956.
11. Carter, P.S., "Antenna Arrays Around Cylinders", Proc. I.R.E., Vol. 31, p. 671, 1943.
12. Knight, P., "Methods of Calculating the Horizontal Radiation Patterns of Dipole Arrays Around a Support Mast", Proc. I.E.E., Vol. 105, Part B, p. 548, 1958.

13. Booker, H.G., "Slot Aerials and Their Relation to Complementary Wire Aerials (Babinet's Principle)", J.I.E.E., Vol. 93, Part IIIA, p. 620, 1946.

14. Monteath, G.D., "Wide-Band Folded-Slot Aerials", Proc. I.E.E., Vol. 97, Part III, p. 414, 1950.

15. Sinclair, G., "The Patterns of Slotted-Cylinder Antennas", Proc. I.R.E., Vol. 36, p. 1487, 1948.

7. APPENDICES

7.1. The z-Component of the Electric Force near a Vertical Aerial Carrying a Sinusoidal Current Distribution

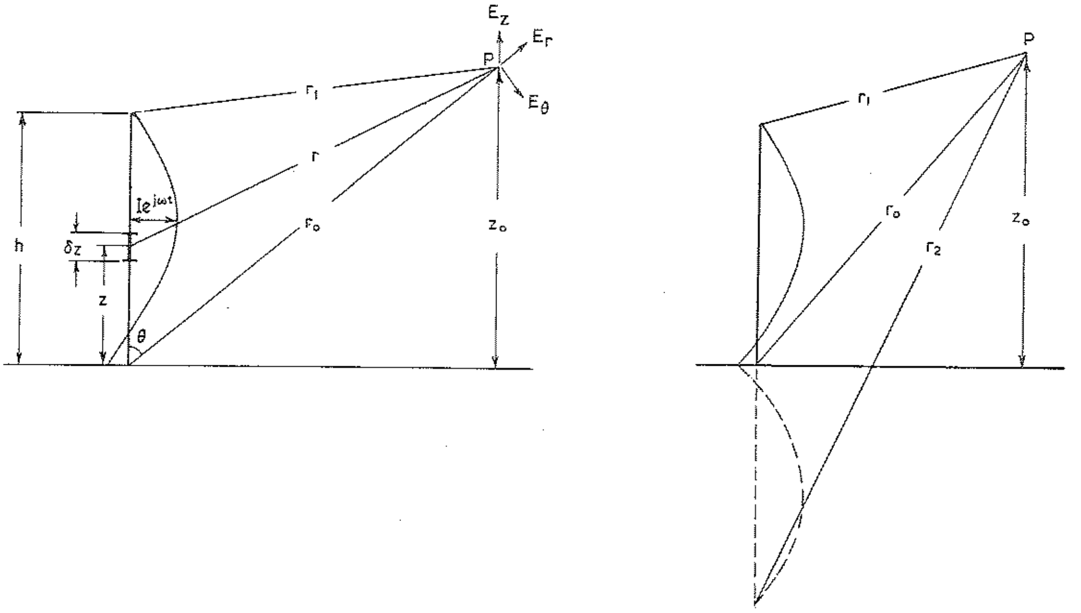

(a) Aerial in free space

(b) Aerial over perfectly-conducting ground

Fig. 7.1

The aerial is equivalent to a number of doublets placed end to end; consider a typical doublet of length δz at a height z, carrying a current $I \sin(\beta\overline{h-z})e^{j\omega t}$, where I is the peak value of the loop current. The electric force at P associated with this element, δE_z, is found by resolving the field components E_θ and E_r given by Equations (1.15) and (1.16). We obtain

$$\delta E_z = 30I\sin(\beta\overline{h-z})\left\{-\frac{j\beta}{r}-\frac{1}{r^2}+\frac{j}{\beta r^3}+(z_0-z)^2\left(\frac{j\beta}{r^3}+\frac{3}{r^4}-\frac{j3}{\beta r^5}\right)\right\}e^{j(\omega t-\beta r)}\delta z \qquad (7.1)$$

For the complete aerial shown in Fig. 7.1(a) E_z is therefore given by

$$E_z = 30I\, e^{j\omega t} \int_0^h \sin(\beta\overline{h-z}) e^{-j\beta r} \left\{ -\frac{j\beta}{r} - \frac{1}{r^2} + \frac{j}{\beta r^3} + (z_0 - z)^2 \left(\frac{j\beta}{r^3} + \frac{3}{r^4} - j\frac{3}{\beta r^5} \right) \right\} dz$$

$$= -j15I\, e^{j\omega t} \left[e^{j\beta h} \int_0^h e^{-j\beta(z+r)} \left\{ -\frac{j\beta}{r} - \frac{1}{r^2} + \frac{j}{\beta r^3} + (z_0 - z)^2 \left(\frac{j\beta}{r^3} + \frac{3}{r^4} - \frac{j3}{\beta r^5} \right) \right\} dz - \right.$$

$$\left. -e^{-j\beta h} \int_0^h e^{j\beta(z-r)} \left\{ -\frac{j\beta}{r} - \frac{1}{r^2} + \frac{j}{\beta r^3} + (z_0 - z)^2 \left(\frac{j\beta}{r^3} + \frac{3}{r^4} - \frac{j3}{\beta r^5} \right) \right\} dz \right]$$

$$= -j15I\, e^{j\omega t} \left[e^{j\beta(h-z-r)} \left\{ \frac{1}{r} + \frac{(z_0 - z)}{r^2} - j\frac{(z_0 - z)}{\beta r^3} \right\} + \right.$$

$$\left. + e^{-j\beta(h-z+r)} \left\{ \frac{1}{r} - \frac{(z_0 - z)}{r^2} + j\frac{(z_0 - z)}{\beta r^3} \right\} \right]_0^h \qquad (7.2)$$

This result is not immediately obvious but may be checked by differentiating the right–hand side of Equation (7.2) with respect to z; note that

$$\frac{\partial r}{\partial z} = -\frac{(z_0 - z)}{r} .$$

Hence
$$E_z = j30I\, e^{j\omega t} \left\{ \cos(\beta h) \frac{e^{-j\beta r_0}}{r_0} - \frac{e^{-j\beta r_1}}{r_1} + \right.$$

$$\left. + j\sin(\beta h) \frac{z_0}{r_0^2} e^{-j\beta r_0} + \sin(\beta h) \frac{z_0}{\beta r_0^3} e^{-j\beta r_0} \right\} \qquad (7.3)$$

where r_0 and r_1 are shown in Fig. 7.1(a).

For an aerial over perfectly–conducting ground, by including the contribution of the image aerial we find

$$E_z = j30I\, e^{j\omega t} \left\{ 2\cos(\beta h) \frac{e^{-j\beta r_0}}{r_0} - \frac{e^{-j\beta r_1}}{r_1} - \frac{e^{-j\beta r_2}}{r_2} \right\} \qquad (7.4)$$

where r_2 is shown in Fig. 7.1(b).

To calculate E_z on the surface of a cylindrical aerial of radius $a(<< \lambda)$ we regard it as equivalent to a large number of thin filaments spaced round the periphery, adding their contributions to find the total field. For points not very near the top

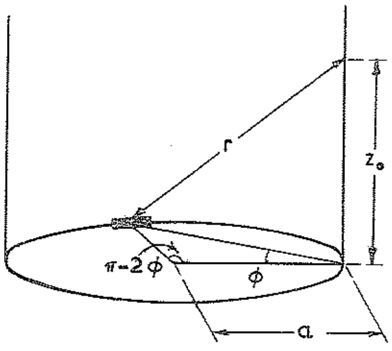

Fig. 7.2

or bottom of the aerial E_z is clearly the same as if the current flowed along the axis of the aerial; but the limiting value at points near the top and bottom needs examination. Since

$$\frac{\sin(\beta r)}{r}$$

is independent of r when r is small there is no difficulty about the real part of E_z. As far as the imaginary part is concerned, when $r \to 0$ we can replace terms of the form

$$\frac{\cos(\beta r)}{r}$$

by $1/r$ and then take the average value of the contributions from all the filaments; from Fig. 7.2 we obtain

$$\frac{2}{\pi}\int_0^{\pi/2}\frac{d\phi}{r} = \frac{2}{\pi}\int_0^{\pi/2}\frac{d\phi}{\sqrt{z_0^2 + (2a\cos\phi)^2}}$$

$$= \frac{2}{\pi z_0\sqrt{1+\left(\frac{2a}{z_0}\right)^2}}\int_0^{\pi/2}\frac{d\phi}{\sqrt{1-\nu^2\sin^2\phi}} = \frac{2}{\pi z_0\sqrt{1+\left(\frac{2a}{z_0}\right)^2}}K(\nu)$$

where
$$\nu^2 = \frac{\left(\frac{2a}{z_0}\right)^2}{1+\left(\frac{2a}{z_0}\right)^2}$$

and $K(\nu)$ is the complete elliptic integral of the first kind. This result is not very different from $1/r_0$, where r_0 is the distance to the centre of the base, except when z_0 is less than about 0·1 a; in any case the assumed current distribution is unrealistic at the ends, since we have neglected the effect of the end caps or, if there are no end caps, the evanescent fields within the top and bottom of the hollow aerial.

Accepting the assumptions that have been made, it is therefore permissible to calculate the electric force at the surface of an aerial as if the current flowed along a filament at the axis.

7.2. The Mutual Impedance Between Similar Vertical Aerials

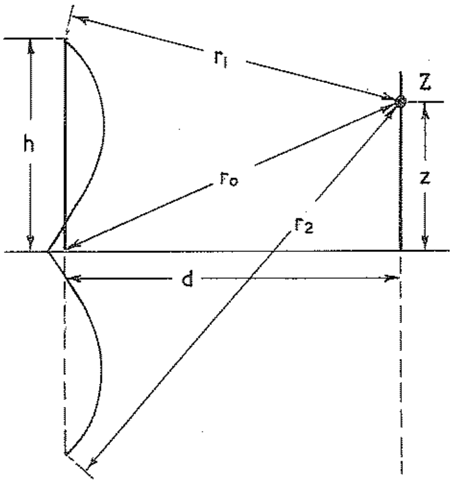

Fig. 7.3 - Calculation of mutual impedance between similar vertical aerials

From Equation (2.22) we have

$$Z_{12} = -j30 \int_0^h \left\{ 2\cos(\beta h)\,\frac{e^{-j\beta r_0}}{r_0} - \frac{e^{-j\beta r_1}}{r_1} - \frac{e^{-j\beta r_2}}{r_2} \right\} \sin(\beta\,\overline{h-z})\,dz$$

$$= -15 \int_0^h \left\{ 2\cos(\beta h)\,\frac{e^{-j\beta r_0}}{r_0} - \frac{e^{-j\beta r_1}}{r_1} - \frac{e^{-j\beta r_2}}{r_2} \right\} \left\{ e^{j\beta(h-z)} - e^{-j\beta(h-z)} \right\} dz \qquad (7.5)$$

Consider an integral of the form $\int_0^h \frac{e^{-j\beta(r_0+z)}}{r_0}\,dz$,

and put $u = \beta(r_0 + z)$ i.e.

$$\frac{du}{dz} = \frac{\beta u}{r_0},$$

since $r_0^2 = z^2 + d^2$.

$$\int_0^h \frac{e^{-j\beta(r_0+z)}}{r_0}\,dz = \int_{\beta d}^{\beta(\sqrt{h^2+d^2}+h)} \frac{e^{-ju}}{u}\,du = \left[Ei(-ju)\right]_{\beta d}^{\beta(\sqrt{h^2+d^2}+h)}$$

where

$$Ei(-jx) = \int \frac{e^{-ju}}{u}\,du = \left[Ci(u) - jSi(u)\right],$$

and $Ci(u)$ and $Si(u)$ are defined in Equations (2.5) and (2.3) respectively.

Similarly, putting

$$u = \beta(r_0 - z), \quad \int_0^h \frac{e^{-j\beta(r_0-z)}}{r_0}\,dz = -\left[Ei(-ju)\right]_{\beta d}^{\beta(\sqrt{h^2+d^2}-h)}$$

Putting $u = \beta(r_1 + z - h)$, $$\int_0^h \frac{e^{-j\beta(r_1+z-h)}}{r_1}\,dz = [Ei(-ju)]_{\beta(\sqrt{h^2+d^2}-h)}^{\beta d}$$

Putting $u = \beta(r_1 - z + h)$, $$\int_0^h \frac{e^{-j\beta(r_1-z+h)}}{r_1}\,dz = -[Ei(-ju)]_{\beta(\sqrt{h^2+d^2}+h)}^{\beta d}$$

Putting $u = \beta(r_2 + z + h)$, $$\int_0^h \frac{e^{-j\beta(r_2+z+h)}}{r_2}\,dz = [Ei(-ju)]_{\beta(\sqrt{h^2+d^2}+h)}^{\beta(\sqrt{4h^2+d^2}+2h)}$$

Putting $u = \beta(r_2 - z - h)$, $$\int_0^h \frac{e^{-j\beta(r_2-z-h)}}{r_2}\,dz = -[Ei(-ju)]_{\beta(\sqrt{h^2+d^2}-h)}^{\beta(\sqrt{4h^2+d^2}-2h)}$$

Substituting and collecting terms we have

$$\begin{aligned} Z_{12} = {} & 15[2\{1+2\cos^2(\beta h)\}Ei(-j\beta d) - \\ & -\{4\cos^2(\beta h) + j\,2\sin(2\beta h)\}Ei\{-j\beta(\sqrt{h^2+d^2}+h)\} - \\ & -\{4\cos^2(\beta h) - j\,2\sin(2\beta h)\}Ei\{-j\beta(\sqrt{h^2+d^2}-h)\} + \\ & +\{\cos(2\beta h) + j\sin(2\beta h)\}Ei\{-j\beta(\sqrt{4h^2+d^2}+2h)\} + \\ & +\{\cos(2\beta h) - j\sin(2\beta h)\}Ei\{-j\beta(\sqrt{4h^2+d^2}-2h)\}] \end{aligned} \tag{7.6}$$

When $d \to 0$ we can write

$$(\sqrt{h^2+d^2}-h) \to d^2/2h, \quad (\sqrt{h^2+d^2}+h) \to 2h, \quad (\sqrt{4h^2+d^2}-2h) \to d^2/4h,$$

$$(\sqrt{4h^2+d^2}+2h) \to 4h, \quad Ci(\beta d) \to \gamma + \log(\beta d), \quad \text{and } Si(\beta d) \to 0.$$

It follows that, as $d \to 0$

$$\begin{aligned} \mathrm{Re}.Z_{12} \to {} & 15\{\sin(2\beta h)Si(4\beta h) - 2\sin(2\beta h)Si(2\beta h) - \\ & -\cos(2\beta h)Ki(4\beta h) + 4\cos^2(\beta h)Ki(2\beta h)\} \end{aligned} \tag{7.7}$$

and is independent of d; $Ki(u)$ is defined in Equation (2.4).

$$\begin{aligned} \mathrm{Im}.Z_{12} \to {} & 15\{-\cos(2\beta h)Si(4\beta h) + 4\cos^2(\beta h)Si(2\beta h) - 2\sin(2\beta h)Ci(2\beta h) + \\ & +\sin(2\beta h)Ci(4\beta h) + \gamma\sin(2\beta h) + \sin(2\beta h)\log(\beta d^2/h)\} \end{aligned} \tag{7.8}$$

Hence as $d \to 0$ Z_{12} contains d only in the form $\log d$.

7.3. The Field in the Direction of a Doublet Mounted Near an Infinitely-Long Cylinder Immersed in a Plane-Wave Field

The field is calculated for a plane wave in the x-z plane incident at an angle θ to the vertical, as the sum of two components. One component is that due to a distant vertically-polarised transmitting doublet, i.e. one with its axis in the plane of incidence and perpendicular to the radius vector; the other is that due to a distant horizontally-polarised transmitting doublet, i.e. one with its axis normal to the plane of incidence. The axis of the cylinder is the vertical z-axis, and the point at which the field is calculated has cylindrical co-ordinates (ρ, z, ϕ).

It follows from the reciprocity theorem that the two field components calculated are respectively the vertically- and horizontally-polarised waves radiated by a transmitting doublet mounted near the cylinder.

7.3.1. Generalised Expression for the Field

Fig. 7.4

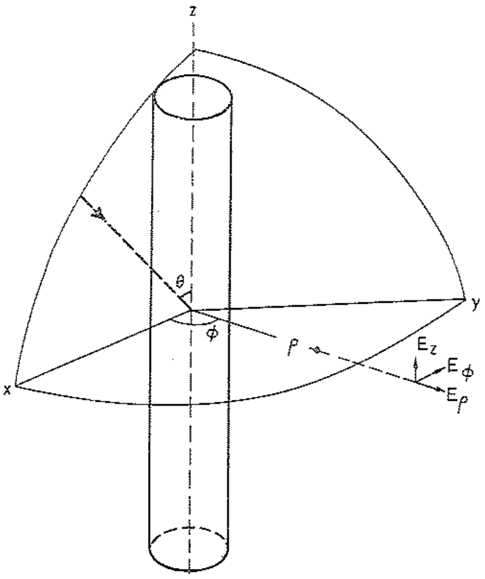

The magnitude of any field component, F, is independent of z, and the phase changes by $\beta\cos\theta$ per unit length along the z-axis; it follows that $\partial F/\partial z = j\beta\cos\theta\, F$. The general expressions for the field in cylindrical co-ordinates become*

$$\mathrm{curl}_\rho\, E = \frac{1}{\rho}\,\frac{\partial E_z}{\partial \phi} - j\beta\cos\theta\, E_\phi = -j\,\omega\mu_0 H_\rho \tag{7.9}$$

$$\mathrm{curl}_\phi\, E = j\beta\cos\theta\, E_\rho - \frac{\partial E_z}{\partial \rho} = -j\,\omega\mu_0 H_\phi \tag{7.10}$$

$$\mathrm{curl}_z\, E = \frac{E_\phi}{\rho} + \frac{\partial E_\phi}{\partial \rho} - \frac{1}{\rho}\,\frac{\partial E_\rho}{\partial \phi} = -j\,\omega\mu_0 H_z \tag{7.11}$$

$$\mathrm{curl}_\rho\, H = \frac{1}{\rho}\,\frac{\partial H_z}{\partial \phi} - j\beta\cos\theta\, H_\phi = j\,\omega\epsilon_0 E_\rho \tag{7.12}$$

---

*E.C. Jordan, "Electromagnetic Waves and Radiating Systems", Prentice-Hall, pp. 16 and 113.

$$\mathrm{curl}_\phi\, H = j\beta\cos\theta\, H_\rho - \frac{\partial H_z}{\partial \rho} = j\,\omega\epsilon_0 E_\phi \tag{7.13}$$

$$\mathrm{curl}_z\, H = \frac{H_\phi}{\rho} + \frac{\partial H_\phi}{\partial \rho} - \frac{1}{\rho}\,\frac{\partial H_\rho}{\partial \phi} = j\,\omega\epsilon_0 E_z \tag{7.14}$$

Eliminating E_ρ, E_ϕ, H_ρ, H_z and H_ϕ we obtain

$$\frac{\partial^2 E_z}{\partial(\beta\rho\sin\theta)^2} + \frac{1}{(\beta\rho\sin\theta)}\,\frac{\partial E_z}{\partial(\beta\rho\sin\theta)} + \frac{1}{(\beta\rho\sin\theta)}\,\frac{\partial^2 E_z}{\partial\phi^2} + E_z = 0 \tag{7.15}$$

The solution can be expressed as the product of two independent functions, one of ρ and the other of ϕ.* We have

$$E_z = f(\rho)\{A\cos(n\phi) + B\sin(n\phi)\}$$

where n is any integer, A and B are constants, and

$$\frac{\partial^2 f(\rho)}{\partial(\beta\rho\sin\theta)^2} + \frac{1}{(\beta\rho\sin\theta)}\,\frac{\partial f(\rho)}{\partial(\beta\rho\sin\theta)} + E_z\left\{1 - \frac{n^2}{(\beta\rho\sin\theta)^2}\right\} = 0$$

This is Bessel's equation of order n; one solution is**

$$f(\rho) = A_n H_n^{(1)}(\beta\rho\sin\theta) + B_n H_n^{(2)}(\beta\rho\sin\theta)$$

where A_n, B_n are constants, and $H_n^{(1)}(z)$, $H_n^{(2)}(z)$ are the Hankel functions of order n of the first and second kinds respectively; these functions are defined by

$$H_n^{(1)}(z) = J_n(z) + jY_n(z)$$

$$H_n^{(2)}(z) = J_n(z) - jY_n(z)$$

where $J_n(z)$, $Y_n(z)$ are the Bessel functions of order n of the first and second kinds respectively.

We have therefore

$$E_z = \{A_n H_n^{(1)}(\beta\rho\sin\theta) + B_n H_n^{(2)}(\beta\rho\sin\theta)\}\{A\cos(n\phi) + B\sin(n\phi)\} \tag{7.16}$$

Since any integral value of n is permissible the most general form of Equation (7.16) is

$$E_z = \sum_0^\infty \{A_n H_n^{(1)}(\beta\rho\sin\theta) + B_n H_n^{(2)}(\beta\rho\sin\theta)\}\{A\cos(n\phi) + B\sin(n\phi)\} \tag{7.17}$$

---

*The general expression for any field component includes an addition factor $e^{j\beta z\cos\theta}$ to take account of the variation of phase with z. Throughout this Section we will omit this factor.

**This solution, and the other formulae in this Section involving Bessel functions will be found in: G.N. Watson, "Theory of Bessel Functions".

Similarly

$$H_z = \frac{1}{\eta_0} \sum_0^\infty \{C_n H_n^{(1)} (\beta \rho \sin\theta) + D_n H_n^{(2)} (\beta \rho \sin\theta)\}\{A \cos(n\phi) + B \sin(n\phi)\} \qquad (7.18)$$

From Equations (7.9) and (7.13)

$$E_\phi = \frac{j}{\beta \sin^2\theta} \left\{ \frac{\cos\theta}{\rho} \frac{\partial E_z}{\partial \phi} + \eta_0 \frac{\partial H_z}{\partial \rho} \right\} \qquad (7.19)$$

From Equations (7.10) and (7.12)

$$E_\rho = \frac{j}{\beta \sin^2\theta} \left\{ \cos\theta \frac{\partial E_z}{\partial \rho} - \frac{\eta_0}{\rho} \frac{\partial H_z}{\partial \phi} \right\} \qquad (7.20)$$

Equations (7.17) to (7.20) can be used to express both the incident wave and the field re-radiated by the cylinder, provided the coefficients A, B, A_n, B_n, C_n and D_n are appropriately chosen.

A solution of this form is convenient for expressing the field re-radiated by the cylinder since, for large values of the argument, Hankel functions of the first and second kinds correspond to inward-travelling and outward-travelling waves respectively; the singularity at the axis $\left(Y_n(z) \to \infty \text{ as } \rho \to 0\right)$ is of no consequence since we are concerned only with values of ρ equal to or greater than the cylinder radius. As we are dealing with radiation into free space we put $A_n = C_n = 0$; A_n, C_n would not be 0 if we had a reflecting surface at some point in space.

It is necessary to express the incident field in the same form as in Equations (7.17) to (7.20) in order to facilitate solving for the arbitrary coefficients. The most convenient form is an infinite series of Bessel functions of the first kind, since there is then no singularity at the axis; in other words, we put $A_n = B_n$ in the general solution.

For a horizontally-polarised transmitting doublet, the E_z component of the incident wave is 0; the cylinder currents are therefore entirely circumferential and the only component of magnetic intensity in the re-radiated field is H_z. It follows from Equation (7.14) that $E_z = 0$ for the re-radiated field also. Correspondingly, for a vertically-polarised transmitting doublet the H_z component of the incident and re-radiated fields are both 0. In Equations (7.19) and (7.20) we therefore put

$$\frac{\partial E_z}{\partial \phi} = \frac{\partial E_z}{\partial \rho} = 0$$

for a horizontally-polarised transmitting doublet, and

$$\frac{\partial H_z}{\partial \rho} = \frac{\partial H_z}{\partial \phi} = 0$$

for a vertically-polarised transmitting doublet.

7.3.2. Values of the Coefficients for a Horizontally-Polarised Transmitting Doublet

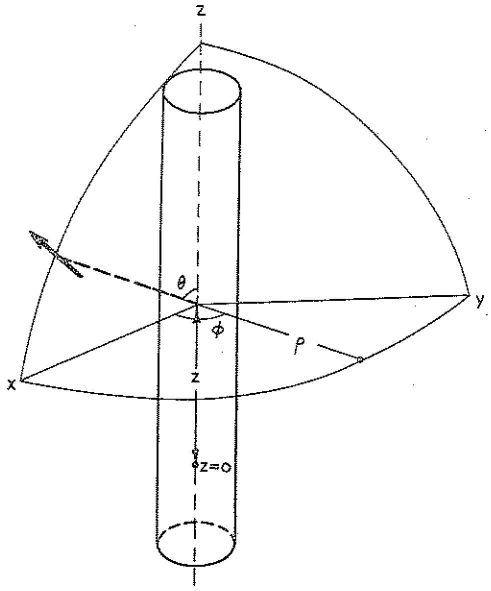

Fig. 7.5

Consider a plane wave arriving at an angle of incidence θ from a distant horizontal transmitting doublet. Let the electric force at the origin be $1\underline{/0}$.

Since the path length from a distant point to the point $(\rho,\ z,\ \phi)$ is less than that to the origin by a length $(z\cos\theta + \rho\cos\phi\sin\theta)$ the incident wave in the plane $z = 0$ can be written

$$\left.\begin{aligned} H_z &= \frac{\sin\theta}{\eta_0}\, e^{j\beta\rho\cos\phi\sin\theta} = \frac{\sin\theta}{\eta_0} \sum_{0}^{\infty} \epsilon_n j^n J_n(\beta\rho\sin\theta)\cos(n\phi) \\ E_z &= 0 \end{aligned}\right\} \qquad (7.21)$$

where ϵ_n is Neumann's number; $\epsilon_n = 1$ for $n = 0$, $\epsilon_n = 2$ for $n \neq 0$.

From Equations (7.19) and (7.21), with

$$\frac{\partial E_z}{\partial \phi} = 0$$

we have for the incident wave

$$E_\phi = j \sum_{0}^{\infty} \epsilon_n j^n J_n'(\beta\rho\sin\theta)\cos(n\phi) \qquad (7.22)$$

where $J_n'(z)$ denotes the derivative of $J_n(z)$ with respect to z, and is given by

$$J_n'(z) = \frac{1}{2}\{J_{n-1}(z) - J_{n+1}(z)\}$$

From Equations (7.18) and (7.19), with

$$C_n = \frac{\partial E_z}{\partial \phi} = 0 \ ,$$

we have for the re-radiated wave

$$E_\phi = \frac{j}{\sin\theta} \sum_{0}^{\infty} D_n H_n^{(2)\prime}(\beta\rho\sin\theta)\{C\cos(n\phi) + D\sin(n\phi)\} \tag{7.23}$$

where $H_n^{(2)\prime}(z)$ denotes the derivative of $H_n(z)$ with respect to z, and is given by

$$H_n^{(2)\prime}(z) = \frac{1}{2}\{H_{n-1}^{(2)}(z) - H_{n+1}^{(2)}(z)\}$$

The sum of the right-hand sides of Equations (7.22) and (7.23) must be zero at the surface of the perfectly-conducting cylinder for all values of ϕ; we have therefore

$$\left.\begin{aligned} D &= 0 \\ CD_n &= -\frac{\sin\theta\,\epsilon_n j^n J_n'(\beta a\sin\theta)}{H_n^{(2)\prime}(\beta a\sin\theta)} \end{aligned}\right\} \tag{7.24}$$

Furthermore, since $E_z = 0$, $B_n = 0$.

7.3.3. Values of the Coefficients for a Vertically-Polarised Transmitting Doublet

Fig. 7.6

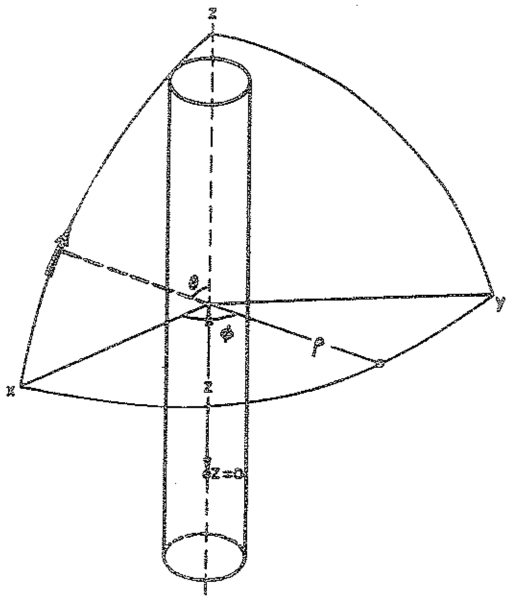

Consider a plane wave arriving at an angle of incidence θ from a distant vertical transmitting doublet. Let the electric force at the origin be 1/$\underline{Q}$.

The incident wave in the plane $z = 0$ may be written

$$\left.\begin{aligned} E_z &= \sin\theta\, e^{j\beta\rho\cos\phi\sin\theta} = \sin\theta \sum_{0}^{\infty} \epsilon_n j^n J_n(\beta\rho\sin\theta)\cos(n\phi) \\ H_z &= 0 \end{aligned}\right\} \qquad (7.25)$$

For the re-radiated wave, E_z is given by Equation (7.17), with $A_n = 0$. Putting the sum of the incident and re-radiated E_z components zero at the surface of the perfectly-conducting cylinder, we have

$$\left.\begin{aligned} B &= 0 \\ AB_n &= -\frac{\sin\theta\,\epsilon_n j^n J_n(\beta a\sin\theta)}{H_n^{(2)}(\beta a\sin\theta)} \end{aligned}\right\} \qquad (7.26)$$

Furthermore, since $H_z = 0$, $D_n = 0$.

7.3.4. Field in Direction of Tangential Receiving Doublet Spaced a Distance b from the Axis of the Cylinder

(i) Component due to horizontally-polarised transmitting doublet

From Equations (7.22, (7.23) and (7.24)

$$E_\phi = j\sum_{0}^{\infty} \epsilon_n j^n \left[J_n'(\beta b\sin\theta) - \frac{J_n'(\beta a\sin\theta)}{H_n^{(2)\prime}(\beta a\sin\theta)} H_n^{(2)\prime}(\beta b\sin\theta) \right]\cos(n\phi) \qquad (7.27)$$

(ii) Component due to vertically-polarised transmitting doublet

From Equations (7.17), (7.19), (7.25) and (7.26)

$$E_\phi = \frac{j\cos\theta}{\beta\rho\sin\theta}\frac{\partial}{\partial\phi}\sum_{0}^{\infty}\epsilon_n j^n \left[J_n(\beta\rho\sin\theta) - \frac{J_n(\beta a\sin\theta) H_n(\beta\rho\sin\theta)}{H_n^{(2)}(\beta a\sin\theta)} \right]\cos(n\phi)$$

Differentiating with respect to ϕ and putting $\rho = b$ we obtain

$$E_\phi = \frac{-j2\cos\theta}{\beta b\sin\theta}\sum_{1}^{\infty} j^n n \left[J_n(\beta b\sin\theta) - \frac{J_n(\beta a\sin\theta)}{H_n^{(2)}(\beta a\sin\theta)} H_n^{(2)}(\beta b\sin\theta) \right]\sin(n\phi) \qquad (7.28)$$

7.3.5. Field in Direction of Vertical Receiving Doublet Spaced a Distance b from the Axis of the Cylinder

(i) Component due to horizontally-polarised transmitting doublet

$$E_z = 0 \qquad (7.29)$$

(ii) Component due to vertically-polarised transmitting doublet

From Equations (7.17), (7.25) and (7.26)

$$E_z = \sin\theta \sum_{o}^{\infty} \epsilon_n j^n \left[J_n(\beta b \sin\theta) - \frac{J_n(\beta a \sin\theta)}{H_n^{(2)}(\beta a \sin\theta)} H_n^{(2)}(\beta b \sin\theta) \right] \cos(n\phi) \qquad (7.30)$$

7.3.6. Field in Direction of Radial Receiving Doublet Spaced a Distance b from the Axis of the Cylinder

(i) Component due to horizontally-polarised transmitting doublet

From Equations (7.18), (7.20), (7.21) and (7.24), when $\rho = b$

$$E_\rho = \frac{j2}{\beta b \sin\theta} \sum_{1}^{\infty} j^n n \left[J_n(\beta b \sin\theta) - \frac{J_n'(\beta a \sin\theta)}{H_n^{(2)'}(\beta a \sin\theta)} H_n^{(2)}(\beta b \sin\theta) \right] \sin(n\phi) \qquad (7.31)$$

(ii) Component due to vertically-polarised transmitting doublet

From Equations (7.17), (7.20), (7.25) and (7.26)

$$E_\rho = j \cos\theta \sum_{o}^{\infty} \epsilon_n j^n \left[J_n'(\beta b \sin\theta) - \frac{J_n(\beta a \sin\theta)}{H_n^{(2)}(\beta a \sin\theta)} H_n^{(2)'}(\beta b \sin\theta) \right] \cos(n\phi) \qquad (7.32)$$

7.3.7. Value of H_z at the Surface of the Cylinder due to Horizontally-Polarised Transmitting Doublet

This result is required in connection with the problem of a longitudinal slot in an infinitely-long cylinder (see Section 4.9).

A vertically-polarised transmitting doublet gives no H_z component. For a horizontally-polarised transmitting doublet the component of H_z for the incident wave is given by Equation (7.21), and for the re-radiated field by Equations (7.18) and (7.24). The resultant is

$$H_z = \frac{\sin\theta}{\eta_0} \sum_{o}^{\infty} \epsilon_n j^n \left[J_n(\beta a \sin\theta) - \frac{J_n'(\beta a \sin\theta)}{H_n^{(2)'}(\beta a \sin\theta)} H_n^{(2)}(\beta a \sin\theta) \right] \cos(n\phi) \qquad (7.33)$$

Since $$J_n(z) H_n^{(2)'}(z) - J_n'(z) H_n^{(2)}(z) = j\,\frac{2}{\pi z} ,$$

Equation (7.33) reduces to

$$H_z = \frac{j}{\eta_0} \frac{2}{\beta \pi a} \sum_{o}^{\infty} \epsilon_n j^n \frac{1}{H_n^{(2)'}(\beta a \sin\theta)} \cos(n\phi) \qquad (7.34)$$